TECHNICAL REPORT STANDARD TITLE PAGE

1. Report No.	2. Government Accession No.	3. Recipient's Catalog No.
FHWA/TX-88+465-1		

4. Title and Subtitle	5. Report Date
AN EXPLORATORY INVESTIGATION OF SHEAR FATIGUE BEHAVIOR OF PRESTRESSED CONCRETE GIRDERS	June 1987
	6. Performing Organization Code

7. Author(s)	8. Performing Organization Report No.
Patrick M. Bachman, Michael E. Kreger, and John E. Breen	Research Report 465-1

9. Performing Organization Name and Address	10. Work Unit No.
Center for Transportation Research The University of Texas at Austin Austin, Texas 78712-1075	11. Contract or Grant No. Research Study 3-5-86-465
	13. Type of Report and Period Covered Interim
12. Sponsoring Agency Name and Address Texas State Department of Highways and Public Transportation; Transportation Planning Division P. O. Box 5051 Austin, Texas 78763-5051	14. Sponsoring Agency Code

15. Supplementary Notes

Study conducted in cooperation with the U. S. Department of Transportation, Federal Highway Administration.

Research Study Title: "Fatigue Strength of Posttensioned Concrete"

16. Abstract

This report presents the results of an exploratory investigation of shear fatigue behavior of precast prestressed girders with unshored cast-in-place slabs. It includes a literature survey of shear fatigue behavior and design specifications related to fatigue of structural concrete. Detailed summaries are given for the fatigue response and ultimate behavior of three full-scale prestressed girders including static and dynamic measurements of load, deflection, crack widths, strand stresses, and stirrup stresses. The controlled variable in this exploratory investigation was the maximum fatigue load. Other variables included in the investigation were concrete strength and prestressing losses. Fatigue data for stirrups in the girders were compared with data from fatigue tests of reinforcing bars in air. Shear fatigue data for the girders were compared and evaluated with results of previous studies and with present design code specifications.

17. Key Words	18. Distribution Statement
prestressed girders, precast, slabs, cast-in-place, unshored, literature, fatigue, structural concrete	No restrictions. This document is available to the public through the National Technical Information Service, Springfield, Virginia 22161.

19. Security Classif. (of this report)	20. Security Classif. (of this page)	21. No. of Pages	22. Price
Unclassified	Unclassified	198	

Form DOT F 1700.7 (8-69)

AN EXPLORATORY INVESTIGATION OF SHEAR FATIGUE BEHAVIOR OF PRESTRESSED CONCRETE GIRDERS

by

Patrick M. Bachman
Michael E. Kreger
and
John E. Breen

Research Report 465-1

Fatigue Strength of Posttensioned Concrete

Research Project 3-5-86-465

conducted for

Texas State Department of Highways and Public Transportation

by

Center for Transportation Research
Bureau of Engineering Research
The University of Texas at Austin

June 1987

The contents of this report reflect the views of the authors who are responsible for the facts and accuracy of the data presented herein. The contents do not necessarily reflect the official views or policies of the Federal Highway Administration. This report does not constitute a standard, specification, or regulation.

PREFACE

The research was sponsored by the Texas State Department of Highways and Public Transportation and the Federal Highway Administration. It was administered by the Center for Transportation Research. The research was conducted in the Phil M. Ferguson Structural engineering Laboratory at the Balcones Research Center, The University of Texas at Austin, Austin, Texas. Close liason with the Texas State Department of Highways and Public Transportation was maintained through their contact representative, Mr. A.B. Matejowsky.

The authors are indebted to the technical staff who worked on this project at Ferguson Laboratory, and particularly to Research Engineer Nobuyuki Matsumoto who conscientiously conducted in-air fatigue tests on deformed reinforcing bars and aided in fabrication and testing of girder specimens.

This report contains a summary of an exploratory study of shear fatigue behavior of prestressed concrete girders.

SUMMARY

This report presents the results of an exploratory investigation of shear fatigue behavior of precast prestressed girders with unshored cast-in-place slabs. It includes a literature survey of shear fatigue behavior and design specifications related to fatigue of structural concrete. Detailed summaries are given for the fatigue response and ultimate behavior of three full-scale prestressed girders including static and dynamic measurements of load, deflection, crack widths, strand stresses, and stirrup stresses. The controlled variable in this exploratory investigation was the maximum fatigue load. Other variables included in the investigation were concrete strength and prestressing losses. Fatigue data for stirrups in the girders were compared with data from fatigue tests of reinforcing bars in air. Shear fatigue data for the girders were compared and evaluated with results of previous studies and with present design code specifications.

I M P L E M E N T A T I O N

Results of this test program demonstrated that a beam, which would have failed in flexure under monotonically increasing load, failed in shear when subjected to fatigue loading. Web-shear cracks were shown to form under fatigue loads which corresponded with a computed maximum diagonal tension stress of less than $4\sqrt{f'_c}$ at h/2 from the face of the support. In addition, brittle fracture of stirrups was observed to occur after diagonal cracks formed. No endurance limit was observed for fracture of stirrups once diagonal cracks formed, even though applied loads were in the approximate range of AASHTO service level design loads.

This study demonstrated that ACI Code and AASHTO Specification provisions for shear in prestressed concrete are inadequate for predicting shear fatigue strength of prestressed concrete girders. Shear fatigue can be minimized by neglecting the concrete contribution to shear strength while designing web reinforcement.

TABLE OF CONTENTS

TABLE OF CONTENTS (continued)

TABLE OF CONTENTS (continued)

LIST OF TABLES

LIST OF FIGURES

LIST OF FIGURES (continued)

LIST OF FIGURES (continued)

LIST OF FIGURES (continued)

LIST OF FIGURES (continued)

LIST OF FIGURES (continued)

CHAPTER 1

INTRODUCTION

1.1 General

The widespread use of prestressed concrete in America is relatively new. In 1950 there was only one precast pretensioning plant in America. By 1975 there were 500 operating plants [15]. The first design codes for prestressed concrete were quite conservative. As behavior of prestressed concrete became better understood through research, and engineers became familiar with design procedures, codes of practice generally became less conservative. This order of events is quite normal in the development of design specifications. However, as design provisions evolve, a greater responsibility is placed on engineers. Generally, the design requires more careful consideration and design equations become more complex. An especially important consequence is that new design limit states may develop which were previously unknown or deemed unimportant. The effect of repetitive loads on the service life of a structure is an example.

The use of standard precast pretensioned concrete I-beams in bridge construction has become popular in America and is probably the most widely used type of bridge construction in Texas. In fact, Texas is one of the few states to develop its own standard sections. Over the past several decades there has been a steady erosion of the excess design capacity of prestressed concrete bridge girders. Allowable loads have been increased reducing effective load factors, while at the same time there has been a general pressure to increase capacity reduction (ϕ) factors and allowable tensile stresses in the precompressed tensile fiber. The combination of these changes leads to higher possibilities of tensile stresses occurring in prestressed girders with consequent cracking and even increased tensile stresses. This makes fatigue resistance a more important consideration, yet at the present time engineers have virtually no guidelines to follow for fatigue design of prestressed concrete. The following questions need to be answered:

1. How is the fatigue life of prestressed concrete beams determined, and can fatigue behavior control the design life?

2. What is the factor of safety against fatigue failure when allowable loads are increased on existing bridges?

3. How do laboratory fatigue conditions with constant-magnitude, steady state loads compare to field conditions?

4. What types of fatigue failure are possible for different loading conditions and span length?

5. Is there any danger of fatigue failures in the shear reinforcement of prestressed girders?

This test program was implemented to study the effect of fatigue on the shear strength of prestressed concrete I-beams with a composite deck.

1.2 Shear in Prestressed Concrete

The basic mechanism for shear transfer in prestressed and reinforced concrete is widely accepted. In an uncracked section, shear strength is mainly provided by shear and diagonal tensile stresses on the gross concrete section. In a cracked section, shear strength is provided by shear stresses in the concrete compressive zone, tensile stresses in the web reinforcement, aggregate interlock, and dowel action. These forces are interrelated. For example, increased web reinforcement will increase the effect of aggregate interlock by decreasing the width of diagonal cracks [6]. Another mechanism for shear transfer, arch action, may develop for beams with a small shear span-to-depth ratio and concentrated loading which introduces vertical compression into the member. Although the basic mechanism for shear transfer is known, it is difficult to assess the percentage of shear carried by each mechanism. When shear strength is exceeded, several modes of shear failure are possible.

Design codes tend to be conservative with respect to shear strength because shear failures can be catastrophic, with no warning of impending failure. The AASHTO and ACI Codes [2,3] present empirical design equations for shear strength of reinforced and prestressed concrete beams based on a concrete contribution and a web reinforcement contribution to shear strength. The concrete contribution is taken to be the load required to cause diagonal cracking. Furthermore, the concrete contribution is assumed to remain constant, regardless of the

stage of loading or the state of cracking. Web reinforcement is designed, based on a 45 degree truss model, to resist only the applied shear in excess of the concrete contribution. Much criticism has been made in recent years of the fact that the concrete contribution is assumed to remain at the same level after diagonal cracking.

In calculating the concrete contribution for prestressed concrete, two types of diagonal cracking are considered. Flexure-shear cracks are those initiated by tensile stresses in the bottom flange due to bending moment which then propagate diagonally through the web as a result of shear stress. Web-shear cracks form at the centroid of the section due to principal tensile stresses. Both types of inclined cracks are shown in Fig. 5.8. The least load required to produce either type of inclined crack is considered as the concrete contribution. In general, web-shear cracks will develop near the supports of a beam while flexure-shear cracks will develop out in the span away from the supports.

The concrete contribution allowed for web-shear strength in prestressed concrete beams is about twice that of the concrete contribution allowed in reinforced concrete beams. This is because of the beneficial effect prestressing has on the principal tensile stresses and the fact that once a web-shear crack develops it will not propagate immediately through the bottom flange because of the high compressive stresses present. Prestressed concrete beams generally have relatively small amounts of web reinforcement compared to reinforced concrete beams because the concrete contribution is relatively high.

The ACI Code equations for shear strength have been determined from results of comprehensive static loading strength tests and produce satisfactory (if complex) designs for static loading. However, the equations may or may not represent shear behavior during fatigue loading since they have not been carefully checked for repeated loading conditions.

1.3 Flexural Fatigue of Prestressed Concrete

The most prevalent form of flexural fatigue damage in prestressed concrete is tensile fatigue fracture of the prestressing strand. Tests conducted by Rabbat et al. [27] in 1978 indicated that fatigue fractures could occur in pretensioned AASHTO highway girders at bottom fiber tensile stresses of $6\sqrt{f'_c}$. Recently a comprehensive investigation of the flexural fatigue

behavior of eleven full-scale pretensioned prestressed beams was concluded at the University of Texas [23] and a study of post-tensioned beams is now underway. This study is an extension of those studies but with emphasis placed on shear behavior during fatigue loading.

1.4 Shear Fatigue of Prestressed Concrete

Although much research has been undertaken to assess the shear strength of prestressed concrete beams under static loading, very little research has been performed on the shear strength of prestressed beams subjected to fatigue loading. Virtually no guidelines are available for shear fatigue design.

The present ACI and AASHTO Code equations for shear strength do not take fatigue behavior into account. Prestressed I beams are especially susceptible to the development of web-shear cracks because of the thinness of the web section. The present design trend is toward use of thinner webs. In fact, present standard prestressed highway girders used by the state of Washington have only a 5-in. web.

The shear fatigue behavior of prestressed beams may change drastically after inclined cracks develop. Usually prestressed beams have minimal web reinforcement because of the high concrete contribution to shear strength allowed by design codes. This allows inclined cracks to propagate with less resistance and results in wider crack openings which leads to a decrease in the shear transferred through aggregate interlock. These considerations are probably inconsequential for static loading but may have dramatic effects under fatigue loading. The use of blanketed strands to reduce top-flange tensile stresses at release may also have an effect on the shear fatigue behavior because inclined cracks can propagate more easily through the bottom flange.

Hanson and Hulsbos performed tests on approximately 1/2-scale specimens [10,12] which were precracked in flexure and shear. They determined that stirrups could fracture and a prestressed beam could fail in shear with no evidence of flexural fatigue distress. Even more alarming, they determined that there are loadings for which a prestressed beam will fail in shear under fatigue loading even though flexural failure would control behavior under static loading conditions. This result has been confirmed for reinforced concrete beams by several authors.

In the tests by Hanson and Hulsbos, enough web reinforcement was provided to develop the flexural capacity. However, this was only approximately one-half of what was required by design specifications. To date, no known tests have been performed on full-scale specimens with sufficient web reinforcement provided to satisfy design code requirements. This present study utilizes full-scale standard prestressed highway girders satisfying all applicable design codes.

1.5 Objectives and Scope of Study

Research projects 300 and 465 were undertaken at the University of Texas to gain a better understanding of the fatigue strength of prestressed concrete beams. The studies were sponsored by the Texas Department of Highways and Public Transportation and the Federal Highway Administration. The investigations were divided into the following phases:

1. Fatigue tests of prestressing strand in air. These tests involved the development of a strand in-air fatigue model based on both previously reported tests and new data. These tests were reported on by Paulson [24]. New tests will be reported by Yates [32].

2. Flexural fatigue tests of pretensioned concrete beams. Eleven full scale pretensioned beams were tested. Primary variables were maximum nominal concrete tensile stress level, girder strand stress ranges, cross sections, strand patterns, passive reinforcement, degree of precracking, presence of occasional overloading, and prestress losses. The first three beams in the series were reported on by Reese [28]. The entire series was reported on by Overman [23].

3. Flexural fatigue tests of post-tensioned partial-beam concrete specimens. A series to investigate the behavior of post-tensioned strand in a specimen simulating beam behavior is underway. Severe effects of fretting corrosion have been noted in tests to date. This series will also be reported by Yates [32].

4. Flexural fatigue tests of post-tensioned girders. A series of large size girder tests is underway. Initial specimens will be reported by Diab [33].

5. Shear fatigue tests of prestressed concrete beams. Three full-scale prestressed beams were tested with the first of this series being a shared specimen with the pretensioned girder flexural fatigue series (see Sec. 4.2). These three specimens are the object of this report. A companion study was performed on the fatigue strength of deformed reinforcing bars in air and was reported on by Matsumoto [18].

Limited test results by Hanson and Hulsbos [10,12] and Price and Edwards [26] have indicated that shear fatigue may be a problem in thin web, prestressed concrete beams. However, less web reinforcement was used in those test specimens than specified by design codes. The objective of this exploratory study is to see if shear fatigue may be a problem in prestressed concrete highway girders which are designed according to present design specifications. Full-scale, Texas Type C girders were used to eliminate any size effects. The emphasis was on the web-shear type of cracking. Specimens were not precracked in shear so that diagonal tensile fatigue of concrete could be explored. After concrete fatigue cracks were developed, the fatigue strength of web reinforcement was studied. Shear-flexural fatigue interaction was also examined. Variables in the three girders tested were maximum fatigue load, and incidental differences in effective prestress and concrete strength.

CHAPTER 2

REVIEW OF PREVIOUS STUDIES

2.1 Introduction

Shear strength of concrete beams is a complex problem. It is known that shear strength is provided by web reinforcement, concrete in the compression zone, dowel action, and aggregate interlock. However, no rational analytical model has been developed to include all these effects. Instead, conservative empirical equations have been developed to predict shear strength under static loading conditions. Most design codes specify that enough shear capacity be present in a beam to develop the flexural capacity and preclude a shear failure. Recent studies are emphasizing a return to the variable angle truss model [34, 35, 36, 37, 38] or the compression strut and tension tie models [39, 40] for improved understanding and design procedures for shear.

Fatigue loading conditions make it more difficult to evaluate shear strength. The present empirical equations with a concrete contribution and a steel contribution to shear strength do not seem to be applicable to fatigue loading when diagonal cracks are present. It has been demonstrated that a concrete beam designed to fail in flexure under monotonically applied loads failed in shear during fatigue loading.

When diagonal cracks are present in a concrete beam, it is the fracture of web reinforcement which generally leads to failure under repeated loads. Therefore, the fatigue resistance of deformed reinforcing bars is very important in the consideration of shear fatigue behavior. Studies have been conducted on reinforcing bars air [11,13,16,17,18,25,29]. However, it is not clear how they apply to similar bars embedded in concrete. Little is known about stresses in reinforcing bars embedded in concrete and subjected to fatigue loading conditions.

Recently there has been concern about shear fatigue of prestressed concrete beams. Generally less web reinforcement is required and many standard prestressed sections utilize a thin concrete web, both of which reduce shear capacity. More importantly, load factors have been reduced in recent years for prestressed concrete bridges where fatigue is of primary concern. Very little research has been conducted up to the present time concerning shear fatigue of prestressed concrete beams.

This chapter presents a comprehensive summary of shear fatigue studies on prestressed concrete beams. In addition, a summary of some of the shear fatigue research for reinforced concrete beams and fatigue of standard deformed reinforcing bars is presented.

2.2 Shear Fatigue of Prestressed Concrete Beams

The earliest research on shear fatigue of prestressed concrete beams in the United States was performed by Hanson and Hulsbos in the 1960's [10]. They set out to determine if a prestressed beam designed to fail in flexure, then subjected to an overload sufficient to develop diagonal tension cracks in the web would be critical in shear instead of flexure for fatigue loading.

They tested two specimens, denoted E10 and E11, with the cross section and loading arrangement shown in Fig. 2.1. The beams were instrumented to obtain load-deflection, concrete strain, and diagonal crack-width data. The beams were reinforced similarly except for the amount of web reinforcement. Beam E10 had 57% and Beam E11 had 43% of the web reinforcement required by AASHTO specifications [1] to develop the ultimate flexural capacity of the sections. However, tests on identical beams confirmed that enough web reinforcement was present to develop a flexural failure under static loads.

The two beams subjected to fatigue tests were initially loaded to 78% of the ultimate flexural capacity to cause inclined cracking during the first load cycle. This load was not high enough to cause yielding of the prestressing strand in the constant moment region. Beam E10 failed in flexural fatigue at a maximum load of 28 kips. Beam E11 failed in shear fatigue at a maximum load of 24 kips. The load history for the beams is given in Table 2.1 and the load-deflection response is shown in Fig. 2.2. It can be seen that both beams were loaded into the nonlinear portion of the load-deflection response during the initial static cycle and during fatigue loading. Discussion will be limited to Beam E11 since shear fatigue is the object of this report.

Hanson and Hulsbos collected much useful information during their test of Beam E11. They noted that diagonal cracks did not open until a load of 10 kips had been applied, and then the crack opening was approximately linear with load. They also

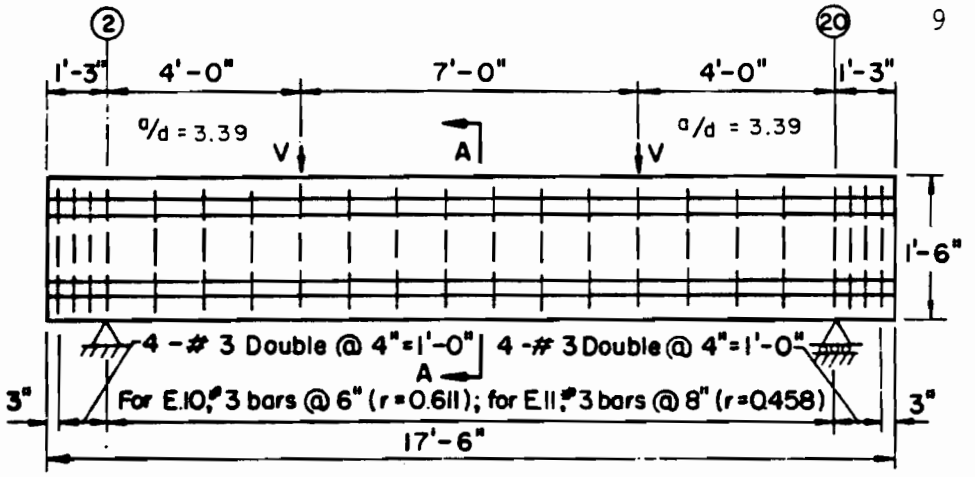

ELEVATION

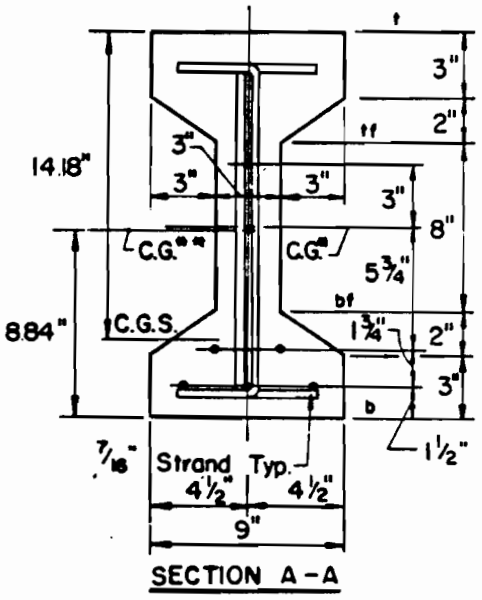

SECTION A-A

SECTION PROPERTIES		
PROPERTY	CONCRETE SECTION	TRANSFORMED SECTION
A	102.0 $in.^2$	105.3 $in.^2$
I	3854 $in.^4$	3986 $in.^4$
Z^t	428.2 $in.^3$	435.2 $in.^3$
Z^b	428.2 $in.^3$	450.9 $in.^3$
Q^{tf}	262.5 $in.^3$	270.9 $in.^3$
Q^{cg}	286.5 $in.^3$	298.5 $in.^3$
Q^{bf}	262.5 $in.^3$	276.3 $in.^3$

MATERIAL PROPERTIES		
PROPERTY	E 10	E 11
f_y,BAR	56 ksi	56 ksi
f_{pu},STRAND	252 ksi	252 ksi
f'_c, TEST	7360 psi	7790 psi

* Concrete Section
** Transformed Section

Fig. 2.1 Cross section, material and section properties, and loading arrangement for beams tested by Hanson and Hulsbos (from Ref. 10)

Table 2.1 Loading History for Beams Tested by Hanson and Hulsbos (from Ref. 10)

Beam	Loading Cycle, N	V_{min} (kips)	V_{max} (kips)	Remarks
E.10	1	0	32	Initial static test: V_c^f = 24 kips; V_c^{dt} = 30 kips, both ends.
	2-6	0,8	18	Static tests.
	7-3,200,000	8	18	Repeated load test at 250 cycles/min.
	3,200,001-4,000,000	8	18	Repeated load test at 500 cycles/min.
	4,000,001-4,526,900	8	28	Repeated load test at 250 cycles/min; fatigue failure in one wire of bottom strand at N = 4,526,900.
E.11	1	0	32	Initial static test: V_c^f = 24 kips; V_c^{dt} = 30 kips, end 2, 28 kips, end 20.
	2-5	0,8	24	Static tests.
	6-2,007,500	8	24	Repeated load test at 250 cycles/min; fatigue failure in stirrup, end 2, at N = 2,007,500.

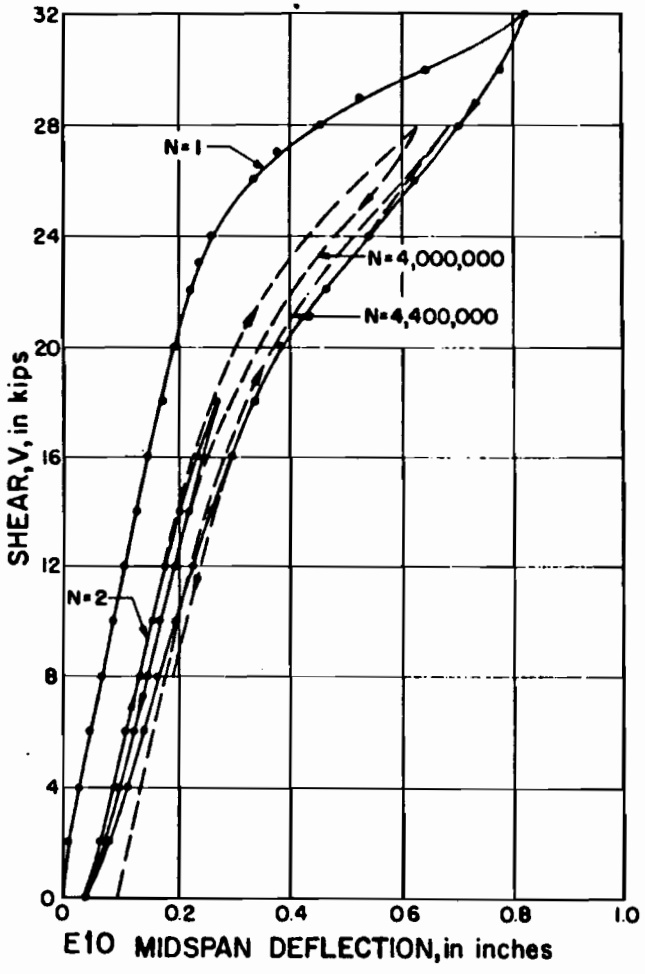

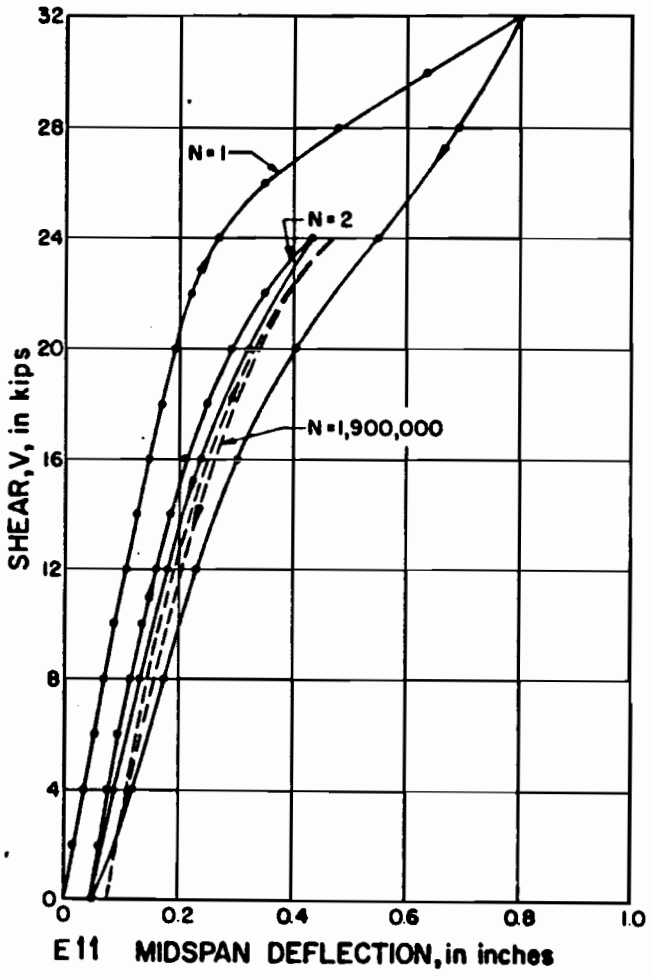

Fig. 2.2 Load-deflection response for beams tested by Hanson and Hulsbos (from Ref. 10)

noted that diagonal-crack width increased greatly before the beam finally failed in shear (Fig. 2.3). The beam failed at 2,008,000 cycles at a fatigue load of 59% of the ultimate static flexural capacity. Figure 2.4 is a photograph of the final fatigue failure. Hanson and Hulsbos described the behavior of Beam E11 as it approached failure:

> The first visual evidence of structural damage was the noticeable increase in width of the diagonal crack, at approximately N = 1,500,000 cycles. Subsequently, noticeable extension of the diagonal crack occurred, particularly in the region of the tension flange. The last static test was conducted at N equal to 1,970,000 cycles, at which time failure appeared imminent. However, the test beam was able to sustain an additional 77,500 load cycles. During this period, the diagonal crack continued to grow in width, until at failure the width was estimated at greater than 3/16 inch, wide enough to see completely through the web of the beam. The width of the crack appeared to increase at a nonuniform rate to be associated with extensions of the diagonal cracking. Final failure occurred suddenly when the diagonal tension crack extended through the compression flange. After the failure, it was observed that the third stirrup from the support was fractured.

Similar behavior was observed in recent tests conducted at the University of Texas (UT) which will be discussed in Sec. 5.1. Hanson and Hulsbos concluded that:

> A prestressed beam subjected to an overload of sufficient magnitude to develop diagonal tension inclined cracking may be more critical in fatigue of the web reinforcement than in fatigue of the longitudinal prestressing strand.

They went on to suggest a method for determining if fatigue failure is probable:

> A criterion for determining if a member is critical in fatigue after inclined cracking is the linearity of the load-deflection curve. That is, if the repeated loadings are within the range which permits the deflection of the member to remain essentially linear, the probability of a

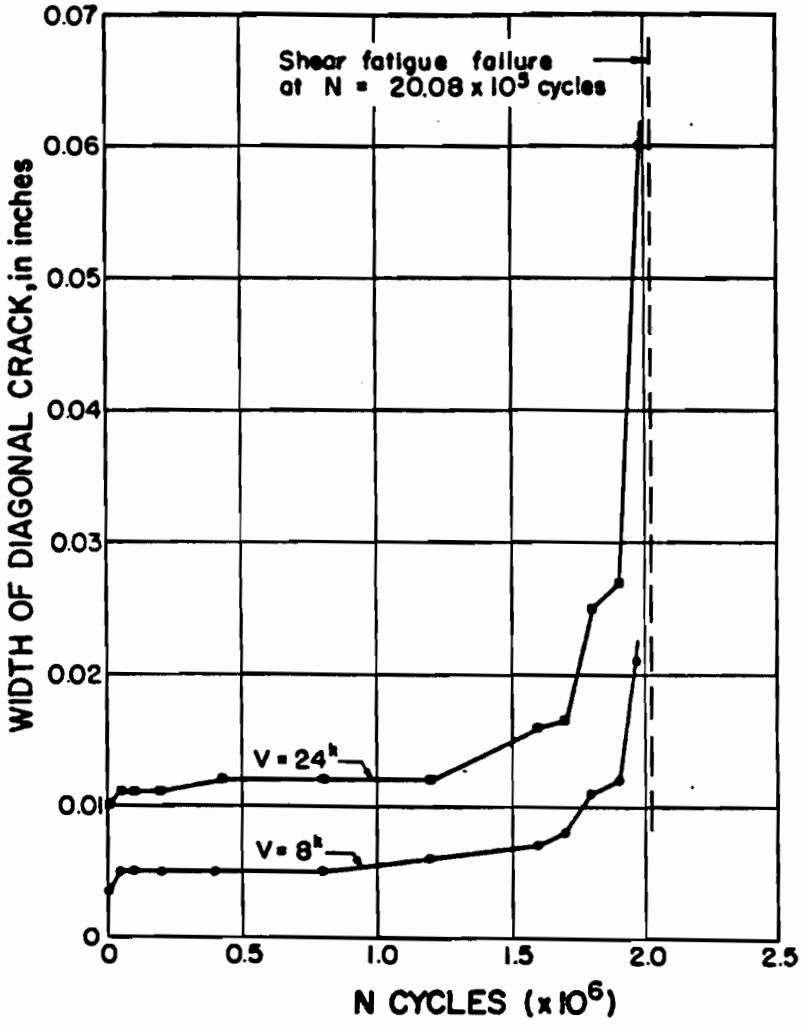

Fig. 2.3 Variation in width of diagonal crack with progressive load cycles applied on Beam E11 (from Ref. 10)

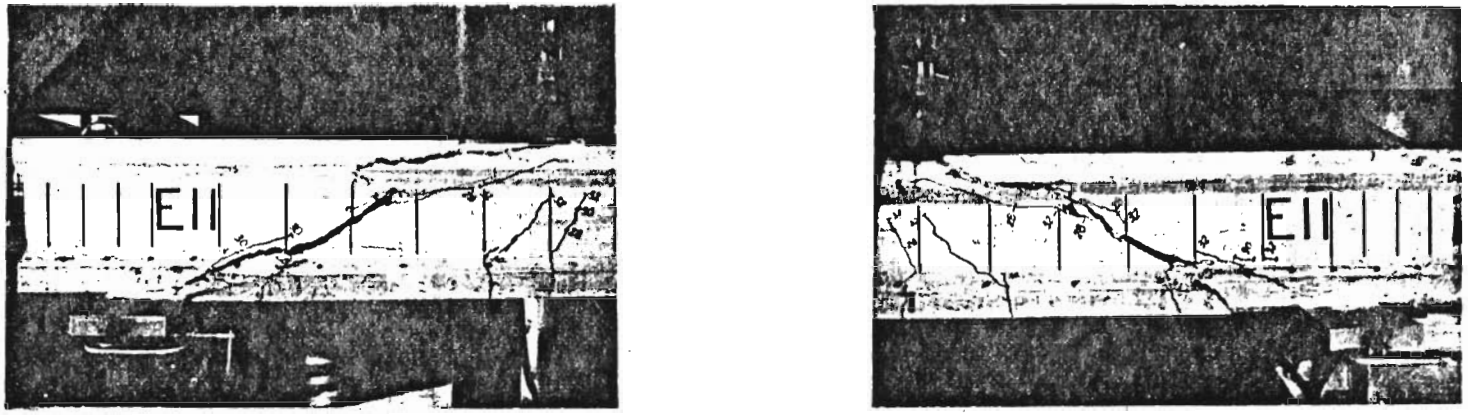

Fig. 2.4 Shear fatigue failure region in Beam E11 (from Ref. 10)

> fatigue failure within the normal life of the member is small.

In the late 1960's Hanson, Hulsbos and Van Horn conducted further research [12] to obtain test information on the fatigue life of prestressed I-beams that had been overloaded to cause flexural and inclined cracking prior to repeated loading. The results of the tests on Beams E10 and E11 had shown that a shear fatigue failure could occur. They tested six beams, denoted H40 through H90, with the same cross section and similar instrumentation as Beams E10 and E11. The only significant difference in materials was that No. 2 reinforcing bars were used for stirrups instead of No. 3 reinforcing bars used in Beams E10 and E11. A similar two-point loading arrangement was used except that the shear span-to-depth ratio was varied from 2.8 to 6.4. The web reinforcement was varied to provide just enough reinforcement to develop the static flexural capacity according to AASHTO provisions. The beams were loaded to approximately 80% of the ultimate static flexural capacity to cause inclined cracking during the first load cycle. They were then subjected to two million cycles of "design" fatigue loading with the upper load producing between $5\sqrt{f'_c}$ and $6\sqrt{f'_c}$ bottom fiber tension at midspan. Then they were subjected to fatigue loading at "above design" loads of $8\sqrt{f'_c}$ to $10\sqrt{f'_c}$ bottom fiber tension at midspan. This caused a fatigue failure in all specimens at the number of cycled listed in Table 2.2. Four of the beams failed as a result of fatigue fractures of prestressing strand at fewer cycles than expected without any indication of shear fatigue damage. The researchers had no explanation for the reduced flexural fatigue life. Beam H70 failed in flexural fatigue after most of the stirrups in both shear spans had failed. Beam H80 failed in shear fatigue without any evidence of flexural fatigue damage. The failure is shown in Fig. 2.5. It is unusual that this specimen had the second highest shear span-to-depth ratio and therefore the second lowest maximum applied shear. In discussing shear fatigue strength, the researchers recognized the difficulty in evaluating the stresses in the shear span:

> It is not possible to evaluate directly the shear fatigue strength of the test specimens, because the stress in the stirrups cannot be calculated theoretically, nor can it be determined from the measured inclined crack widths or vertical deformation.

From measurement of the inclined cracks, the researchers determined that the stirrups were subjected to transverse

Table 2.2 Cycles of Loading Causing Damage and Failure of Beams Tested by Hanson, Hulsbos, and Van Horn (from Ref. 12)

Beam	ρ/ρ_d	NUMBER OF CYCLES OF ABOVE-DESIGN LOADING		
		First Indication of Damage		End of test
(1)		Flexural fatigue (2)	Shear fatigue (3)	(4)
H-40	2.82	304,000	None	458,000
H-50	3.53	455,000	None	570,000
H-60	4.23	714,000	None	906,000
H-70	4.94	576,000	267,000	691,000
H-80	5.66	None	274,000	401,000
H-90	6.35	1,082,000	None	1,201,000

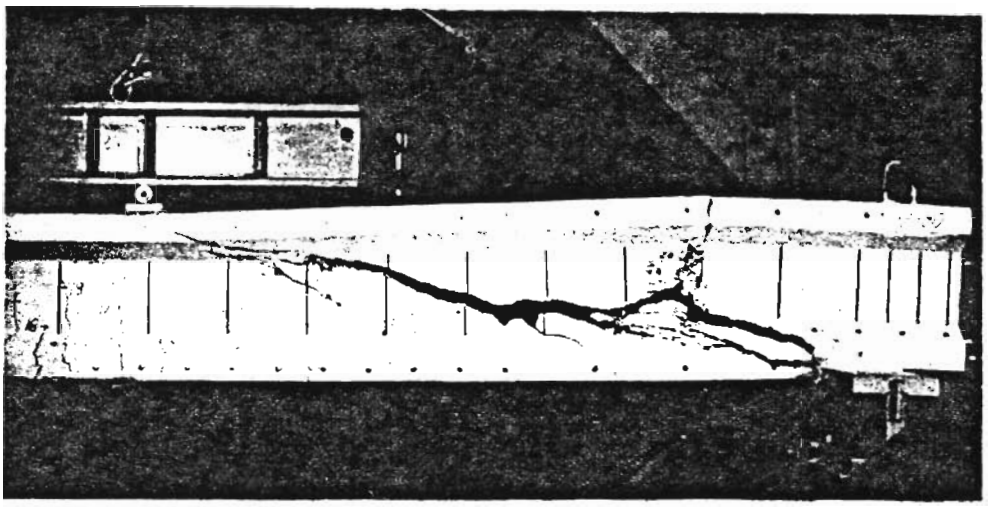

Fig. 2.5 Failure region in Beam H-80 tested by Hanson, Hulsbos, and Van Horn (from Ref. 12)

deformations and this had a large influence on the stirrup fatigue life. They also noted that the beams that experienced stirrup fractures (H70 and H80) had the largest inclined crack openings as shown in Fig. 2.6. In conclusion, the researchers said the following about shear fatigue of prestressed concrete beams:

> The tests demonstrated that prestressed concrete beams have a remarkable shear fatigue resistance. Prestressed beams, with enough web reinforcement to develop their flexural capacity, can be subjected to overloads which cause extensive cracking without subsequent danger of a shear fatigue failure under design loads. Furthermore, shear fatigue failures do not occur suddenly, but rather give considerable warning as indicated by increasing deflection and increasing inclined crack width before failure occurs. In the tests reported herein, and in previously reported tests, shear fatigue failures did not occur when the range in inclined crack width was less than 0.006 inch under application of repeated load.

Price and Edwards conducted research on shear fatigue of post-tensioned concrete beams that concluded in 1970 [26]. They set out to determine the effect of fatigue on the diagonal cracking strength and to determine stress range versus number of cycles to first stirrup fracture. They tested 17 post-tensioned, thin-webbed I-beams with the cross section and loading arrangement shown in Fig. 2.7. The beams were instrumented to obtain load-deflection, concrete strain, stirrup strain, and diagonal crack width data. The only variables considered in the tests were maximum fatigue load. Minimum load was kept constant at 25% of V_u. Four strength tests were performed to obtain the static strength in shear. The remaining beams were tested under fatigue loading. If failure had not occurred by three million cycles, the beams were loaded statically to failure. Two of the fatigue specimens, S10 and S11, were tested at a load below the diagonal cracking load to determine the fatigue strength of concrete in diagonal tension. The remaining fatigue specimens were loaded to produce inclined cracking during the first cycle. A summary of the results of the fatigue specimens is listed in Table 2.3.

Price and Edwards observed that the onset of diagonal cracking caused a major redistribution of stresses in the shear span. They estimated that when diagonal cracks formed, approximately one-half of the total applied shear was carried by

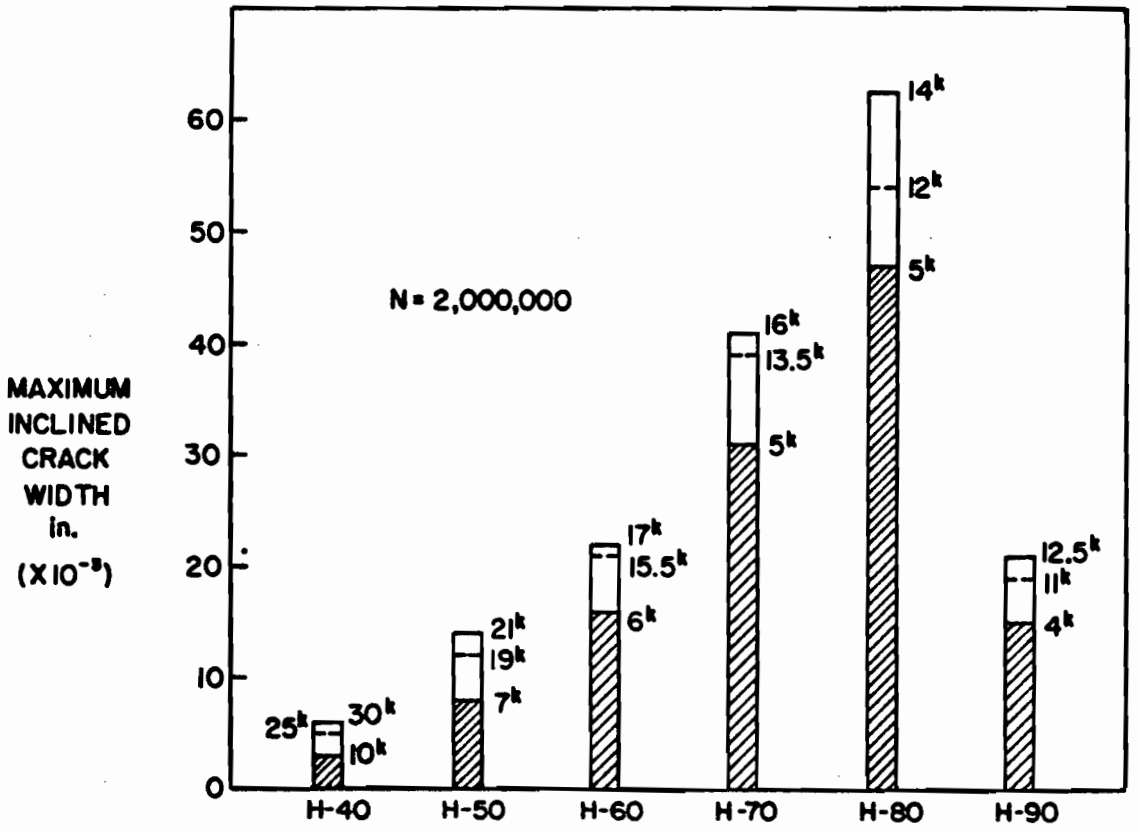

Fig. 2.6 Maximum crack width at start of above-design loading for beams tested by Hanson, Hulsbos and Van Horn (from Ref. 12)

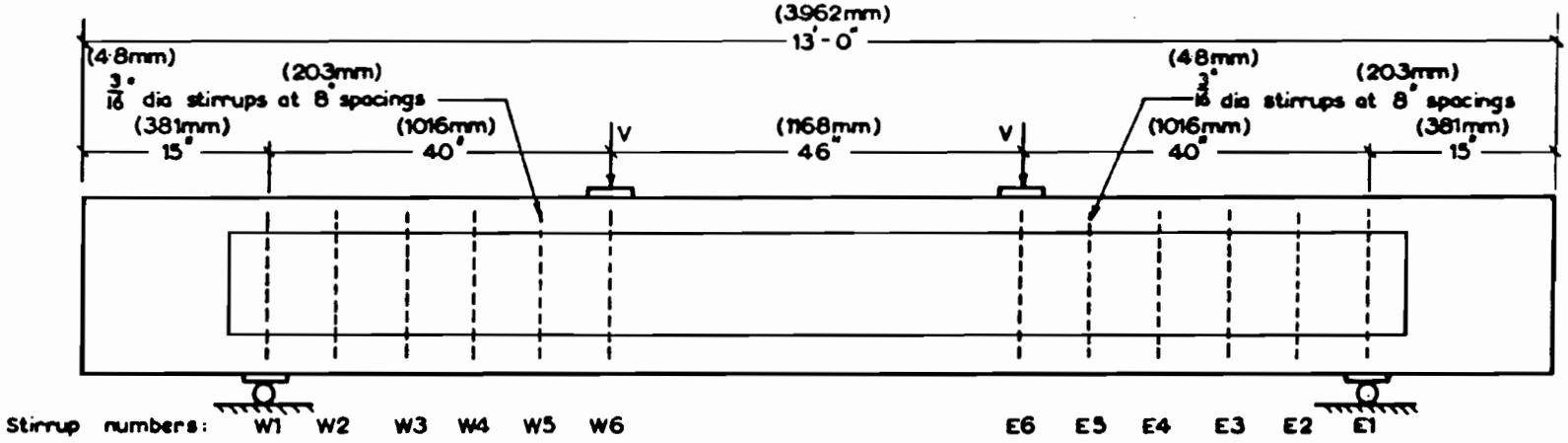

GENERAL ELEVATION

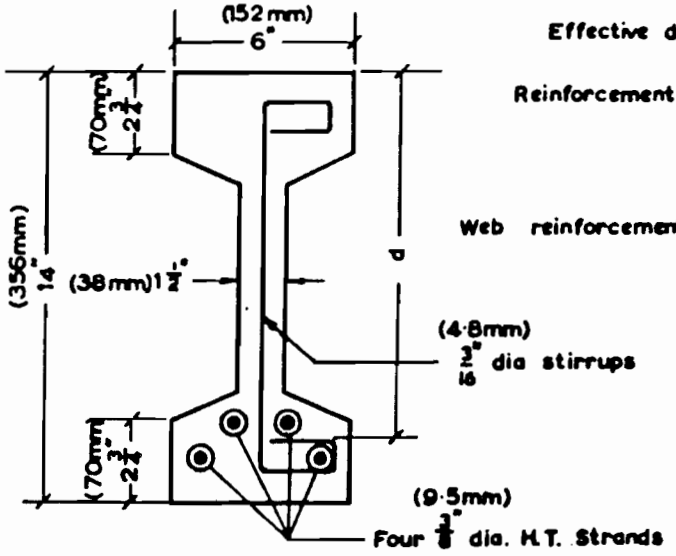

SECTION

Material Properties

$\overline{f'_c}$ = 7975 psi

f_y = 65 ksi

Effective depth, d = 11 7/8" (302mm)

Reinforcement ratio, p = 0·76%

$\frac{a}{d}$ = 3·40

Web reinforcement ratio, r = 0·23%

$\frac{r.f_{smy}}{100}$ = 145

Fig. 2.7 Cross section, material properties, and loading arrangement for beams tested by Price and Edwards (from Ref. 26)

Table 2.3 Results of Shear Fatigue Tests on Beams Tested by Price and Edwards (from Ref. 26)

Beam No.	Maximum load level $\frac{V_{max}}{V_u}$, percent	Number of cycles to first stirrup fracture N_1		Number of cycles to complete beam collapse N_f	Shear span in which complete collapse occurred	Number of stirrup fractures at collapse
		Shear span W	Shear span E			
S3	63	1,007,000	—	2,700,000	W	4
S10	63 (56)	3,871,000†	3,871,000†	3,871,000*(1,696,000)	—	—
S12	63	808,500	2,815,000	4,962,000*	—	—
S13	63	3,932,000†	3,932,000†	3,932,000*	—	—
S4	70	—	463,000	828,000	E	4
S6	70	304,000	285,000	350,000	E	4
S9	70	240,000	631,000	734,000	W	4
S15	70	320,200	503,400	1,010,000	W	4
S2	77	—	159,000	226,000	E	2
S7	77	83,000	130,000	137,000	E	2
S14	77	34,000	—	48,600	W	2
S16	77	79,300	56,100	82,000	E	2
S11	77 a	—	—	2,800	W	—

*Tests stopped before collapse.
†Tests stopped before stirrup fracture.

$\frac{V_{min}}{V_u}$ = 25 percent

V_u = 16,020 lb (7268 kgf)

( ) = Load level and number of cycles to diagonal tension cracking

a - Beam loaded to 55% of V_u for 3,088,000 cycles to attempt to induce inclined cracking in fatigue. Inclined cracking induced by static overload at this time

the stirrups. In their tests, stirrup strains did not increase appreciably with additional load cycles (Fig. 2.8). However, the diagonal crack widths did increase with additional cycles (Fig. 2.9). This discrepancy was attributed to bond breakdown between the stirrups and surrounding concrete. The researchers noted that the failure in fatigue was similar to the failure under static loading as shown in Fig. 2.10. They also noted, as did Hanson and Hulsbos, that beams could sustain many additional cycles of fatigue loading after the first stirrup fracture and that as the number of cycles to first stirrup fracture increased, so did the number of cycles to final failure. This is shown graphically in Fig. 2.11. Figure 2.12 shows the maximum fatigue load versus number of cycles to first stirrup fracture which was developed from their series of tests. The outer curves indicate the 5% confidence limit for probability of failure. This data may indicate a trend of behavior for the generalized case of shear fatigue. However, the applicability of their curves is restricted because of the limited test variables examined in their study.

In summary it may be said that previous research on shear fatigue of prestressed concrete beams has led to many interesting observations. However, not much has been determined in the form of useful analytical models to predict fatigue response for general conditions.

2.3 Shear Fatigue of Reinforced Concrete Beams

One of the earliest studies in shear fatigue of reinforced concrete beams was conducted by Chang and Kesler [7] in the 1950's. Their purpose was to develop simple and sufficient expressions for the static strength of beams failing in shear, and to determine the strength of reinforced concrete beams unreinforced for shear subjected to repeated loading. The remainder of this discussion will pertain to their research on fatigue loading.

Chang and Kesler tested 39 specimens that had a 4 x 6 in. cross section with no web reinforcement. The specimens were 60 in. long, simply supported, and loaded at the one-third points with equal loads. The shear span-to-depth ratio for all specimens was 3.53. They considered concrete strength, percentage of longitudinal reinforcement, and maximum applied shear as their primary variables. The tests were continued to failure or ten million cycles at which time a static strength test was performed. Information related to initial diagonal

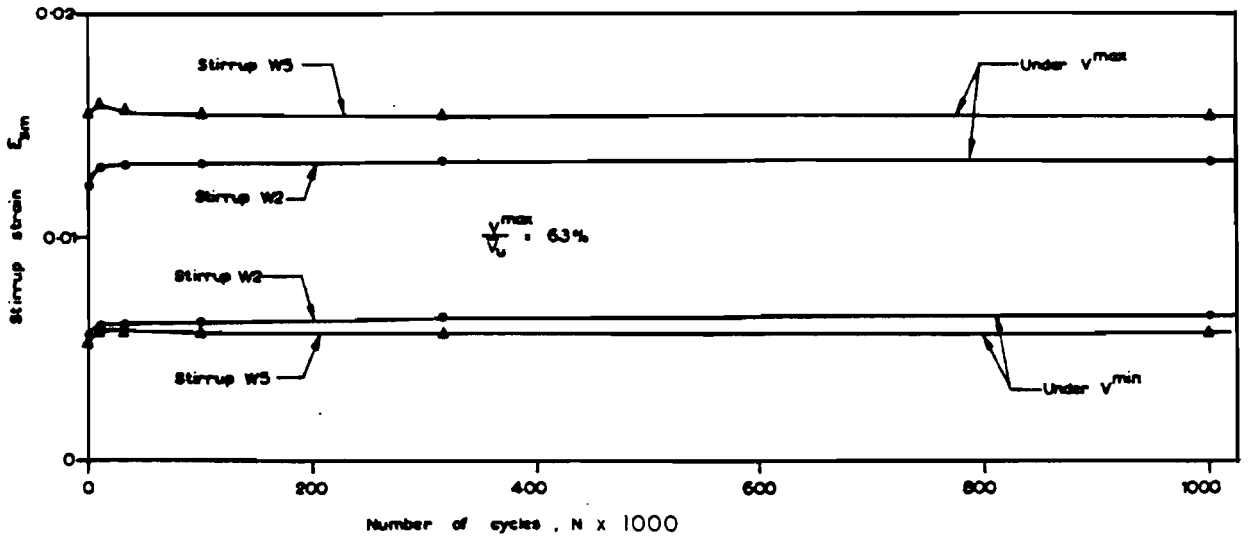

Fig. 2.8 Stirrup strain versus number of cycles for Beam S3 (from Ref. 26)

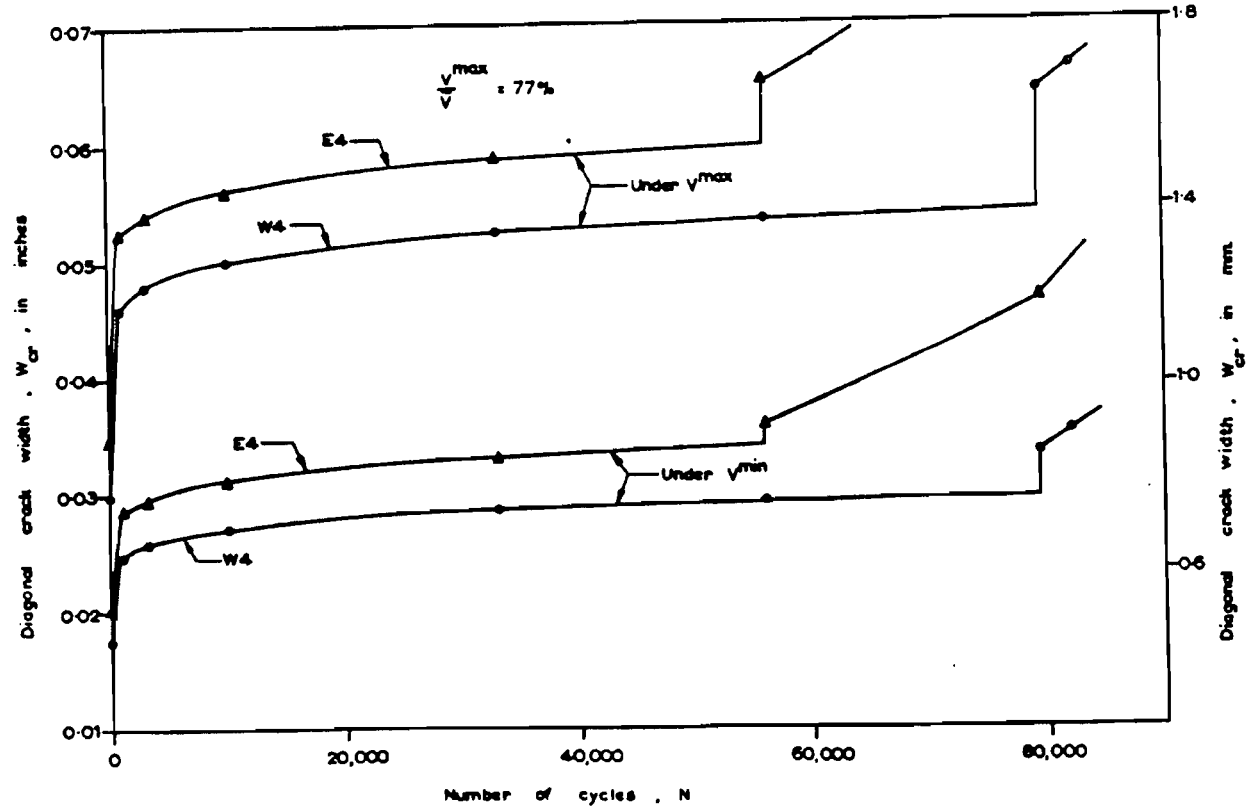

Fig. 2.9 Diagonal crack width versus number of cycles for Beam S16 (from Ref. 26)

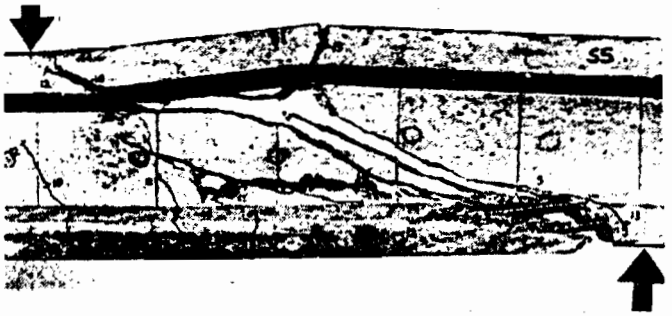

Fig. 2.10 Typical ultimate failure under static or fatigue conditions for tests by Price and Edwards (from Ref. 26)

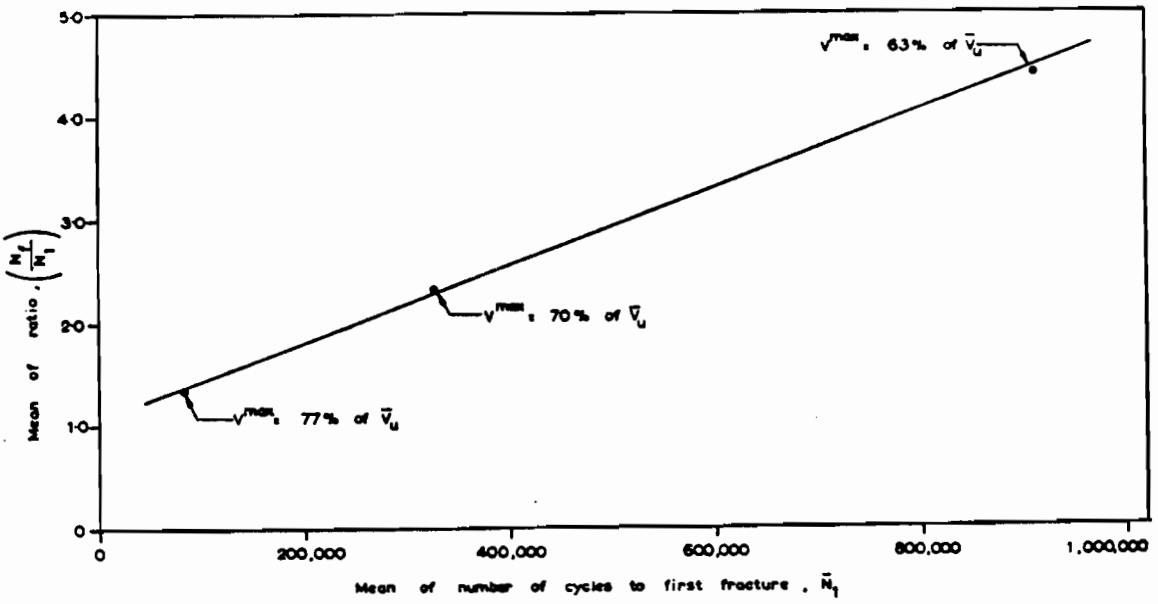

Fig. 2.11 Ratio of number of cycles to final failure (N_f) to number of cycles to first stirrup fracture (N_1) versus mean number of cycles to first stirrup fracture ($\bar{N}_1$) for tests by Price and Edwards (from Ref. 26)

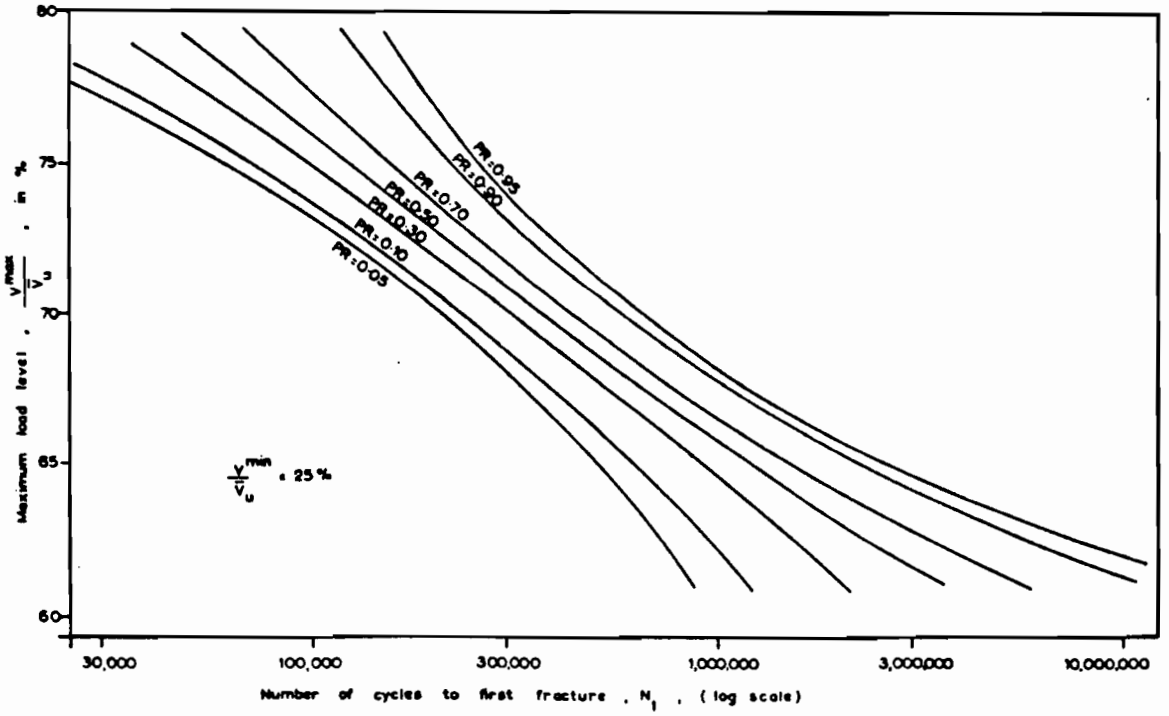

Fig. 2. rcent of ultimate load level versus number of cycles to first stirrup fracture for tests by Price and Edwards (from Ref. 26)

cracking and final failure of the beams, if they did not fail when diagonal cracking occurred, was obtained. Chang and Kesler observed three types of fatigue failure:

1. Fatigue of longitudinal reinforcement in the constant moment region with inclined cracking present (Fig. 2.13b).

2. Diagonal cracking (Fig. 2.13c).

3. Shear compression (Fig. 2.13d).

Important conclusions reached in the study included:

1. The fatigue strength of the type of specimens tested was influenced by the percentage of steel and concrete strength, to the same extent as static strength.

2. For fatigue loading up to 100,000 cycles, the cracking load was reduced at a more rapid rate than the ultimate failure load.

3. If a beam did not crack diagonally under fatigue loading, neither the diagonal tension cracking load, nor the ultimate moment capacity were affected. If a beam was cracked diagonally under fatigue loading but did not fail, the static load capacity was not affected.

In another study by Chang and Kesler [8], they tested 25 more specimens of identical cross section and loading arrangement. This time they lowered the amount of longitudinal tensile reinforcement in order to study the complicated fatigue behavior of a reinforced concrete beam that would fail in flexure at a static load only slightly less than that which would produce a shear failure. They had three control specimens to determine the ultimate static load and to verify that flexural behavior would dominate during static load tests. The fatigue specimens exhibited the same three types of failure as the previous study except that in addition, fatigue of the longitudinal reinforcement in the constant moment region with no inclined cracks was possible (Fig. 2.13a). In general, low amplitude repeated loads resulted in a flexural fatigue failure, while high amplitude repeated loads resulted in a shear fatigue failure. Chang and Kesler were probably the first researchers to demonstrate that a reinforced concrete beam, which would fail in flexure when loaded monotonically, could fail in shear when subjected to fatigue loads. This was an extremely important

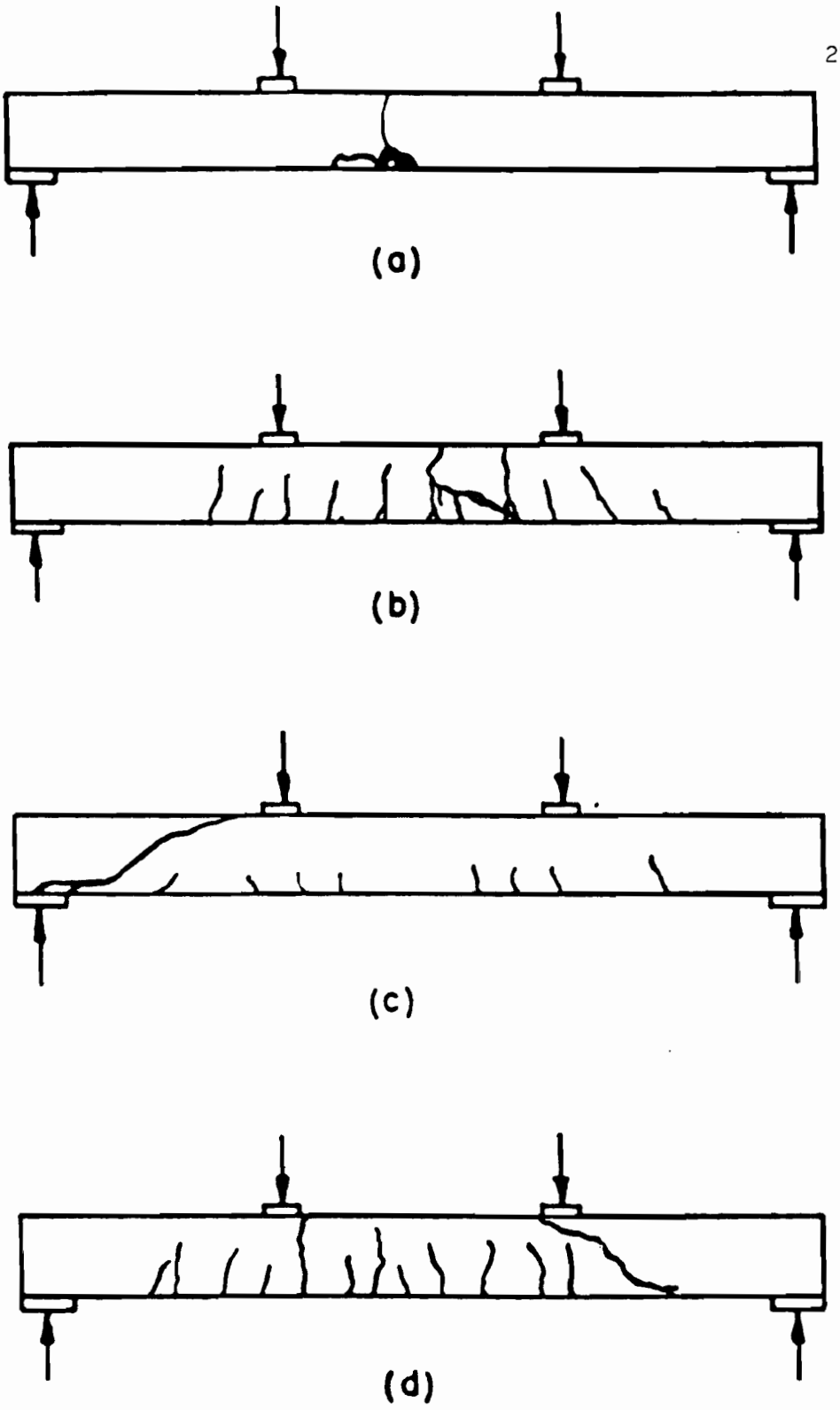

Fig. 2.13 Various fatigue failures encountered by Chang and Kesler (from Ref. 8)

discovery because it implied that fatigue loading could change the limit state for design.

Ruhnau conducted a fatigue study of reinforced concrete beams in West Germany in the early 1970's [30]. His purpose was to determine stresses in the web reinforcement as they pertained to:

1. Design criteria for web reinforcement.
2. Inclined crack width control.
3. Fatigue strength of web reinforcement.

He tested five beams with the primary variable being web thickness. Some important conclusions were:

1. After inclined cracking, use of the ACI-AASHTO concept of maximum shear being composed of a concrete contribution and a reinforcement contribution was not valid. During additional load cycles, the stirrups were subjected to stresses immediately upon loading; it was not necessary to first exceed the concrete contribution.
2. After diagonal cracking, stirrups had residual stresses upon unloading. More load repetitions led to an increase in maximum stirrup stresses.
3. Stirrup stress after diagonal cracking could be represented by the equation

$$f_v = k_1 + k_2 V_{max} s/j_d A_v$$

where, f_v = stirrup stress,

V_{max} = maximum applied shear force,

s = stirrup spacing,

j_d = internal lever arm,

A_v = area of web reinforcement in a distance "s",

k_1 = residual stress, and

k_2 = proportion of shear force carried by stirrups.

For comparison, the ACI-AASHTO equation would result in

$$f_v = (V_{max} - V_c)\, s/j_d A_v$$

where V_c = shear force carried by concrete.

The equations are compared graphically in Fig. 2.14. Ruhnau reported that constants were mainly dependent on the level of previous loading, but indicated research would be required to obtain their values for general conditions. In his tests, the value of k_1 ranged from 4 ksi to 18 ksi and the value of k_2 ranged from 0.45 to 0.60.

In recent years, much research has been conducted in Japan on shear fatigue of reinforced concrete beams. Most of this research has been under the supervision of Hajiimee Okamura. An analytical model was proposed to describe shear fatigue behavior and to predict stirrup strains at any number of loading cycles. The model is based on the ACI concept of a concrete contribution and a web reinforcement contribution to resist applied shear, with the following modifications.

1. The concrete contribution to shear strength is assumed to decrease logarithmically with additional load cycles.

2. The applied shear resisted by the web reinforcement is reduced at the supports and at points of concentrated load.

A detailed discussion of the equations developed by Okamura et al. and their applicability to this study is presented in Sec. 5.2.

In 1978 Higai [14] tested 130 rectangular and T-shaped reinforced concrete beam sections to determine their shear response when subjected to moving loads and fatigue loads. He studied the effect of shear span-to-depth ratio and its effect on the fatigue failure mechanism. It was observed for beams with no web reinforcement and a small a/d ratio that the beam would not fail immediately upon initiation of inclined cracks, while at some larger a/d ratio the same beam would fail immediately upon

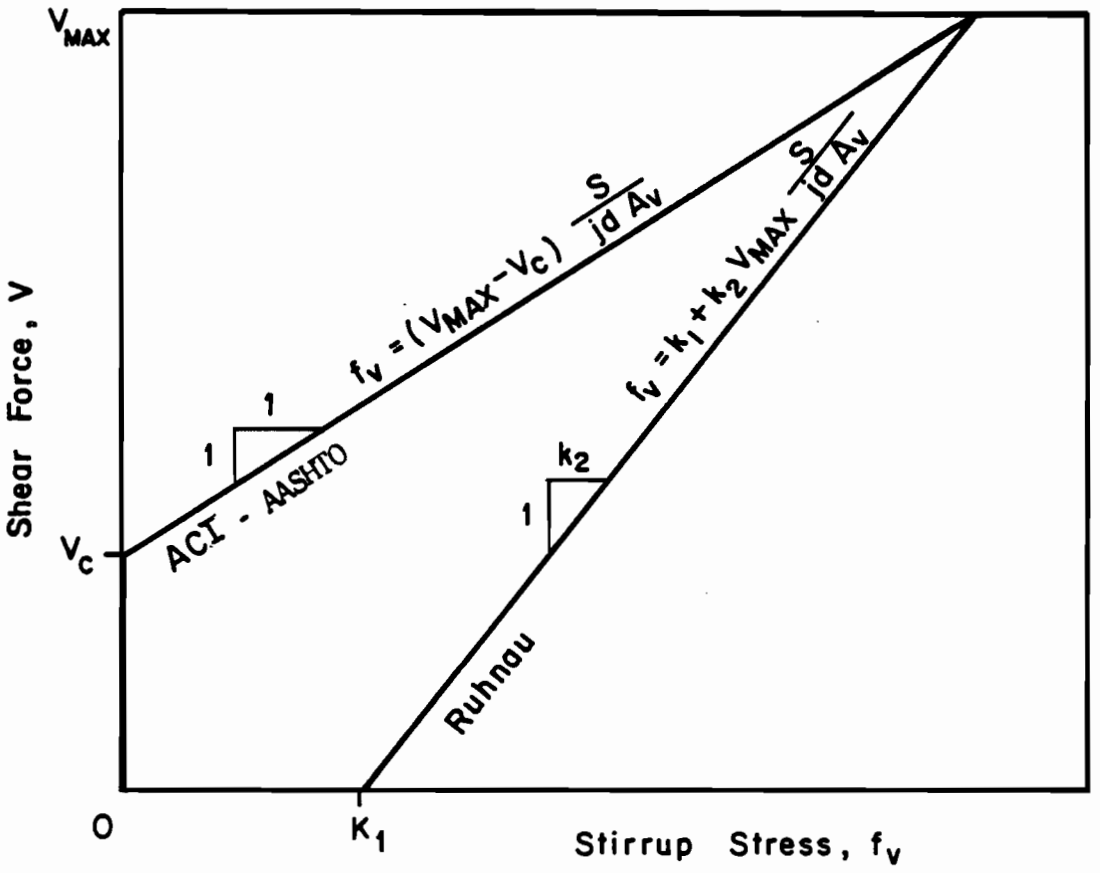

Fig. 2.14 Comparison of Ruhnau's equation for stirrup stress with ACI equation for stirrup stress

initiation of inclined cracking. He proposed that at low a/d ratios the arch-mechanism failure load, instead of diagonal cracking, controlled the behavior of the beam. As a result, the beam would not fail upon initiation of diagonal cracks. At high a/d ratios, the diagonal cracking load instead of the arch-mechanism failure load controlled failure. He proposed that under fatigue loading, the diagonal cracking load was reduced by a certain amount at a given number of cycles. Therefore, beam with an a/d ratio such that it would fail at initiation of a diagonal cracking under static load, would not fail but would develop arch action under fatigue load. This concept is shown graphically in Fig. 2.15. Higai also discussed the well-known phenomenon of increased shear strength near supports or concentrated loads. He proposed that for design purposes it would be better to consider a reduction in applied shear force near supports or concentrated loads. He suggested a form for a relationship to describe such a reduction.

In 1979 Okamura and Farghaly conducted a test on a reinforced concrete T-beam to further investigate the distribution of shear stresses in the cross section [19]. They proposed that the reduction in shear force near supports and concentrated loads should be applied only to the web reinforcement. They also modified the equation for the reduction, so that shear forces would be reduced to a distance 1.5d from supports and 1.0d from concentrated loads. A graphic illustration is shown in Fig. 5.3.

In 1981 Okamura, Farghaly, and Ueda conducted shear fatigue tests on 17 beams with web reinforcement [21], paying careful attention to stirrup strains. Some of their conclusions were:

1. Inclined cracks that had developed during the first cycle of loading continued to grow in width and length during fatigue loading; however, seldom did new cracks form during fatigue loading.

2. From stirrup strain readings it was determined that significant redistribution of stresses took place under fatigue loading before any stirrups fractured.

3. Forty-one of 42 broken stirrups fractured at the location of the bottom bend where the stirrups joined the longitudinal steel. The authors suggested the fatigue life of the stirrup at a bend was approximately one-half of the fatigue life of a straight section.

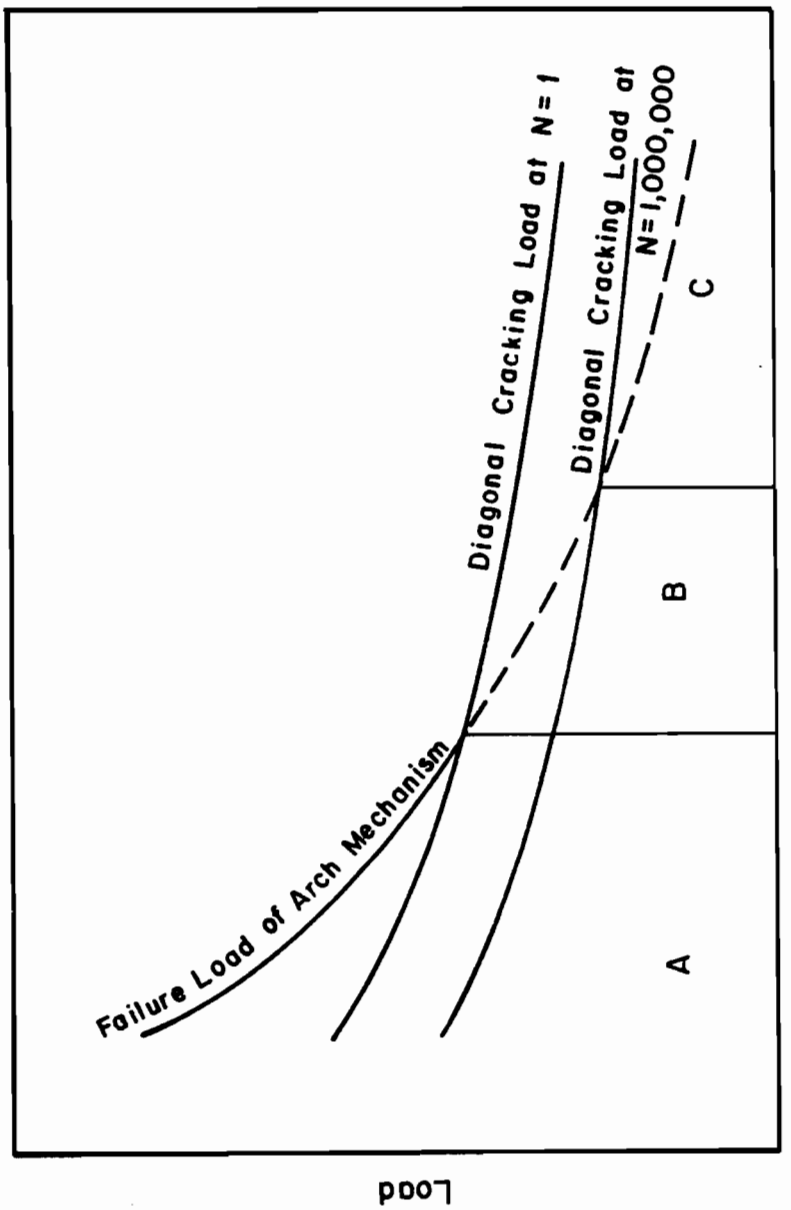

A - arch action regardless of number of cycles

B - arch action possible, depending on number of cycles

C - arch action not possible for less than 1,000,000 cycles; immediate failure upon diagonal cracking

Fig. 2.15 Failure mechanism in a reinforced concrete beam with no web reinforcement (from Ref. 14)

4. Fracturing of stirrups caused longitudinal tensile reinforcement to be subjected to greater dowelling action and caused longitudinal fatigue fractures in some specimens.

5. Stirrup stress and stress ranges increased with progressive number of load cycles. These increases were accompanied by increases in associated diagonal crack widths.

The authors developed an equation for the stirrup stresses which took into account the increase in stirrup stress and stress range with additional cycles. They did this by developing an equation to describe the concrete resistance which decreased with load cycles.

In 1983 Okamura and Ueda reported on additional shear fatigue tests [22]. They modified the previously developed equation for stirrup stress to include the influence of load range on concrete shear strength. They also modified the strain range equation to make it less conservative. A detailed discussion of their equations is presented in Sec. 5.2. The authors continued the development of their shear fatigue model in an attempt to apply it to general repeated loading such as that found in actual bridge structures.

The most recent research on shear fatigue of reinforced concrete beams was conducted in Switzerland in 1983 by Thurlimann and Frey [9]. They performed tests on six beams with web reinforcement and eleven beams without web reinforcement. The specimens were loaded at midspan and had a shear span-to-depth ratio of 7.4. The variables they considered were web thickness, web reinforcement and longitudinal reinforcement. Some of the conclusions reached in the investigation that have not been presented previously are:

1. Stirrups with small initial strains displayed larger increases in strain than those with larger initial strains. The capacity for redistribution was more pronounced in beams with a larger ratio of longitudinal to web reinforcement.

2. With the same web and longitudinal reinforcement, a larger web thickness led to smaller stirrup strains and smaller increases in strains during cycling.

3. Variations of strain in longitudinal reinforcement and in the compression flange indicated a truss mechanism was developed to resist shear after cracking.

4. The fatigue resistance of the stirrups in concrete corresponded with that for fatigue resistance in air.

5. Although the upper and lower load levels remained constant, the reinforcement was subjected to a multi-step test due to the increase in strain with cycling.

Although the results of shear fatigue of reinforced concrete do not apply directly to shear fatigue of prestressed concrete, much of the behavior is similar.

2.4 Fatigue of Standard Deformed Reinforcing Bars

A series of axial tension fatigue tests on No. 3 standard deformed reinforcing bars was conducted as a companion investigation to this study [18]. Through these tests comparisons could be made between the fatigue behavior of bars in air and bars of the same mill heat embedded in prestressed concrete beams. Statistical analysis was employed to interpret the fatigue test data and to develop S-N relationships. The application of fracture mechanics to the fatigue behavior of deformed reinforcing bars was also explored. The study was conducted in two phases.

In Phase I, 30 reinforcing bars were tested using nine different stress ranges. The minimum stress for all tests was 6 ksi. The frequency of loading for all specimens was 10 Hz. Results of the Phase I study are listed in Table 2.4. Photographs of a typical fractured section are shown in Fig. 2.16. A statistical analysis was performed on the data and the following S-N equation was proposed:

$$\log N = 14.80 - 5.65 \log SR$$

where N = number of cycles to failure

SR = stress range (greater than 32 ksi)

R = -0.89 (correlation coefficient)

S_e = 0.184 (standard error of estimate)

Table 2.4 Summary of Results of Phase I In-Air Fatigue Tests on Deformed No. 3 Reinforcing Bars (from Ref. 18)

Specimen Desig.	Test Seq.	Stress Range S_r (ksi)	Min. Stress S_{min} (ksi)	Fatigue Life N	Frac. Section Position l*	Location of crack Initiation
30-6-1	2	30.0	6.0	4,060,500	0.01	lug base
30-6-2	27	30.0	6.0	5,000,000+**	——	——
30-6-3	29	30.0	6.0	2,362,000	-0-	lug base
30-6-4	30	30.0	6.0	5,000,000+	——	——
33-6-1	18	33.0	6.0	5,000,000+	——	——
36-6-1	1	36.0	6.0	5,000,000+	——	——
36-6-2	17	36.0	6.0	1,369,530	0.26	lug base
39-6-1	4	39.0	6.0	675,890	0.39	lug base
39-6-2	8	39.0	6.0	613,980	0.26	lug base
39-6-3	15	39.0	6.0	1,225,400	0.12	lug base
39-6-4	20	39.0	6.0	659,000	0.15	lug base
39-6-5	26	39.0	6.0	296,250	-0-	lug base
40-6-1	6	40.0	6.0	1,802,070	0.14	lug base
40-6-2	9	40.0	6.0	607,990	0.25	lug base
42-6-1	3	42.0	6.0	238,120	0.11	lug base
42-6-2	7	42.0	6.0	298,340	0.20	lug base
42-6-3	13	42.0	6.0	376,500	-0-	lug base
42-6-4	16	42.0	6.0	439,120	0.16	lug base
42-6-5	23	42.0	6.0	284,970	0.26	lug base
45-6-1	5	45.0	6.0	609,280	0.01	lug base
45-6-2	10	45.0	6.0	142,090	0.01	lug base
45-6-3	12	45.0	6.0	423,550	0.42	lug base
45-6-4	21	45.0	6.0	369,330	-0-	lug base
45-6-5	24	45.0	6.0	99,670	0.07	lug base***
48-6-1	11	48.0	6.0	224,880	0.09	lug base
48-6-2	14	48.0	6.0	344,520	-0-	lug base
48-6-3	19	48.0	6.0	226,080	-0-	lug base
48-6-4	22	48.0	6.0	121,810	-0-	lug base
48-6-5	25	48.0	6.0	138,000	-0-	lug base
54-6-1	28	54.0	6.0	131,600	0.20	lug base

* 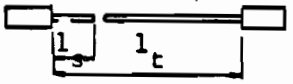 $l = l_s/l_t$

** Did not fail until 5,000,000 cycles

*** Defect was observed in fracture section

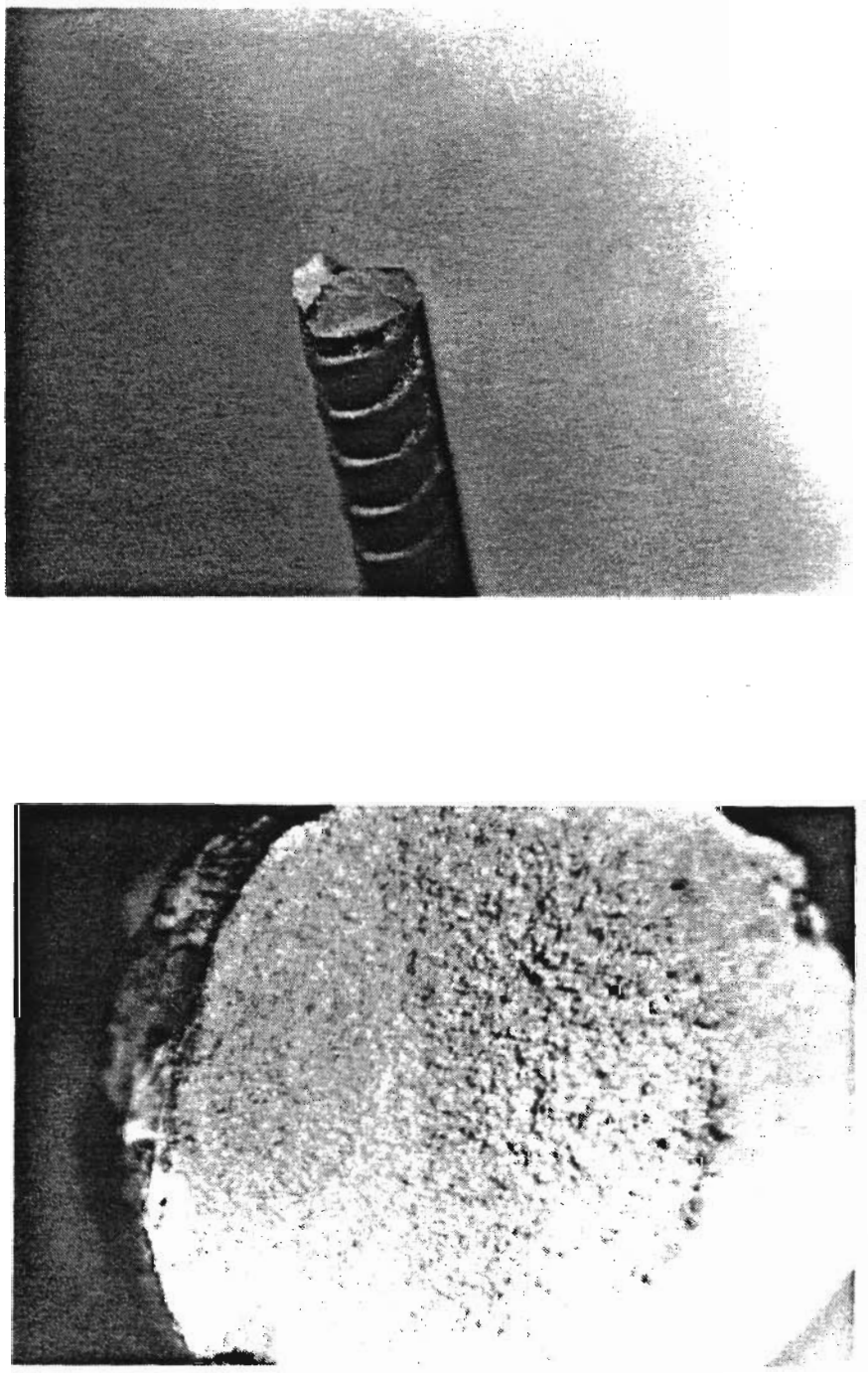

Fig. 2.16 Fatigue fracture and magnified view of fracture (from Ref. 18)

Specimens which sustained greater than five million cycles were considered run-out data and were excluded from the analysis. The equation and data points are shown in Fig. 2.17.

In Phase II, eight specimens were tested to investigate the effect of pre-strain on fatigue life. Previous studies showed that the fatigue strength for bent bars was less than for straight bars. A possible reason for this was the prestrain induced by cold bending. Table 2.5 is a summary of the results of the Phase II study. In general, a trend in reduction of fatigue life with increase of prestrain was observed. However, the fatigue lives of all the prestrained specimens fell within the 95% confidence interval obtained in the Phase I study.

Conclusions reached by Matsumoto were:

1. A reasonable fatigue limit for the reinforcing bars tested was 32 ksi, which corresponded with a two million cycle fatigue life.

2. The square root of the lug-base radius seemed to be an appropriate variable for controlling fatigue life of reinforcing bars based on a fracture mechanics approach.

3. Reinforcing bars subjected to an increasing stress range exhibited different fatigue behavior than reinforcing bars subjected to a constant stress range.

4. Tensile pre-strain of less than 5% did not significantly affect the fatigue strength of reinforcing bars.

Many other tests have been conducted on fatigue of standard deformed reinforcing bars. There is wide agreement that the primary variables affecting fatigue behavior are stress range and bar deformation geometry. Other factors affecting fatigue behavior are minimum stress level, bar size, yield and tensile strength of bars, bending of bars, and welding of bars. Some of the previous tests conducted on deformed reinforcing bars are summarized in the following paragraph.

Rehm [29] concluded that stress range has the most influence on the fatigue life and proposed a permissible stress range of 28 ksi. He also observed that bent bars had approximately a 50% lower stress limit than straight bars. Pfister and Hognestad [25] concluded that bar yield strength, test beam cross section, and magnitude of minimum stress had only a minor influence on the stress range at the fatigue limit;

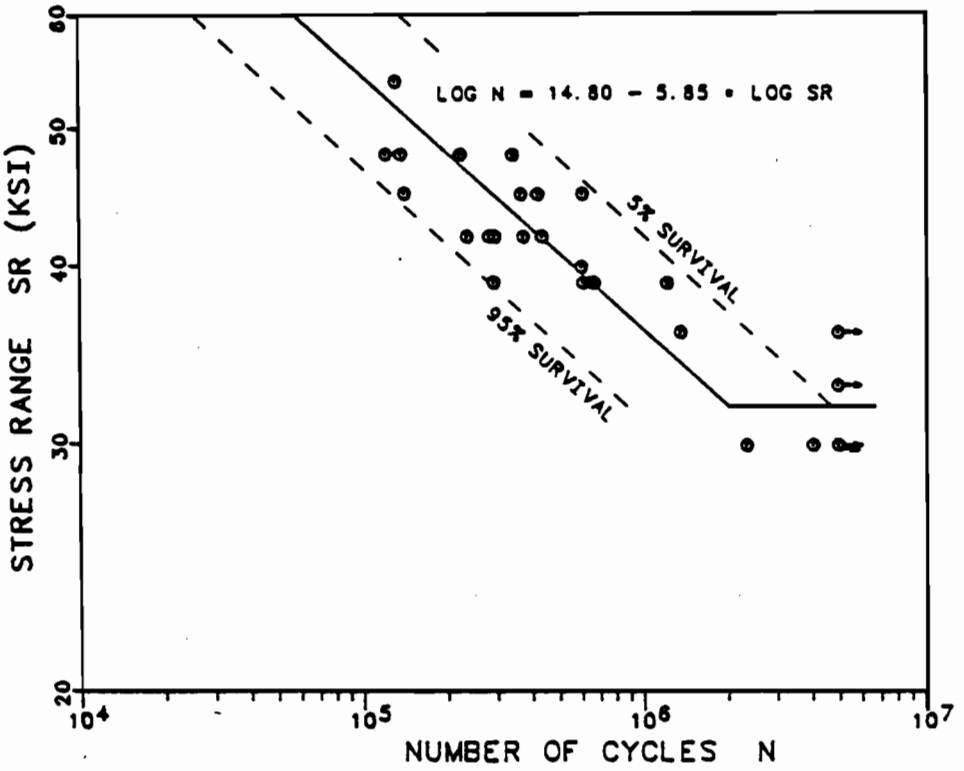

Fig. 2.17 S-N line for Phase I fatigue test data (from Ref. 18)

Table 2.5 Fatigue Test Results of Phase II Study (from Ref. 18)

Lot	No.	Pre-Strain (% elong.)	Yield Stress S_y (ksi)	Maximum Stress S_{max} (ksi)	Fatigue Life N
1	1	-0-	----	----	194,400
	4	3.8	67.9	87.3	116,880
	3	6.2	67.9	96.0	78,830
	2	11.3	68.4	100.9	136,300
2	3	-0-	----	----	371,900
	4	0.2	72.5	72.5	367,650
	2	1.6	73.6	76.1	322,800
	1	3.0	70.7	88.9	199,360

however, bar deformations had considerable influence. Hanson, Burton, and Hognestad [11] investigated the effect of the bar deformation pattern and concluded that the radii at the base of lugs had a significant influence on fatigue strength. Jhamb and MacGregor [16,17] reported that the fatigue strength of bars tested in air was lower than for bars embedded in beams. Helgason, Hanson et al. [13] investigated the effect of bar size and deformation pattern. They developed an equation for the fatigue limit which was adopted by AASHTO and recommended by ACI Committee 215. The variables in the equation are minimum stress level and ratio of the radius at the base of a bar deformation to the height of the deformation. This equation is discussed further in Sec. 5.5.3.

Based on the research conducted up to the present, the following may be said about the fatigue behavior of standard deformed reinforcing bars:

1. Fatigue life is primarily controlled by applied stress range.

2. Fatigue resistance is dependent upon geometry of the bar surface.

3. The relationship between fatigue properties from air tests and fatigue results from beam tests is not well defined.

CHAPTER 3

TEST PROGRAM

3.1 Introduction

The purpose of the test program was to study the effects of fatigue loading on the shear behavior of prestressed concrete girders. Full-scale Texas Type C pretensioned girder specimens were used throughout the test series. The only controlled variable in the test series was maximum fatigue load.

A series of flexural fatigue specimens preceded this study. The same basic test set-up was used for both series of tests. This chapter is a summary of the test program; additional details may be found in References 23 and 28. Major differences in the test program, such as loading arrangement and stirrup instrumentation, are discussed in detail in this chapter.

3.2. Description of Test Specimen

All three pretensioned girder specimens used in the test program were Texas Type C-16 with a clear span of 48 ft. They all utilized 16 seven-wire, 1/2 in. diameter, Grade 270, stress-relieved strands in a straight pattern. Section properties (from Texas Department of Highways and Public Transportation [TDHPT] drawing GpA) and strand pattern (from TDHPT drawing GpSS-OD) are shown in Figs. 3.1 and 3.2 respectively. All shear and confining reinforcement conformed to TDHPT drawing GpA. The basic shear reinforcement consisted of No. 3 hairpin stirrups spaced at 1 ft on center. Additional shear and confining reinforcement was placed at the ends of the member. Two No. 5 longitudinal bars were placed in the top flange to reduce tension stresses at release. Pickup loops were placed at each end of the member. The pickup loop placement and its effect on the shear strength of the girders is further discussed in Chapter 4. The steel cage, except for stirrups which were instrumented to detect fatigue fractures, was tied with standard wire ties. Stirrups instrumented to detect fatigue fractures were tied with nylon ties. See Sec. 3.4.4 for further discussion of the method used for detecting fatigue fractures. Electrical strain gage wires were neatly tied to the longitudinal reinforcement in the top flange along the length of the beam. Figure 3.3 shows the shear and confining reinforcement layout, and stirrup dimensions.

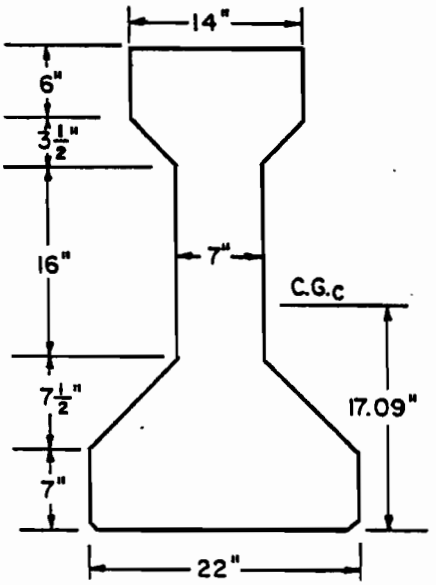

A = 494.9 in^2

Cb = 17.09 in

Ct = 22.91 in

I = 82,602 in^4

Sb = 4833 in^3

St = 3605 in^3

Fig. 3.1 Texas Type C girder properties

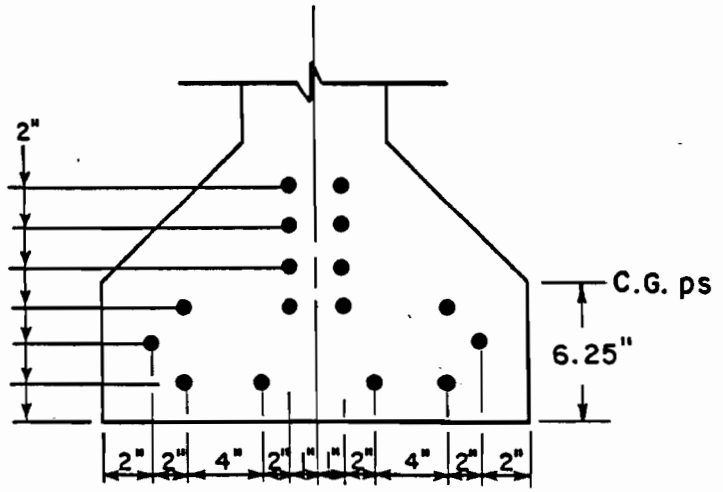

Fig. 3.2 C-16 strand pattern

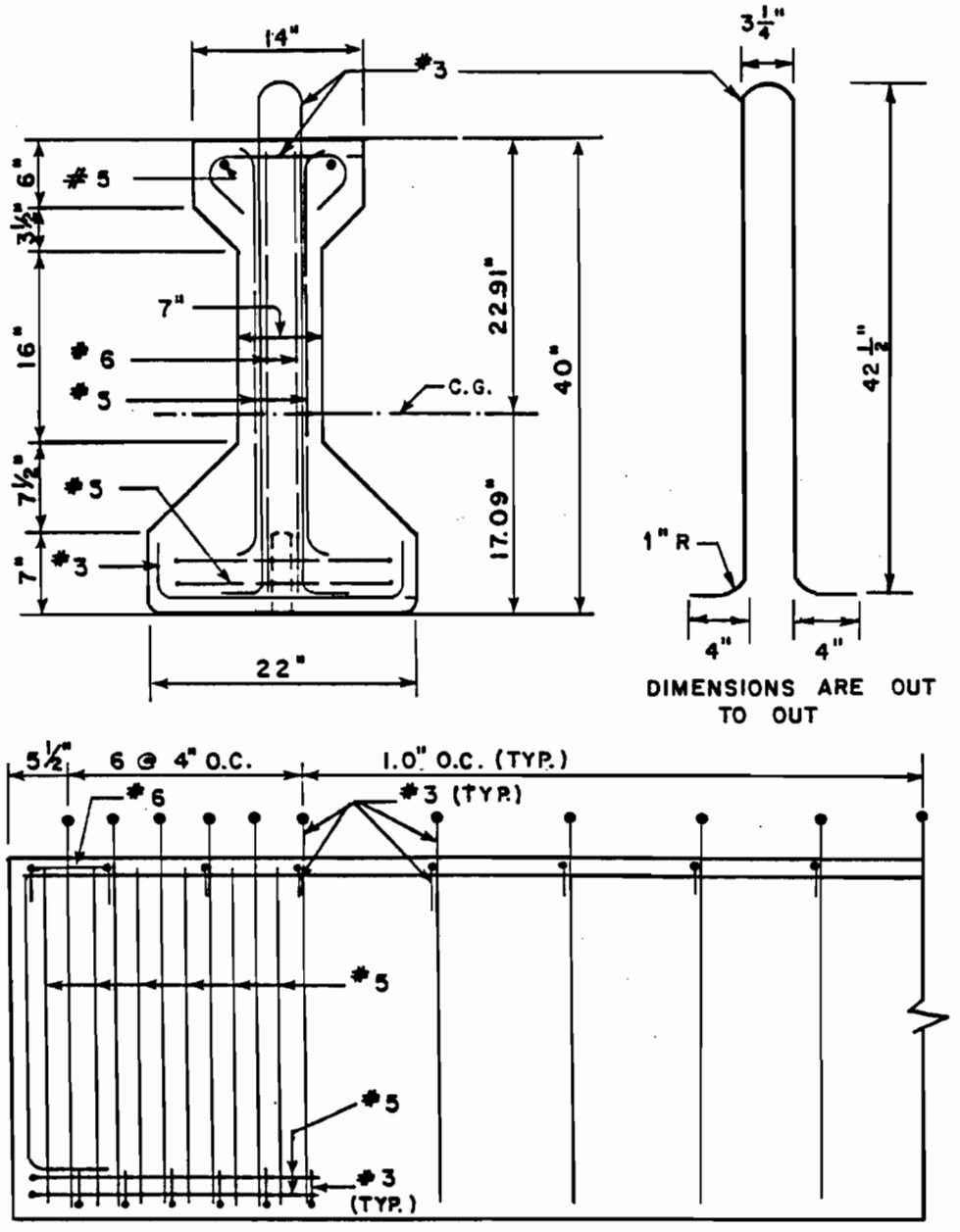

Fig. 3.3 Shear and confining reinforcement, and stirrup dimensions for a Texas Type C girder

Figure 3.4 is a photograph of the end anchorage confining reinforcement and the shear reinforcement at midspan with strain gages in place.

Unshored cast-in-place slabs were added to the girders to form the composite section shown in Fig. 3.5. Each deck slab was reinforced with two mats as indicated in the figure. All test specimens were fabricated in the Phil M. Ferguson Structural Engineering Laboratory. A complete description of procedures used in fabrication of the test specimens can be found in Ref. 23.

3.3 Material Properties

3.3.1 Concrete for Girder and Slab. The concrete mixes were designed using TDHPT standard specifications. Concrete used for the girders was Class H and had a required strength of 5000 psi. Concrete used for the slabs was Class C. The concrete consisted of Type I portland cement, Colorado river sand, and crushed limestone coarse aggregate (maximum size 1 in.). Table 3.1 lists the concrete strengths and mix proportions for the three girders and slabs.

3.3.2 Web Reinforcement and other Mild Steel. All reinforcement used for the girders and slabs conformed with TDHPT specifications. All bars were ASTM A615 Grade 60 and were purchased from a local supplier. All stirrups used in the shear spans were produced from the same mill heat. Straight 20 ft bars were also obtained from the same mill heat for use in the companion study (see Secs. 2.4 and 5.4 and Ref. 18. A stress versus strain curve for the stirrups is shown in Fig. 3.6. Material properties and other data for the stirrups are shown in Table 3.2.

3.3.3 Prestressing Strand. One-half in. diameter, Grade 270, seven wire, stress relieved strand, manufactured under ASTM Specification A-416-74, was used for all three girders. All strand was from a single 12,000 ft spool which was stored inside the laboratory to prevent corrosion.

A stress versus strain curve was provided by the manufacturer and was confirmed by laboratory tests. The modulus of elasticity for the strand was 29,000 ksi. The modulus of elasticity for a single wire (required to interpret electrical strain gage readings) was 30,500 ksi. The curves are shown in Fig. 3.7.

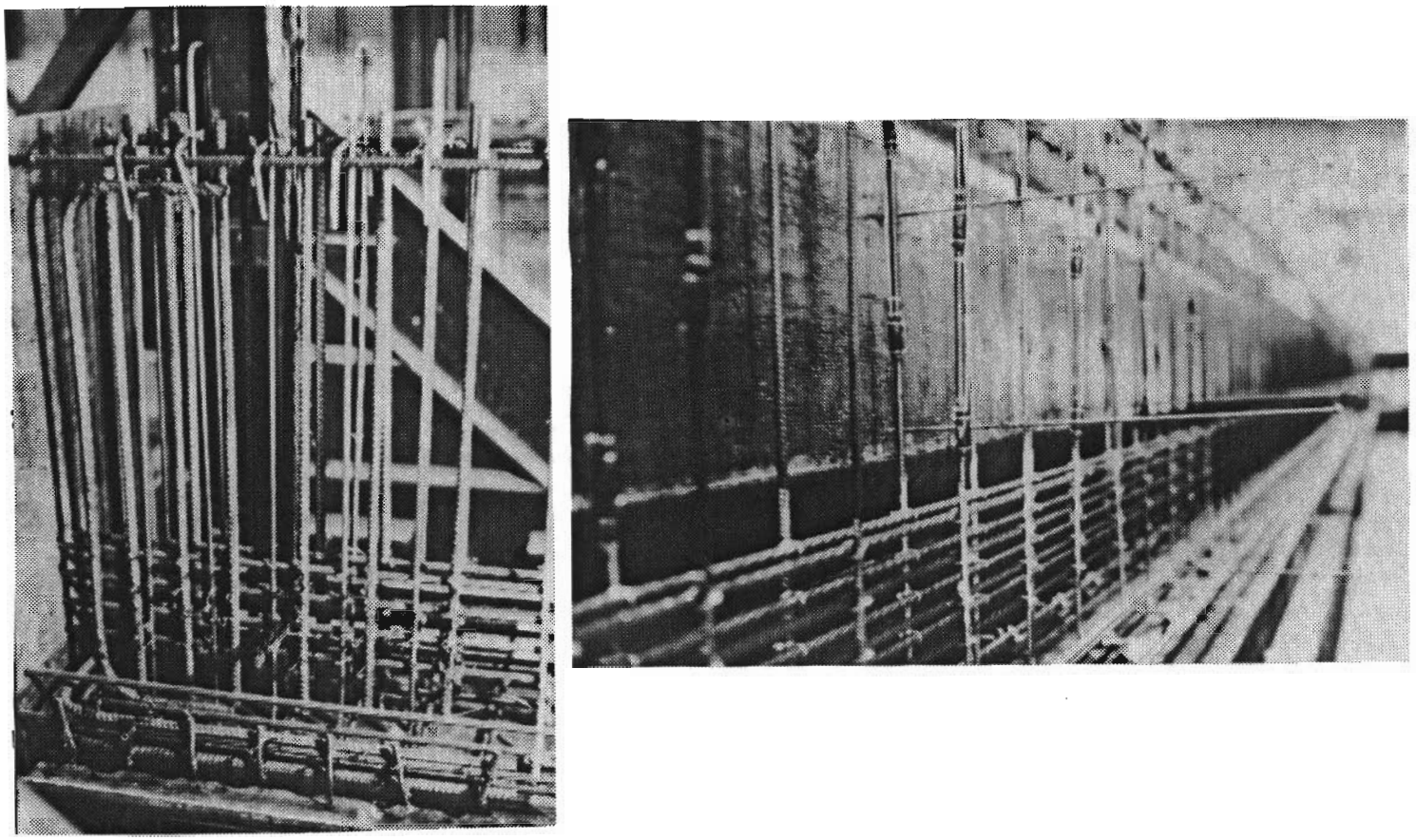

Fig. 3.4 Photograph of Texas Type C end anchorage reinforcement (left) and midspan shear reinforcement (right) with strain gages on stirrups

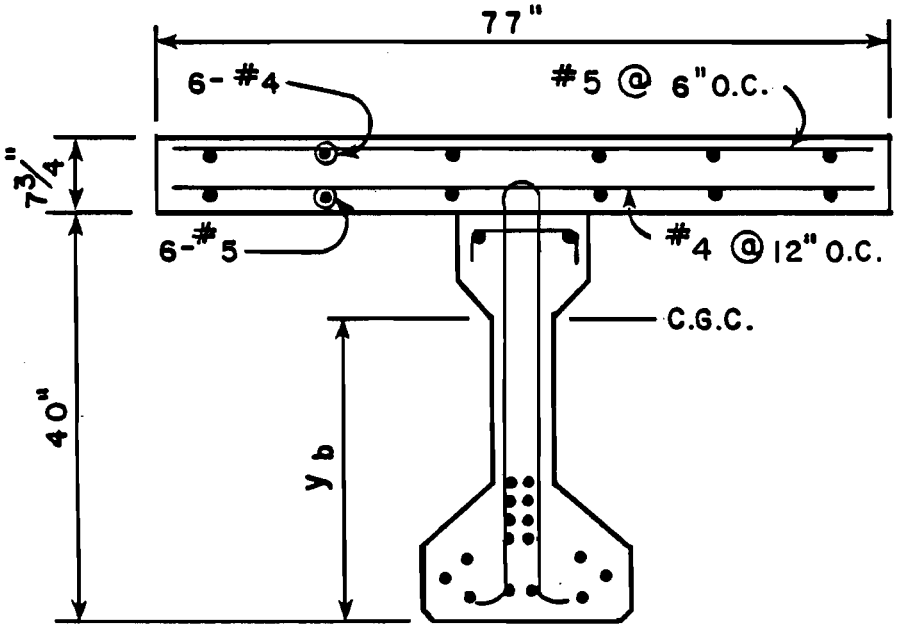

Fig. 3.5 Texas Type C slab reinforcement

TABLE 3.1 Concrete Properties for Test Specimens

Specimen		Weights per Cubic Yard (lb)				Slump (in.)	W/C Ratio	Cement Factor (sacks)	Compressive Strength (psi)		
		Coarse Aggregate	Fine Aggregate	Cement	Water (gal)				Initial[b] (days)	28-Day	Test (days)
1[a]	Girder	2028	1217	679	236 (28)	3.5	0.35	7.20	4950 (6)	6690	6870 (35)
	Slab	1984	1330	560	247 (30)	4.0	0.44	6.00	4430 (5)	5910	4950 (7)
2	Girder	1991	1195	667	253 (30)	6.0	0.38	6.97	5820 (12)	6700	6840 (39)
	Slab	1978	1325	558	255 (31)	6.0	0.46	5.93	3600 (2)	5790	5460 (22)
3	Girder	1989	1193	666	257 (28)	7.0	0.39	6.96	4210 (3)	5810	5680 (25)
	Slab	1987	1331	560	237 (28)	8.0	0.42	5.96	4210 (3)	5470	5360 (8)

[a] Beam C-16-NP-6.0-NO-1.91 in flexural series of tests [23].
[b] Initial strength for girder is at release of prestress force, initial strength for slab is at removal of forms.

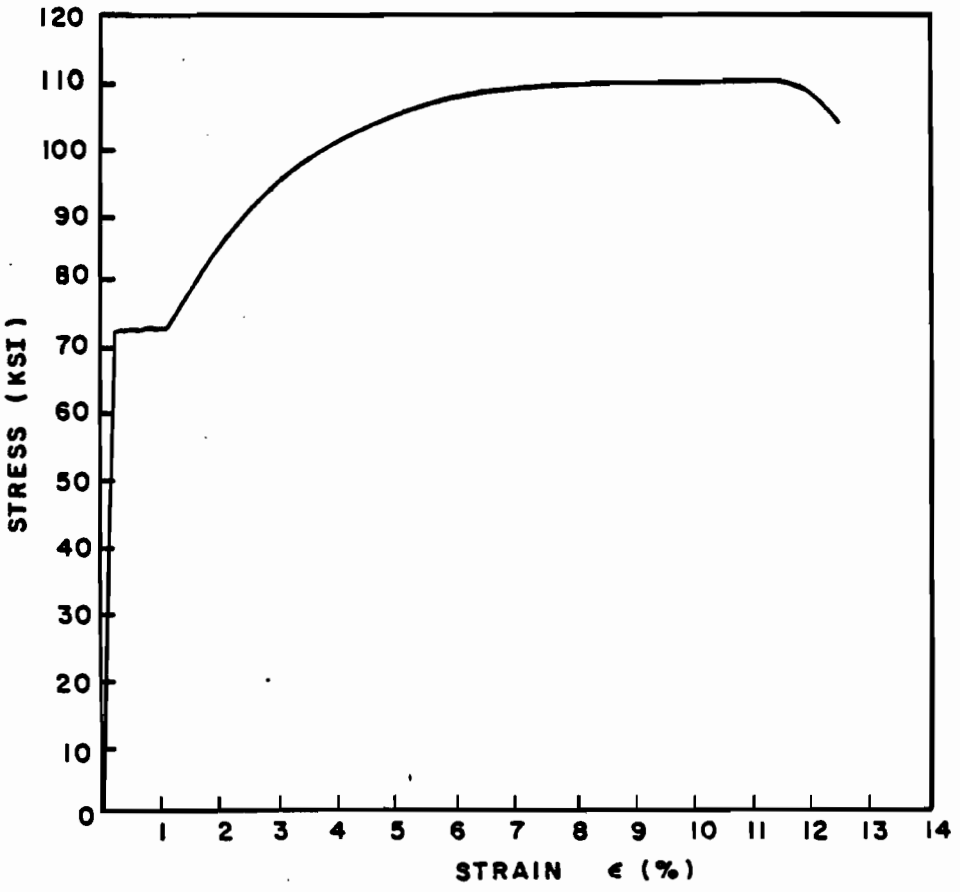

Fig. 3.6 Stress-strain curve for No. 3 deformed bar

Table 3.2 Material Properties for No. 3 Deformed Bars

Items	Values
Grade Designation	ASTM A615 [9] Grade 60 Deformed Billet-Steel Bar for Concrete Reinforcement
Heat Number	69803
Form of Product	No. 3 (3/8 in.) bar
Surface Condition	As - rolled
Lug Height	0.016 in.
Lug Spacing	0.24 in.
Tensile Strength	109,500 psi
Yield Point	72,000 psi
Elongation	12.5 % in 8 in. gage length
Modulus of Elasticity	29,500,000 psi
Chemical Composition:	
C	0.42%
M_n	1.07%

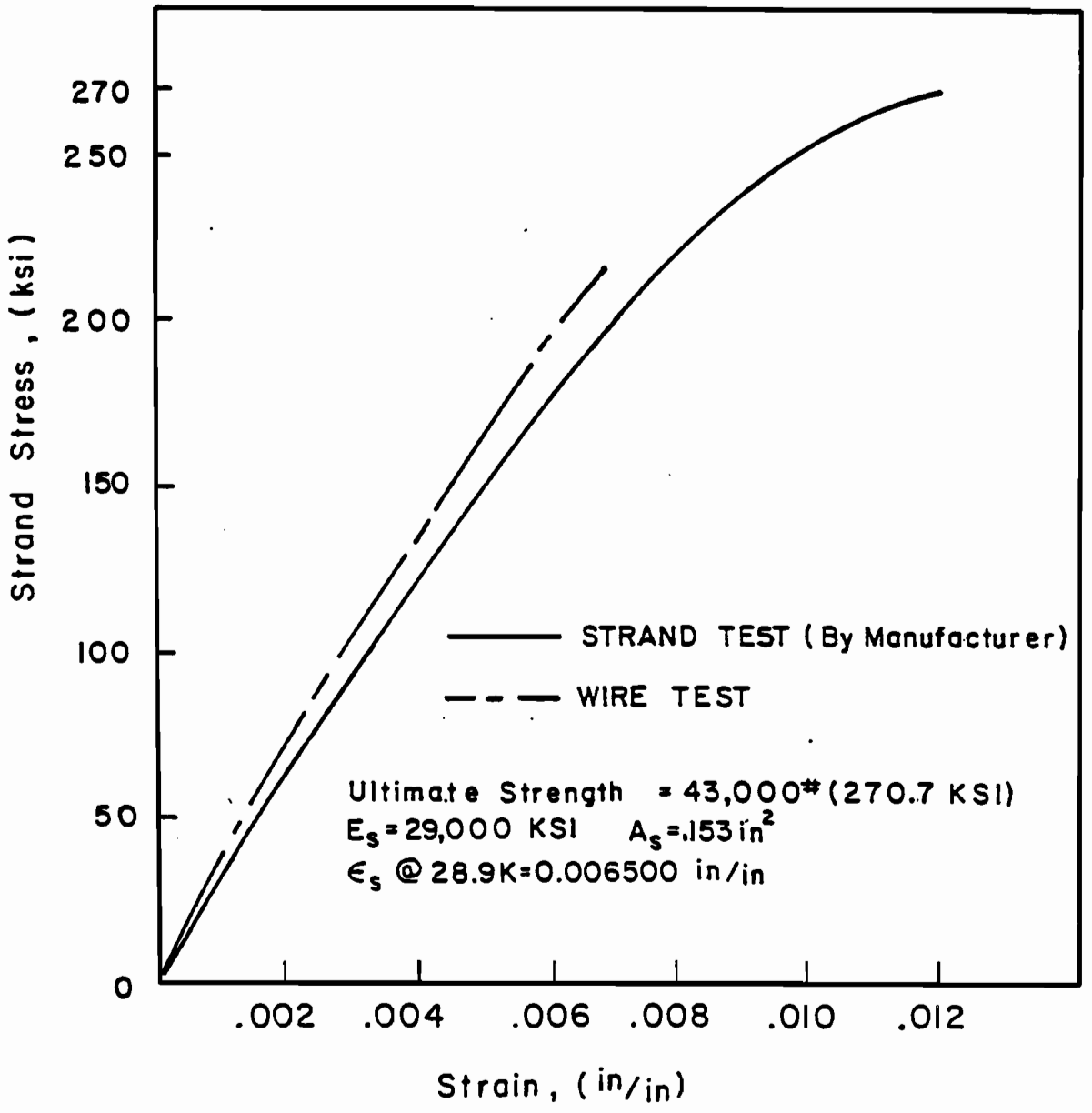

Fig. 3.7 Stress-strain curves for the prestressing steel used in the test series

3.4 Instrumentation and Data Acquisition for Static and Fatigue Testing

3.4.1 General. Data were collected through electrical and mechanical systems. The intent was to verify data by collecting them through more than one method. Following is a brief description of the equipment used to monitor data collected through electrical systems.

1. An MTS Model 464 electronic signal peak detector was used to monitor load range, centerline deflection range, inclined crack-width range, selected stirrup and prestressing strand strain ranges, and centerline deflections during static and fatigue testing. Up to six channels of input could be monitored at one time.

2. A Vishay Model 2310 four channel power supply/amplifier was used to amplify voltage inputs to the electronic signal peak detector.

3. A Houston Instruments Model 2000 plotter was used to plot data during static tests. Typical curves produced were load-deflection, load-strain, and load-inclined crack opening response.

4. An Acurex Autodata Ten/10 electronic scanner was used during static testing to monitor up to 72 channels of electrical strain gages, load cells, and displacement transducers. The Acurex Autodata system was used for Beam 1 and up to 210,000 cycles for Beam 2 when a malfunction developed.

5. Strain indicators with switch-and-balance boxes were used to record up to 60 channels of strain gage output for Beam 3 and for Beam 2 after the Acurex Autodata system malfunctioned.

3.4.2 Stirrup and Prestressing Strand Instrumentation. Electrical strain gages (Micro Measurements EA-06-062AP-120) were placed on individual wires of four prestressing strands before they were initially tensioned. For Beam 1, 14 gages were placed on bottom strands in the constant moment region to monitor strand stress range. For Beam 2 and Beam 3, 20 gages were placed on top and bottom strands in the constant moment region and in the shear span. The intent was to monitor strand stress range in the constant moment region and to examine the effect of inclined cracking on strand stress at various sections.

Electrical strain gages (Micro Measurements EA-06-250BG-120, for Beam 1, Tokyo Sokki Kenkyujo FLA-6-11 for Beam 2 and Beam 3) were placed at four points on selected stirrups, as shown in Fig. 3.8, so that they were distributed throughout the thin web portion of the girder. Placement of instrumented stirrups along the length of the shear span is shown in Figs. 4.3 and 4.4 (Beam 1), 4.12 and 4.13 (Beam 2), and 4.32 (Beam 3). Reinforcing bar deformations were carefully removed so no stress concentrations were created at the location of a strain gage. Three-wire leads were used for all strain gages to eliminate effects of lead wire length.

3.4.3 Concrete Instrumentation. Demec mechanical strain gages were used to measure concrete strains and crack opening widths. Demec targets were installed on the lower flange at nine locations prior to application of the prestress force. Effective prestress force strains were recorded with a 6-in. Demec gage. Demec targets were also placed on both sides of selected flexural and inclined cracks after they developed and were read with a 2-in. Demec gage to measure crack opening width. The strain indicated by the Demec gage was multiplied by the 2-in. gage length to determine crack widths. It was assumed that the concrete strain adjacent to the crack was negligible compared to the crack width. Demec targets were placed across inclined cracks such that vertical and horizontal components of crack opening could be recorded. A 2-in. displacement transducer was also placed across selected inclined cracks to monitor the crack-width range during static and fatigue loading. Locations are shown in Figs. 4.3 and 4.4 (Beam 1), 4.12 and 4.13 (Beam 2), and 4.32 (Beam 3).

3.4.4 Stirrup Fracture Detection System. At the start of the test series it was believed that a stirrup fracture would be apparent by a noticeable change in beam load-deflection response, inclined crack width, or stirrup stress range. This was found to be false for Beam 1, so a more precise method of detecting stirrup fractures was developed for Beam 2 and Beam 3.

The system was very simple and detected fractures during fatigue or static loading with only an ohmmeter. Lead wires were attached to each stirrup leg at the bottom of the stirrup with hose clamps as shown in Fig. 3.8. After the stirrups were tied to the prestressing strand the lead wires were taped to the bottom of the prestressing bed. After the girder was cast and transported to the testing platform, the lead wires were exposed. To test for a fracture, an ohmmeter was connected between the

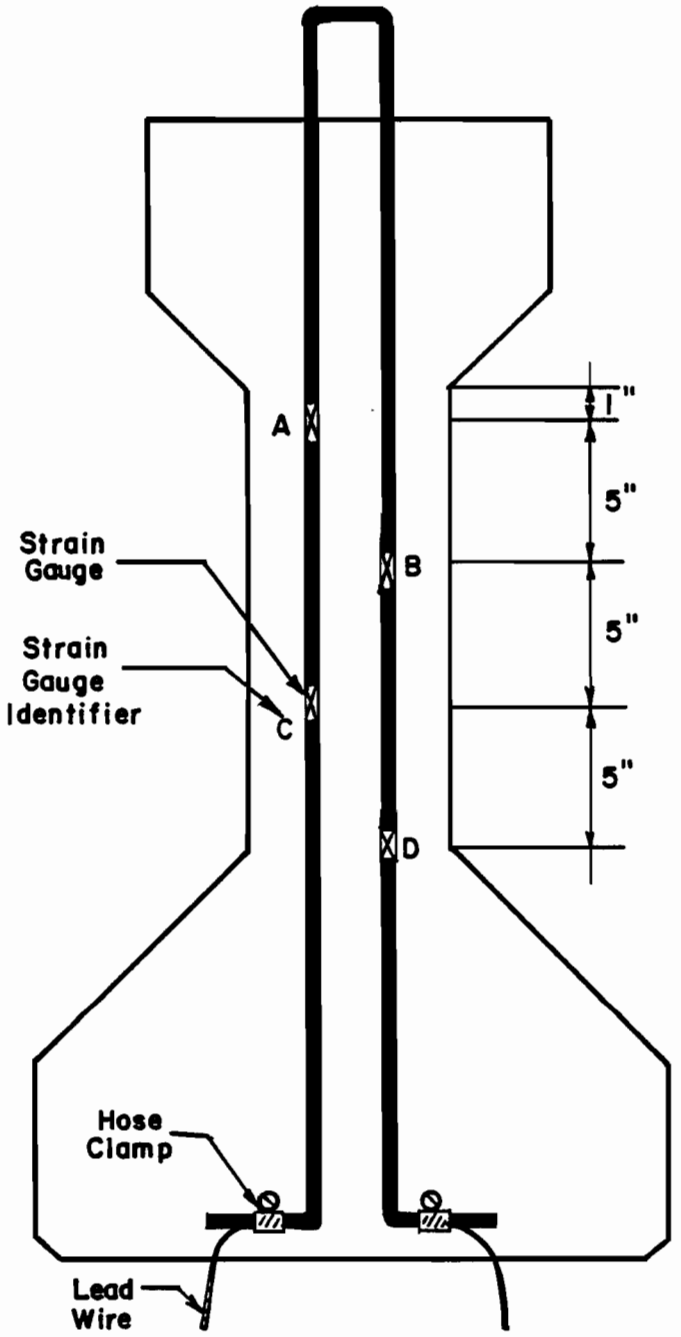

Fig. 3.8 Electrical strain gage placement and lead wires for detecting stirrup fractures

lead wires. If the stirrup was not fractured, a negligible amount of resistance was measured (less than one ohm). If the stirrup was fractured, greater than 50 ohms resistance was measured across the stirrup. Resistance did not increase to infinity after a fracture because some amount of electrical continuity existed in the concrete.

In order for this system to work as described, stirrups had to be electrically insulated from the prestressing strand and reinforcing steel to which they were attached. This was accomplished by coating the stirrups with epoxy at all points of attachment, then wrapping them with duct tape at all points of attachment. Nylon ties were used for attachment. After casting the girder, electrical isolation could be checked by placing an ohmmeter between a stirrup lead wire and an exposed strand at the end of the girder.

Eleven stirrups were instrumented in each shear span as shown in Figs. 4.12 and 4.13 (Beam 2), and 4.32 (Beam 3). When testing was complete, all stirrups were uncovered to verify fractures and in all cases the stirrup fracture detection system was accurate.

3.4.5 Deflection Measurements. Deflection was measured by electrical and mechanical systems. Two displacement transducers were placed at midspan of the girder and were used to monitor deflections during static and fatigue testing. Dial gages were placed at midspan, third span, quarter span (load points), and 3 ft from each end, for use in static tests. A limit switch was also placed at midspan to stop fatigue testing when the centerline deflection increased significantly.

3.4.6 Load Measurements. Applied loads were measured with Strainsert 100 kip load cells bolted to each loading ram between the hydraulic piston and the spherical head mounted on the deck slab. Load readings were taken during fatigue and static testing using the MTS electronic signal peak detector. Loads were substantiated by the pressure gages on the console of the load pulsator.

3.5 Test Setup

Test specimens were subjected to a two-point loading by 150 kip single acting Miller rams attached to a pair of steel bents. The bents were located at quarter spans of specimens for the shear series of this study. The loads were placed so that

shear rather than flexure should govern the fatigue behavior. Beam 1 (Beam C-16-NP-6.0-NO-1.91) was used in both series of tests. It was precracked in flexure with load applied at the third points. The bents were then moved to the quarter points for the remaining portion of the test on Beam 1 and for all subsequent testing on Beam 2 and Beam 3. Photographs showing placement of the load frames for each series of tests are shown in Figure 3.9. Additional details for the loading frame and hydraulic loading system are presented in Ref. 23.

3.6 Test Procedure

3.6.1 Static Testing. Static tests were performed before fatigue loading to obtain initial readings. Two or three complete load cycles were performed. In general, the maximum applied static load was the same as the maximum fatigue load, except for Beam 1 which was precracked in flexure with loads in a different position (see Sec. 4.2.2). None of the specimens were precracked in shear at the beginning of the test.

Fatigue testing was started after the two or three cycles of static testing and was stopped at various intervals to perform additional similar static tests, such as when inclined cracks developed, deflections increased significantly, or stirrups fractured.

3.6.2 Fatigue Testing. Fatigue loading was used to develop inclined cracks and then to determine the fatigue strength of the web reinforcement after inclined cracks had formed. A minimum or lower load level of 10 kips was used for all three beams so that the rams would remain seated in the spherical loading heads. Upper load levels ranged from 67.5 to 80 kips for the various beams. Load, midspan deflection, inclined crack opening, selected stirrup and stand strain ranges, and load pulsator frequency were monitored during fatigue loading. The fatigue load fluctuated from its desired range at most 3 kips (approximately 4%) and generally less than 1 kip (approximately 1%). Fatigue testing was continued until a sudden large increase in load-deflection response occurred. This happened after several stirrup or strand fractures as discussed in Chapter 4.

3.6.3 Strength Testing. After substantial fatigue damage and prior to the final strength test, a 5-in. neoprene pad was placed between the girder ends and the concrete pedestal to accommodate increased girder rotations. A monotonically

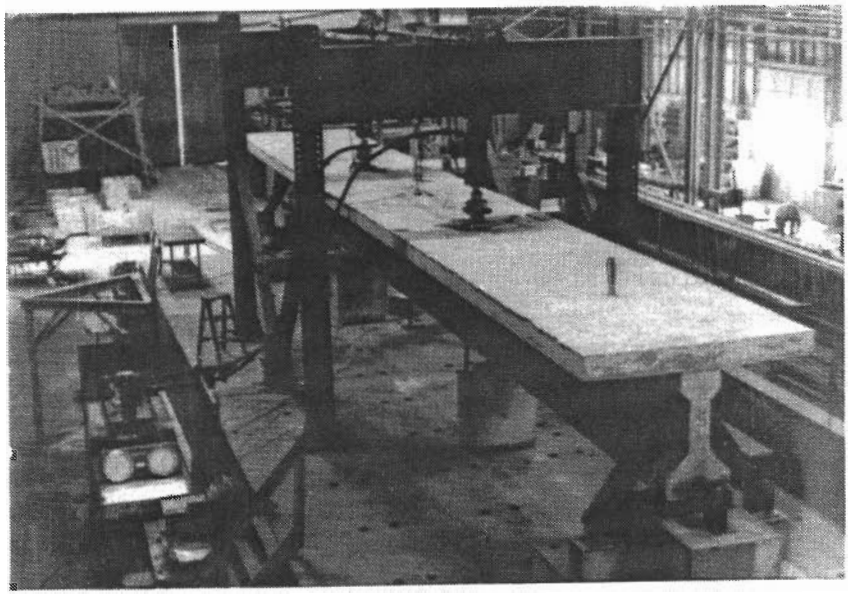

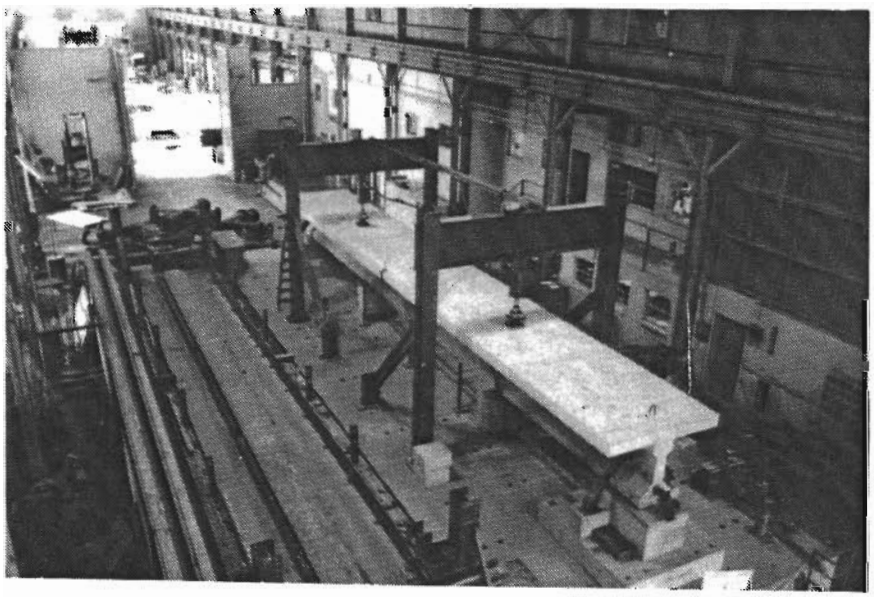

Fig. 3.1 Test setup

increasing load was applied until an ultimate load was established as indicated by increases in deflection with no increase (or a decrease) in load.

Following the strength test, concrete cover was removed from stirrups to verify fractures and their locations. A photograph of a beam with the web concrete removed to expose fractures is shown in Fig. 4.30.

CHAPTER 4

TEST RESULTS

4.1 Introduction

This chapter deals primarily with the shear behavior of the test specimens. A summary of the prestress data is presented in Table 4.1. The "actual effective stress" listed in Table 4.1 was determined experimentally for each girder after flexural cracks formed in the constant moment region. The load corresponding with the zero-tension condition at the bottom of each girder was determined during static load cycles with the aid of a linear potentiometer placed across a flexural crack at the bottom of the girder. The sudden change in slope of the load versus displacement plot for the potentiometer was taken to coincide with the onset of tension in the bottom of the girder. As a result, the load corresponding with this change in slope was considered to be the zero-tension load. The effective prestress force was calculated using the zero-tension load, dead load moment, live load moment, and girder cross section dimensions as input. Actual losses tabulated in Table 4.1 were based on the estimated actual effective prestress for each girder.

A summary of the flexural fatigue behavior is presented in Table 4.2. For more details on flexural fatigue, see Ref. 23, "Flexural Fatigue Behavior of Pretensioned Concrete Girders." Figure 4.1 illustrates how the three shear specimens fit on the S-N curve established in the study mentioned above. The superscripts "F" and "V" refer to flexural and shear fatigue failures respectively, where flexural fatigue is associated with broken strands, and shear fatigue with broken stirrups.

Table 4.3 is a summary of material and beam cross section properties at initiation of each test. None of the specimens were precracked in shear prior to fatigue loading. The intent of each test was to observe two different stages of behavior. In the first stage, fatigue strength for inclined cracking of the concrete was to be explored. Once the inclined cracks formed in the second stage, the fatigue behavior of the stirrups could be observed.

Only one of the flexural tests in Overman's study developed inclined cracks during fatigue loading. The load level

TABLE 4.1 Summary of Prestress Data

Girder	Decompression Load[a] P_o (k)	Flexural Cracking Load P_{cr} (k)	Ultimate Flexural Load[c] P_u (k)	Pretension Stress[d] f_{si} (ksi)	Predicted Effective Stress[c] f_{se} (ksi)	Predicted Loss (%)	Actual Effective Stress[e] f_{se} (ksi)	Actual Loss (%)
1	50	93[b]	156	187	164	12.2	155	17.1
2	46	86[c]	157	189	169	10.8	147	22.0
3	40	76[c]	157	189	156	17.7	137	27.4

[a] Determined experimentally with load-deflection data (see Sec. 3.9.1, Ref. 23).
[b] This load is an actual cracking load since this specimen was precracked in flexure.
[c] Calculated with analytical program PBEAM [31] (see Sec. 5.3, Ref. 23).
[d] Determined experimentally as explained in Sec. 3.2.2., Ref. 41.
[e] Calculated by using the experimentally determined decompression load (see Sec. 5.4.2, Ref. 23).

Loading Arrangement:

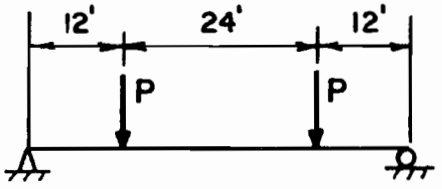

TABLE 4.2 Summary of Flexural Fatigue Data

Girder	Load Range (k)	Dynamically Amplified Load Range[a] (k)	Calculated Stress Range[b] (ksi)	Maximum Measured Stress Range[c] (ksi)	Bottom Fiber Tension[b] (psi/ $X\sqrt{f'_c}$)	No. of Cycles to Flexural Fatigue Cracking	Ultimate Failure Mode at No. of Cycles
1	10-80	10-83.0	27.8	18.3	500/6.03	Precracked	Flexure @ 1,911,000
2	10-75	10-77.6	26.4	14.1	443/5.36	10,000	Shear @ 891,000
3	10-67.5	10-69.2	19.8	10.7	414/5.49	1,000,000	Flexure @
	10-71.3	10-73.1	24.8	13.8	471/6.25		3,272,000

[a] Determined by comparing static and dynamic deflection readings (see Sec. 5.4.4, Ref. 23).
[b] Calculated with analytical program PBEAM [31] (see Sec. 5.4.5.1, Ref. 23).
[c] Measured with electrical strain gage.

Loading Arrangement:

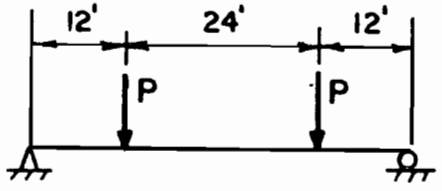

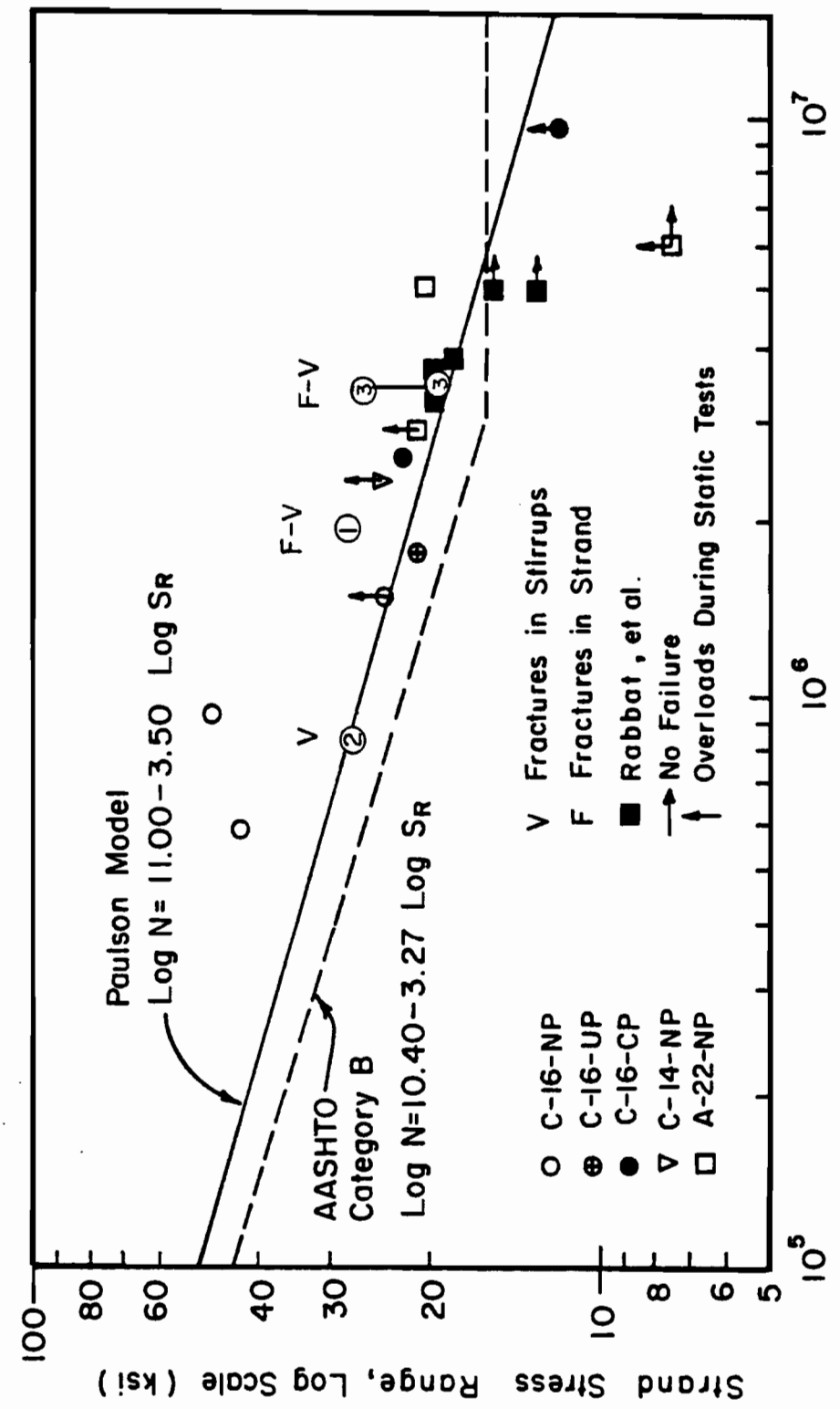

Fig. 4.1 Shear fatigue data plotted with previous tests, Paulson model, and AASHTO model

TABLE 4.3 Summary of Composite Material and Cross Section Properties

Specimen	Concrete Strength First Day of Load Application		Effective Slab Width	Center of Gravity Measured from Bottom of Section	I_{TOTAL}
	$f'_{c\,girder}$ (psi)	$f'_{c\,slab}$ (psi)	(in.)	(in.)	($in.^4$)
1	6870	4950	65.36	30.64	264,700
2	6840	5460	68.79	30.98	269,400
3	5680	5360	74.81	31.54	277,100

for that specimen was 75 kips which corresponded with the highest fatigue load in his series of tests. That load was taken as an upper estimate for the series of shear fatigue tests (the first specimen tested was a shear-flexure specimen). A lower load of 10 kips was chosen for all tests. All forces used in this discussion refer to loads applied by one of two hydraulic rams used to load test specimens. No overloads were imposed on the specimens during static testing (except for Beam 3 which was cracked in shear at 3,133,000 cycles), although some overload (less than 4%) was imposed as the result of electronic drift in the hydraulic pulsator. The frequency of the pulsating load was maintained at approximately 2.5 Hz throughout all tests to minimize dynamic amplification.

When testing of a specimen was complete, a post-mortem investigation was carried out to verify stirrup fatigue fractures and their locations. In all cases fractures occurred in both legs of a stirrup at similar locations.

4.2 Description of the Behavior of Beam 1

4.2.1 General. Testing of Beam 1 began 35 days after the girder was cast. The specimen was precracked in flexure because the specimen was the last in a series of flexural fatigue tests as well as the first in the series of shear fatigue tests; it was a common specimen in the two different test programs. In the previous test program it was denoted Specimen C-16-NP-6.0-NO-1.91. For more information about the flexural portion of the test, see Sec. 4.5, Ref. 23. A schedule of the loading program over the life of the girder is shown in Fig. 4.2. Illustrations showing the instrumentation, crack pattern at ultimate, and fatigue breaks for the north and south shear spans are shown in Figs. 4.3 and 4.4, respectively. No post-mortem investigation was performed to reveal fatigue fractures on the north shear span because that portion of the specimen was disposed of prematurely. The number of cycles to fatigue fracture is not shown on the north or south shear span because it was not possible to accurately determine from strain gages when the stirrups fractured. The Acurex data acquisition system was used to monitor electrical strain gages. In future specimens, a positive method for identifying stirrup fractures while fatigue testing was in progress was developed.

Pick up loops (4-1/2 in. diameter, 7-wire prestressing strand) for transporting the girder were placed 5 ft from each end of the girder without considering their effect on shear

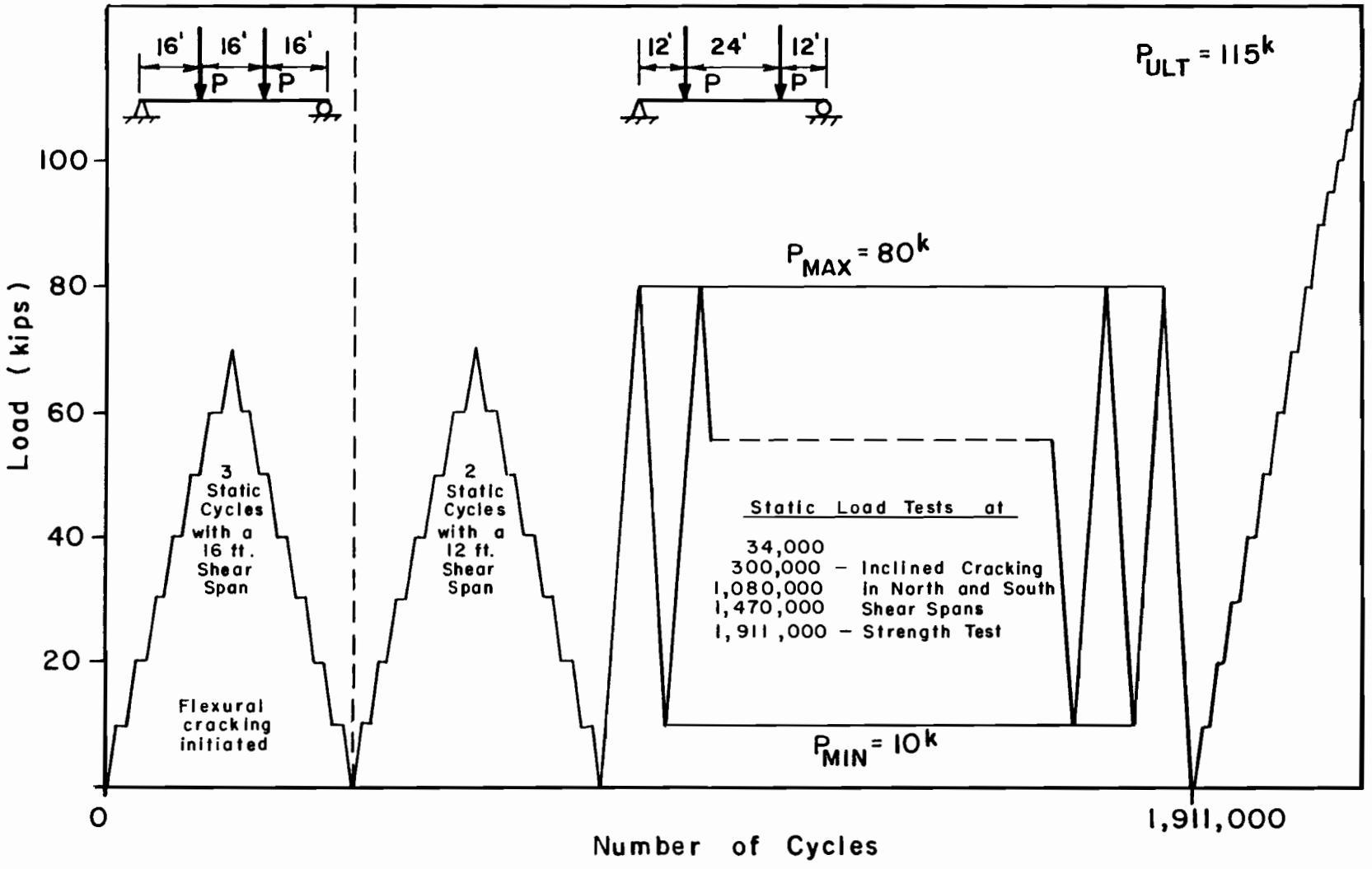

Fig. 4.2 Load program for Beam 1

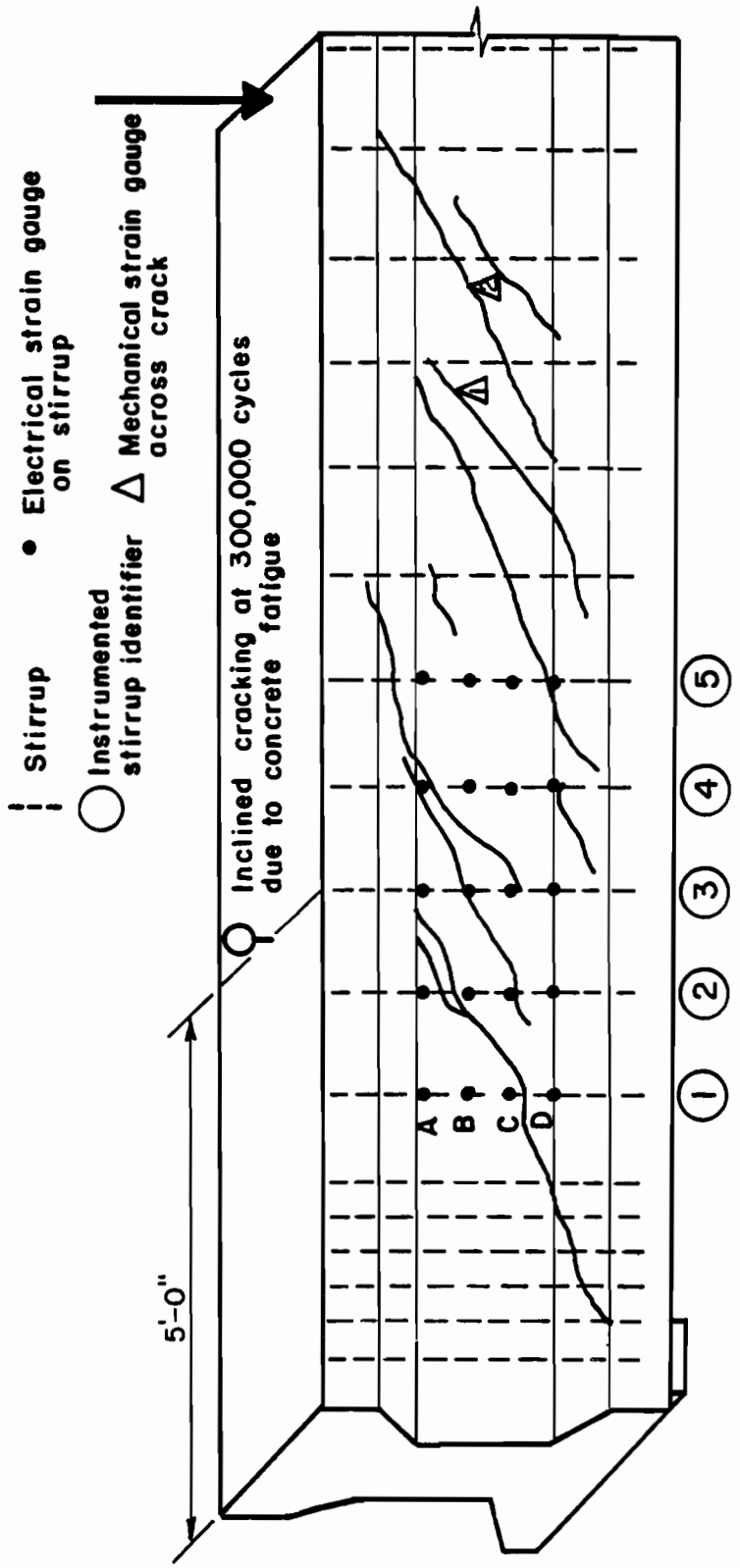

Fig. 4.3 Beam 1, north shear span; instrumentation and crack pattern

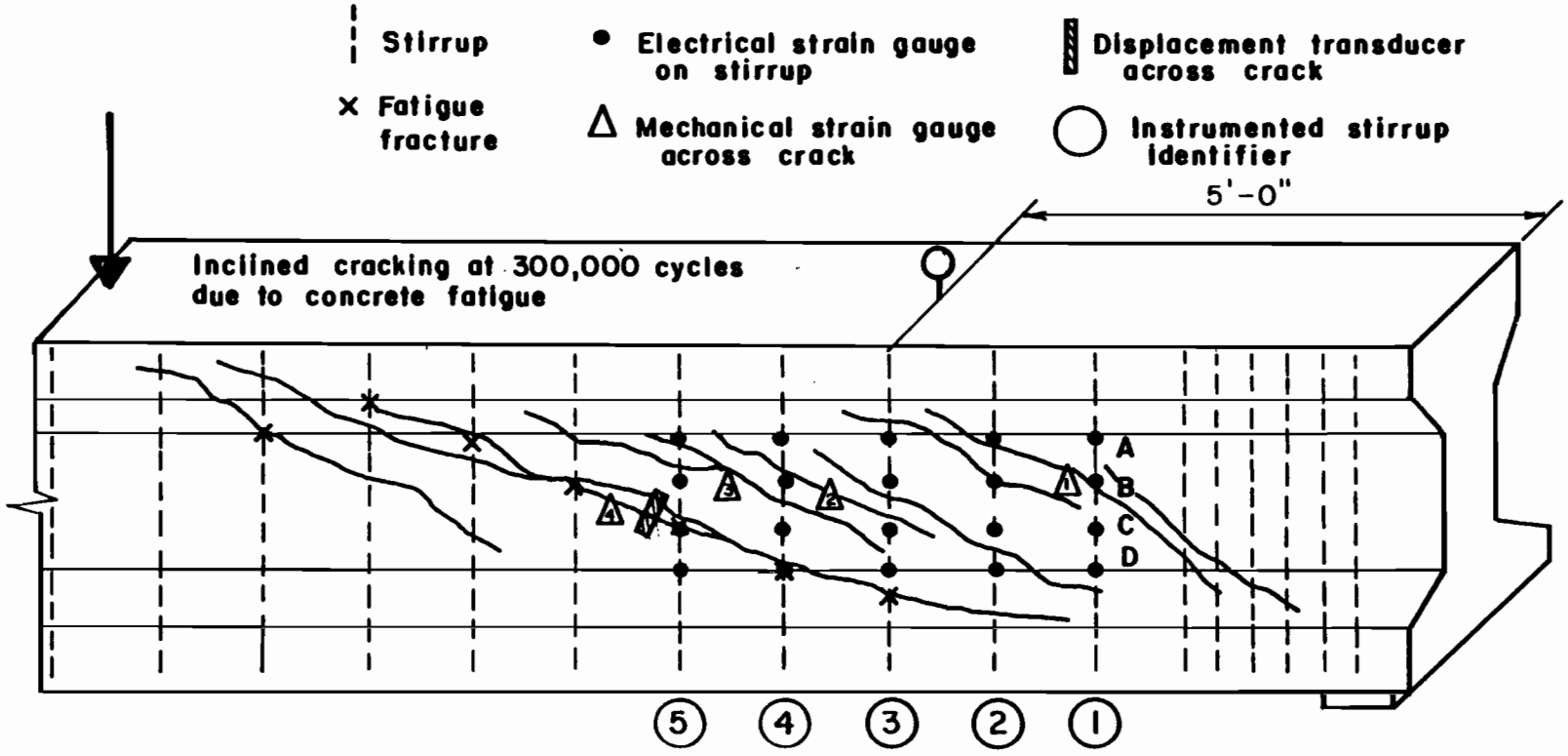

Fig. 4.4 Beam 1, south shear span; instrumentation, crack pattern, and fatigue fractures

strength. In fact, it appears that the pickup loops increased the shear fatigue strength of the girder which resulted in a flexural fatigue failure.

4.2.2 Uncracked Behavior. Testing was initiated by performing three cycles of static load with a 16-ft shear span to check the data acquisition system and crack the specimen in flexure. The load frame was then moved to produce a 12-ft shear span which was used throughout this test and all subsequent tests. Two additional static load cycles were performed after the load frame was moved. An upper fatigue load of 80 kips was chosen because it simultaneously provided desired flexural stresses at midspan and diagonal tension stresses near the ends of the span. The maximum computed diagonal tension stress was 328 psi or $3.96\sqrt{f'_c}$ at a section at the top of the web, 24 in. (h/2) from the face of the support. The corresponding maximum uncracked section bottom fiber tensile stress at midspan was 500 psi or $6.03\sqrt{f'_c}$.

A static test was performed at 34,000 cycles to record data throughout one load cycle and check for cracks. No inclined cracks were detected.

Fatigue loading was continued until 300,000 cycles when inclined cracks were detected while fatigue loading was in progress. Inclined cracks were recorded and mechanical strain gage targets were mounted across selected cracks (for location see Figs. 4.3 and 4.4) to record changes in crack widths during the remainder of the test.

4.2.3 Post-Cracking Behavior. After inclined cracks developed, shear was carried by truss action, with stirrups acting as vertical tension members and concrete as compression struts. This was confirmed by stress readings taken from instrumented stirrups during static load cycles. As fatigue loading continued, the inclined crack pattern developed extensively in both shear spans with several well-distributed cracks. The crack distribution appeared to be the result of the pickup loop which was placed near the middle of each shear span.

Crack widths were measured during each static test. The only crack to show significant change over the life of the specimen was the crack monitored by mechanical strain gage S4 (S and N denote south and north shear span respectively) shown on Fig. 4.4. Figure 4.5 illustrates that the crack grew quite rapidly until late in the life of the specimen when the rate of growth declined for both the absolute and residual crack width.

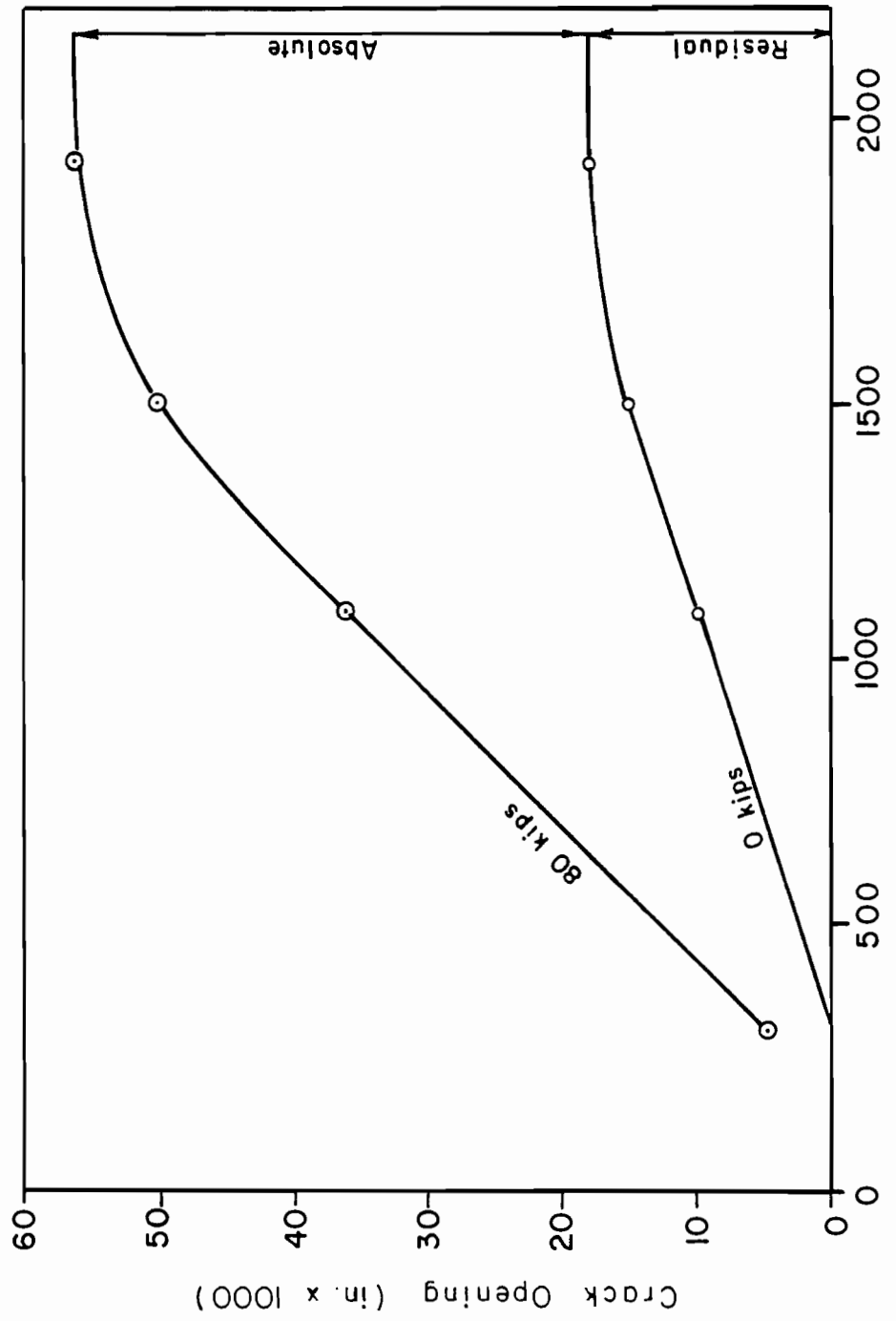

Fig. 4.5 Growth of crack monitored by mechanical strain gage S4

This was probably due to the influence of the pickup loops. At the time the strength test was conducted, seven stirrups had fractured in fatigue between the load point and the pickup loop in the south shear span. The crack monitored by mechanical strain gage S4 increased in width as additional stirrups failed along the crack. After all stirrups along the crack had fractured, the pickup loop anchored the crack which could propagate no further unless the pickup loop also failed.

Near the end of the specimen life, following the fracture of the seven stirrups, a second shear-truss mechanism was evident. Figure 4.6 illustrates this shear truss mechanism with the pickup loop vertical tension member and two concrete compression struts. The inclined crack pattern of Fig. 4.4 reflects the locations of the compression struts.

At 1,080,000 cycles, slip of prestressing strand was observed at the north end of the member as shown in Fig. 4.7. Notice some strand ends are recessed. At 1,470,000 cycles, flexural fatigue damage was observed in the constant moment region as shown in Fig. 4.8. Extensive spalling had occurred and two strands were exposed with visible breaks in the wires. A static load cycle was performed before continuing fatigue loading. The load pulsator automatically turned off at 1,911,000 cycles due to a large increase in specimen deflection. The static strength test was performed at this time.

It is possible that the flexural fatigue damage may have been influenced by the development of inclined cracks in the shear spans. Shear cracks had propagated through the top two levels of prestressing strand since 300,000 cycles. The lower strands in the section were not crossed by inclined cracks. The cracks were prevented from propagating through the lower part of the tension flange by the presence of the pickup loops. The repeated opening and closing of the inclined cracks probably resulted in debonding of the upper layers of prestressing strands along a significant portion of their length. This would result in a higher stress range in the remaining prestressing strands at flexural cracks and shorten the fatigue life. This interpretation is supported by the fact that some of the top strands had slipped at the ends of the span during fatigue loading. In addition, after all the strands were broken at midspan during the final static strength test, it was observed that some of the top strands near midspan had withdrawn into the specimen more than 1 in.

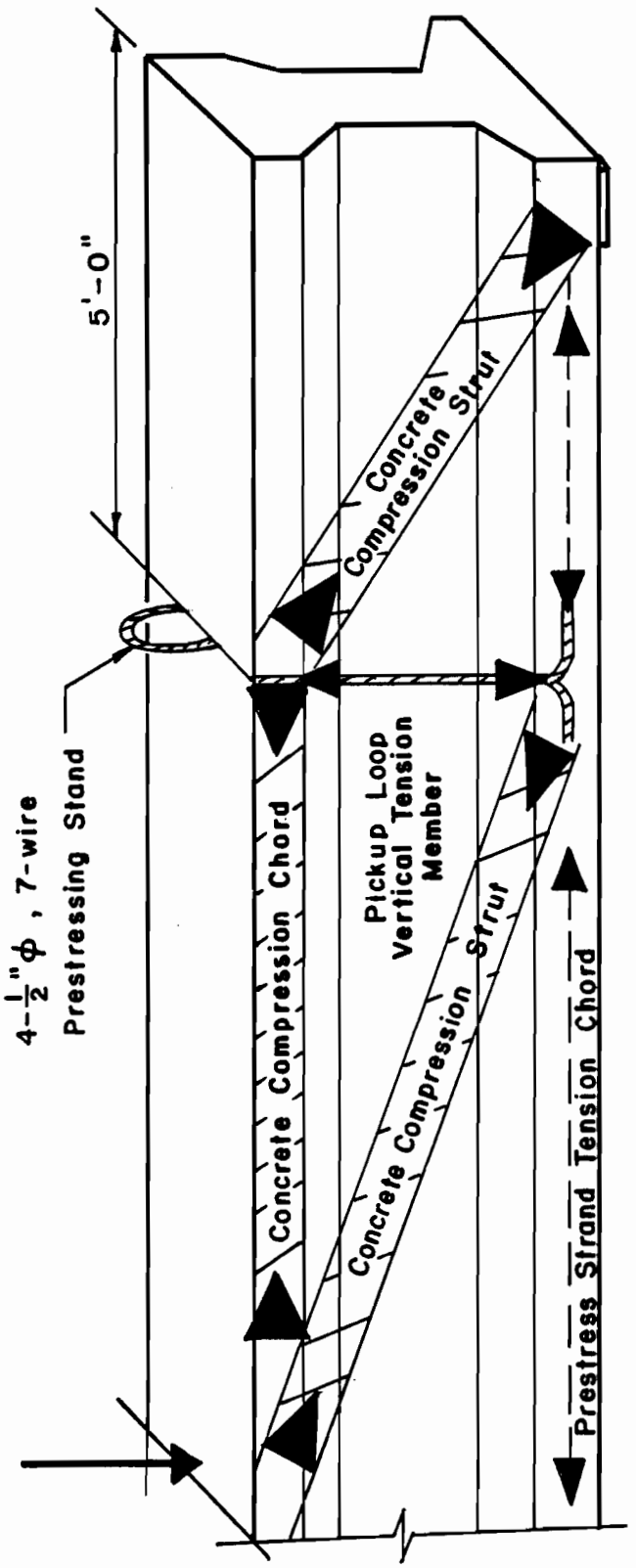

Fig. 4.6 Secondary shear truss action with pickup loop as vertical tension member

Fig. 4.33

Strand slip at

1.080 million cycles

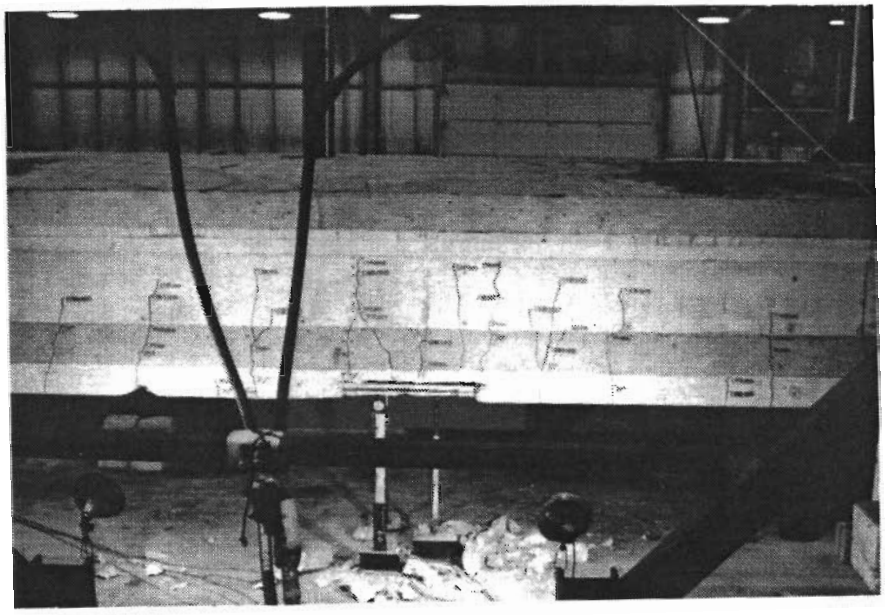

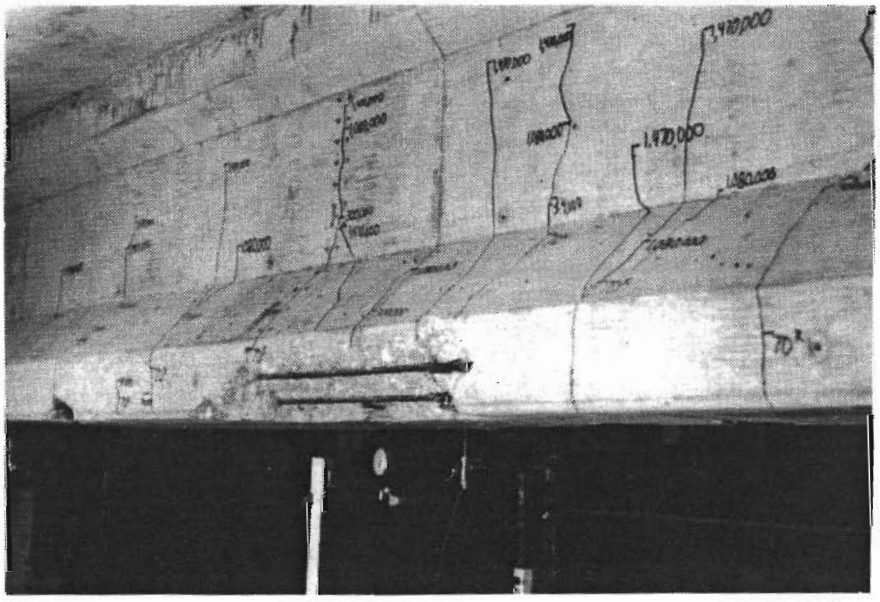

Fig. 4.37 Concrete spalling after approximately 1.5 million cycles

4.2.4 Ultimate Behavior. The specimen reached a load of 115 kips before it failed in flexure. This represented 71% of the calculated ultimate flexural capacity.

Stirrup S1 fractured during the strength test at the location of strain gage S1B (for location see Fig. 4.4). This was detected through the stresses inferred from strain gage data collected during the strength test. Figure 4.9 is a plot of the crack opening at the location of the displacement transducer (LVDT) in the south shear span (for location see Fig. 4.4) during the strength test. It can be seen that the crack almost regained its original width after the specimen failed in flexure. Figure 4.10 shows the north and south shear spans after the strength test.

4.3 Description of the Behavior of Beam 2

4.3.1 General. Testing was started 39 days after the girder was cast. The specimen was not precracked in flexure or shear. A schedule of fatigue testing over the life of the girder is shown in Fig. 4.11. Fatigue loading varied from 10 kips to 75 kips. Illustrations showing the instrumentation, crack pattern at ultimate, and fatigue fractures for the north and south shear span are shown in Figs. 4.12 and 4.13, respectively. The pickup loops for transporting the girder were placed 1 ft from each end of the beam so that they would not influence shear strength as they did in Beam 1. The data acquisition system for collecting electrical strain gage signals in Beam 2 malfunctioned and was changed to strain indicator with switch-and-balance boxes at 500,000 cycles into the test.

Beam 2 was the most informative of the three shear fatigue specimens. Inclined cracking and stirrup fatigue breaks were developed in each shear span. A technique was used to detect fatigue fractures while fatigue loading was in progress (see Sec. 3.4.4). The strength of the girder was dominated by shear behavior. Unlike Beam 1, there was little interaction between flexural behavior at midspan and shear behavior in the shear spans. As a result, shear could be studied independently. Throughout the fatigue history of Beam 2, shear was resisted by three different mechanisms:

1. Concrete in diagonal tension with stirrups providing almost no resistance as indicated by electrical strain gage readings.

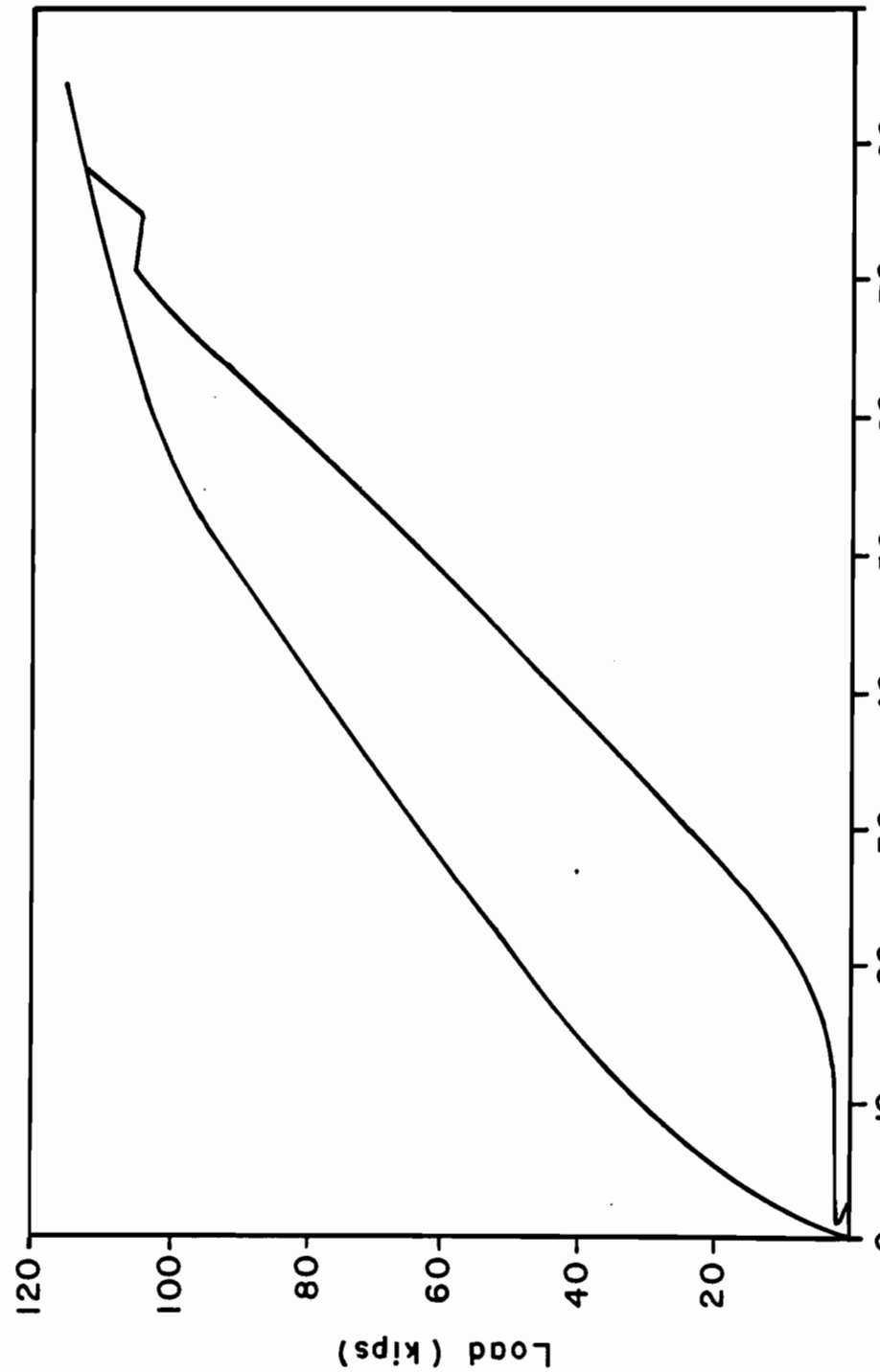

Fig. 4.9 Crack opening in south shear span during strength test

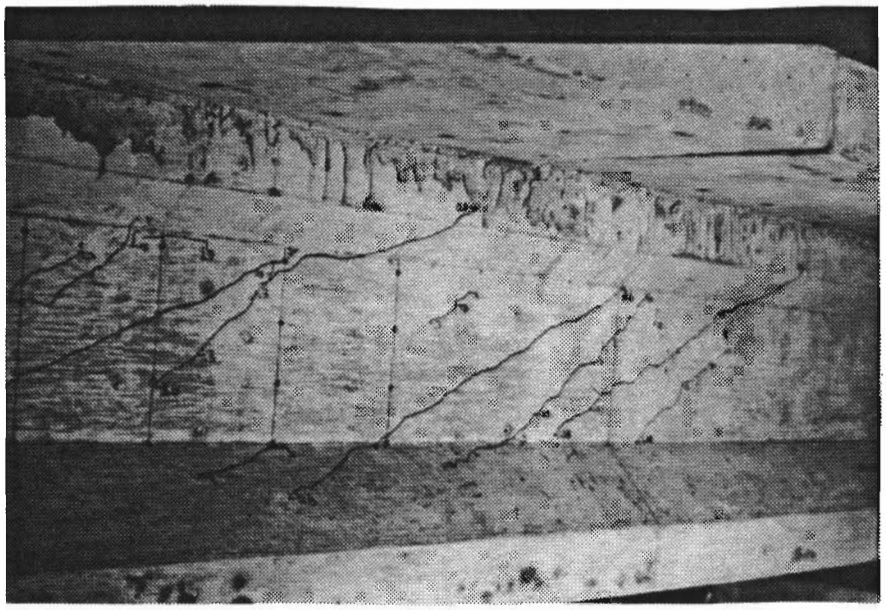

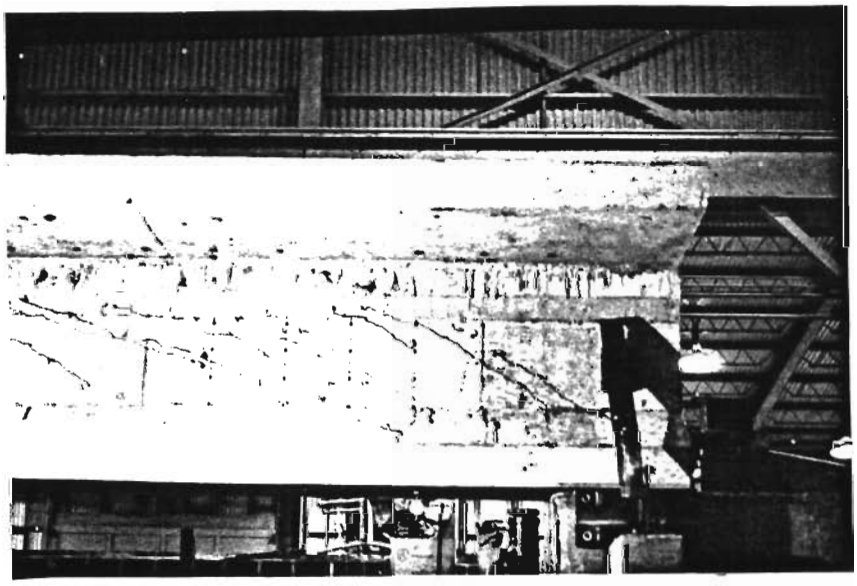

Fig. 4.10 Inclined crack pattern in north (top) and south (bottom) shear spans after the strength test

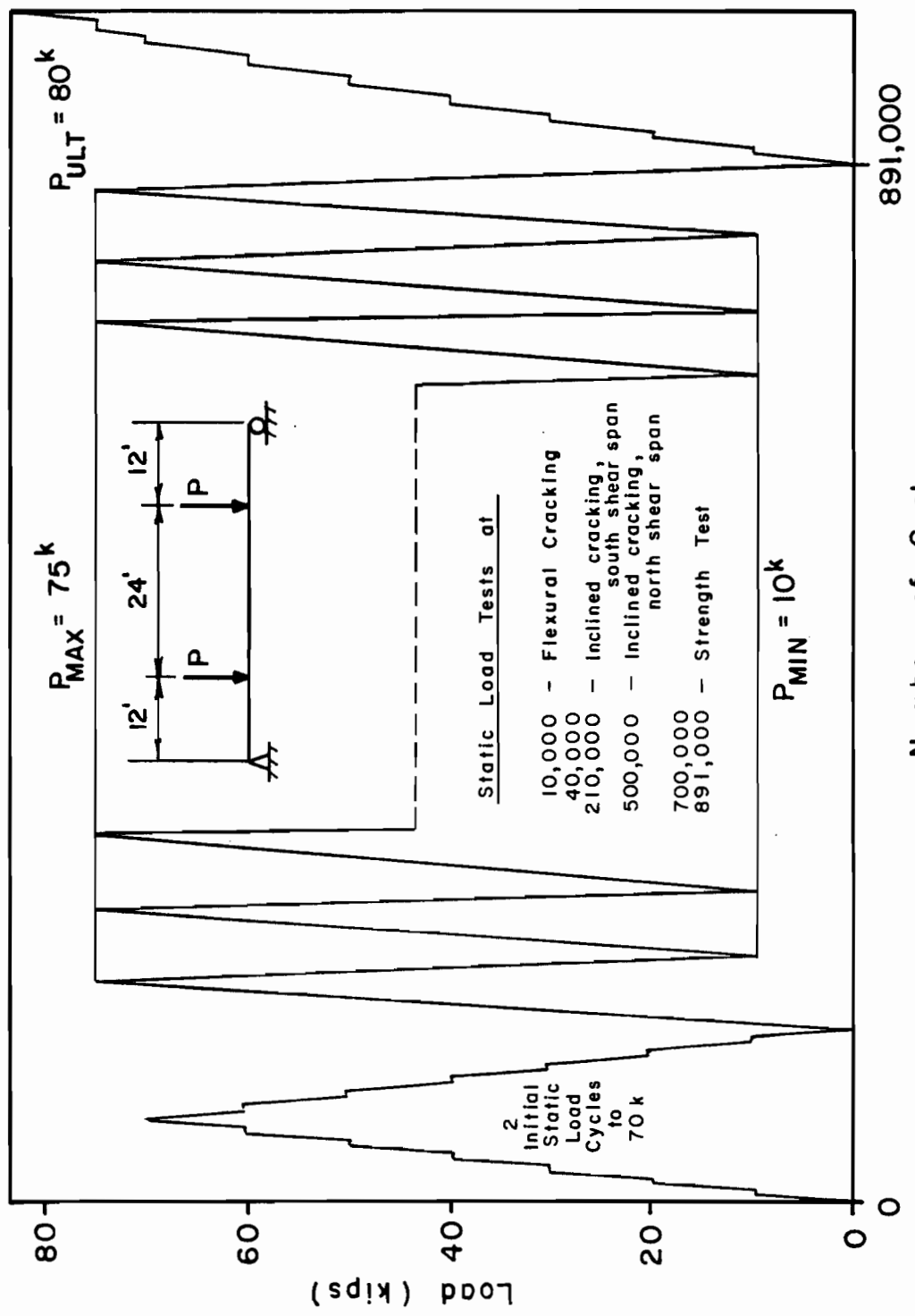

Fig. 4.11 Load program for Beam 2

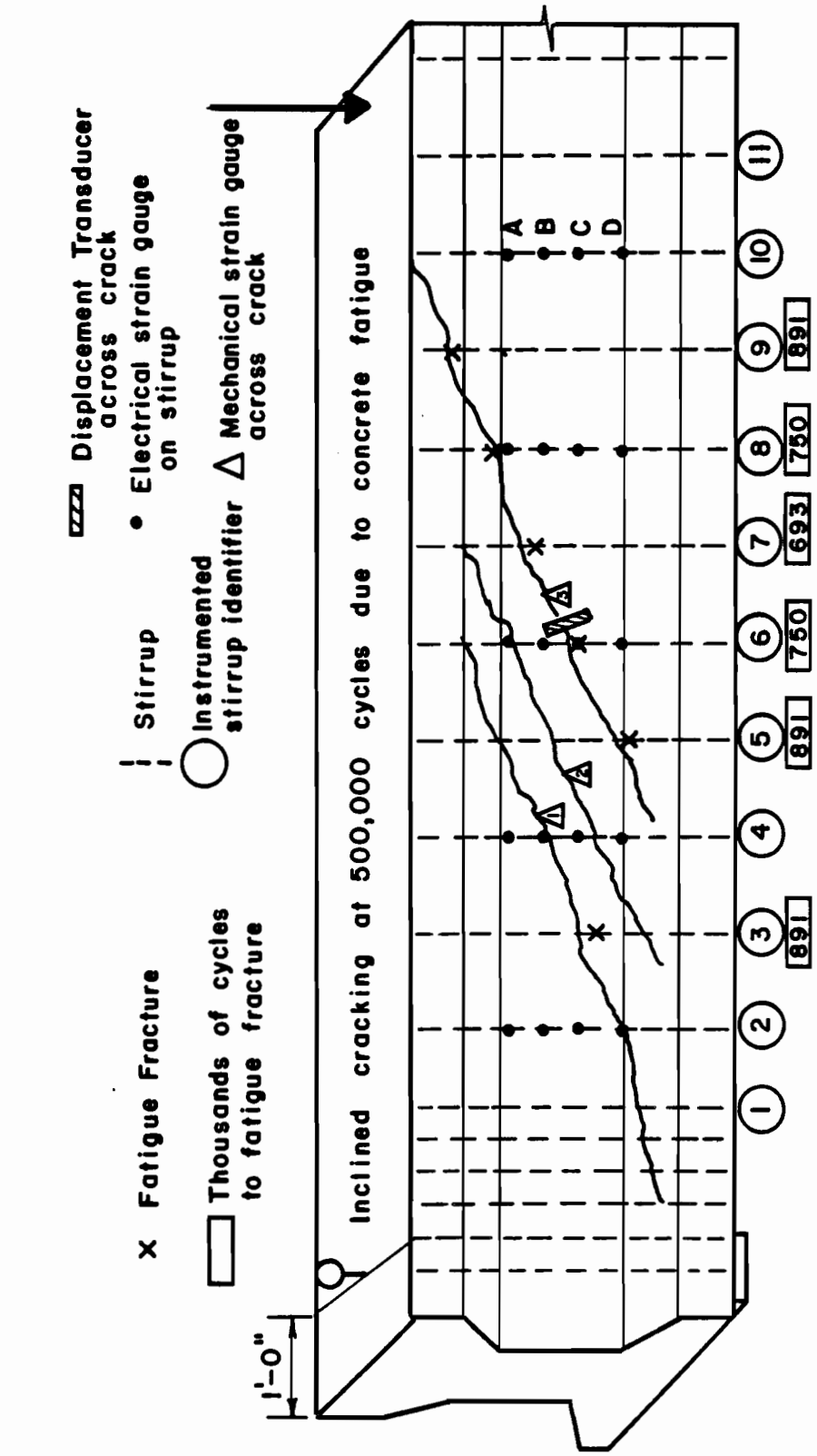

Fig. 4.12 Beam 2, north shear span; instrumentation, crack pattern, and fatigue fractures

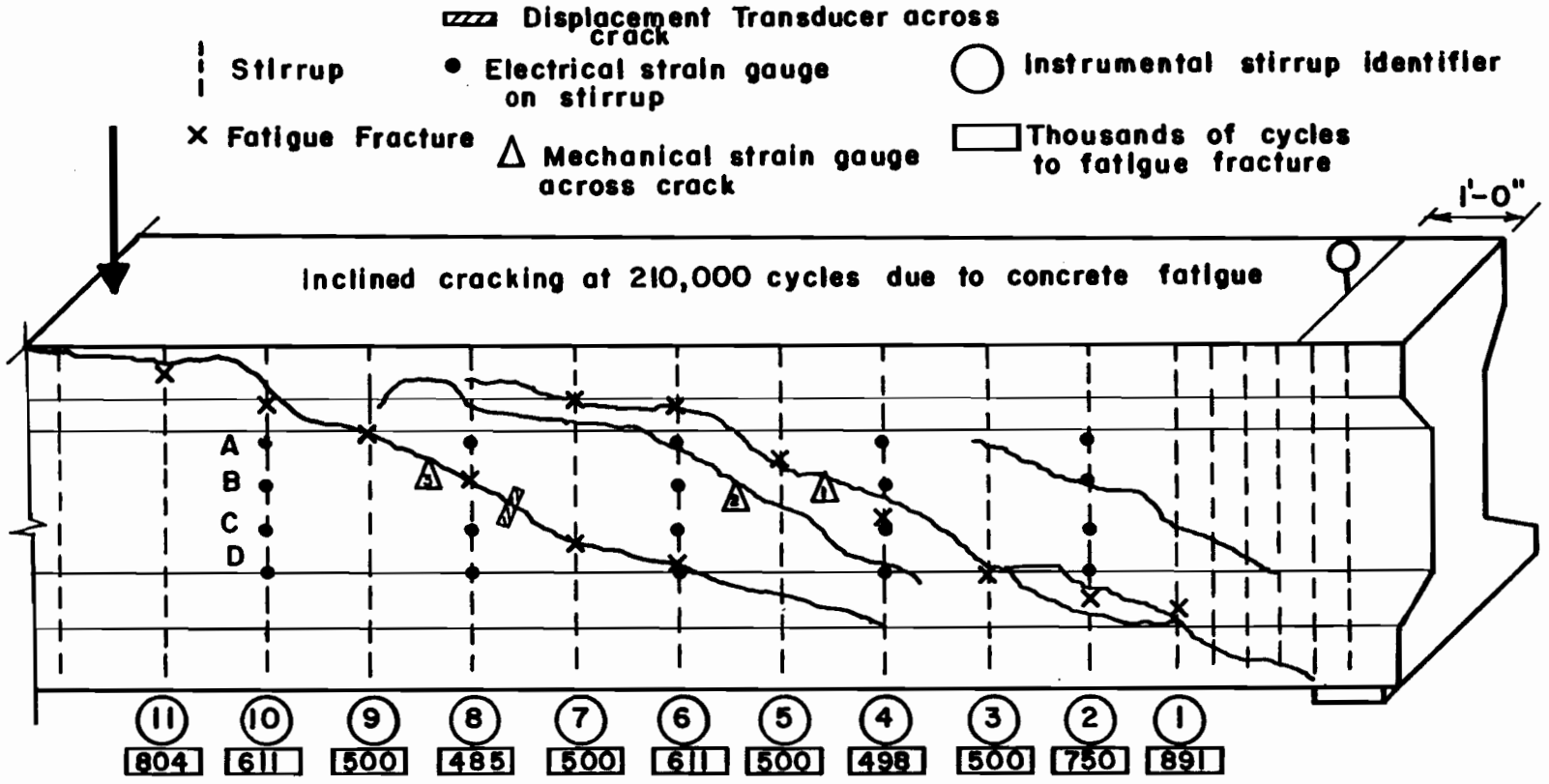

Fig. 4.13 Beam 2, south shear span; instrumentation, crack pattern, and fatigue fractures

2. Shear truss after cracking with stirrups acting as vertical tension members and concrete as inclined compression struts.

3. Tied arch, after several stirrups fractured, with concrete forming an arch and prestressing strand acting as a tension tie.

The transfer from the shear truss to the tied arch mechanism was not sudden but gradual.

4.3.2 Uncracked Behavior. Initially, two cycles of static load up to 70 kips were applied to check the data acquisition system. This load did not initiate flexural or inclined cracking. Stirrup stresses were recorded but were less than 1 ksi as expected for an uncracked section. Fatigue loading was applied with an upper load of 75 kips, which was 5 kips less than the upper load for Beam 1. The maximum fatigue load is compared with AASHTO service loads in Sec. 5.1. The maximum computed diagonal tension stress was 311 psi or $3.76\sqrt{f'_c}$ at a section at the top of the web, 24 in. (h/2) from the face of the support. The corresponding maximum bottom fiber tensile stress at midspan was 443 psi or $5.36\sqrt{f'_c}$.

Fatigue loading was stopped at 10,000 cycles to perform a one-cycle static load test and to examine the girder for new cracks. The maximum applied load for this test and subsequent static load tests was 75 kips. Seven flexural cracks were detected in the constant moment region extending a maximum of 11 in. from the bottom of the girder. This demonstrated that flexural cracking can occur for a flexural stress less than $6\sqrt{f'_c}$ under fatigue conditions. Flexural cracks did not change appreciably throughout the remaining life of Beam 2. Only one additional crack was detected at 40,000 cycles, and none of the cracks ever propagated into the web of the section (14.5 in. from the bottom of the girder).

Inclined cracking in the south shear span was detected at 210,000 cycles while fatigue loading was in progress. Three major cracks were easily visible and extended across the web of the girder at an angle of approximately 35 degrees from the horizontal. One cycle of static load was performed at this time to mount mechanical strain gages across cracks, measure crack openings, and record strain versus load measurements for some of the electrical strain gages near inclined cracks. It was established that the stirrups were experiencing significant stresses with the highest stress ranges being 35, 20, and 33 ksi

on gages S4C, S6A, and S8B respectively (S denotes south shear span, N denotes north shear span). These gages may be located in Fig. 4.13. The girder was effectively transferring shear through truss action. Inclined cracks were easily visible with no load on the girder at this stage in the test. Fatigue loading was resumed with an upper load of 75 kips.

Inclined cracking was detected in the north shear span at 500,000 cycles. As with the south shear span, three major cracks formed at an angle of approximately 35 degrees from the horizontal. Mechanical strain gages were mounted across the cracks and a cycle of static load was performed to measure crack openings and stirrup stresses. The highest stress ranges were 29, 32, and 35 ksi at gages N4B, N6C, and N8A respectively. These gages may be located in Fig. 4.12. As for the south shear span, cracks were easily visible with no load applied on the girder.

It is interesting that the north shear span cracked 300,000 cycles later than the south shear span. Both hydraulic rams were operated from the same pulsator piston, so it is unlikely that the loads were different in the north and south shear span. It is likely that this discrepancy reflects the scatter inherent in concrete tensile fatigue strength.

4.3.3 Post-Cracking Behavior. The first cracking encountered during fatigue testing was flexural cracking. As previously mentioned, cracks did not propagate significantly and flexural response remained relatively constant throughout the life of the girder. This was not the case with inclined cracking.

After inclined cracks developed in the south and north shear spans, LVDT's were mounted across the cracks so that the changes in crack opening could be monitored continuously with an electronic signal peak detector. The location of the LVDT's is shown in Fig. 4.12 and 4.13. Figure 4.14 illustrates the rapid increase in crack width during fatigue loading over the life of the specimen. The change in the south shear span crack opening was approximately linear throughout the life of the girder. The change in the north shear span crack opening was not linear; crack opening increased dramatically late in the life of the girder to nearly the same level as the south shear span crack opening.

Stirrup strain ranges near crack openings were also monitored continuously on the electronic signal peak detector

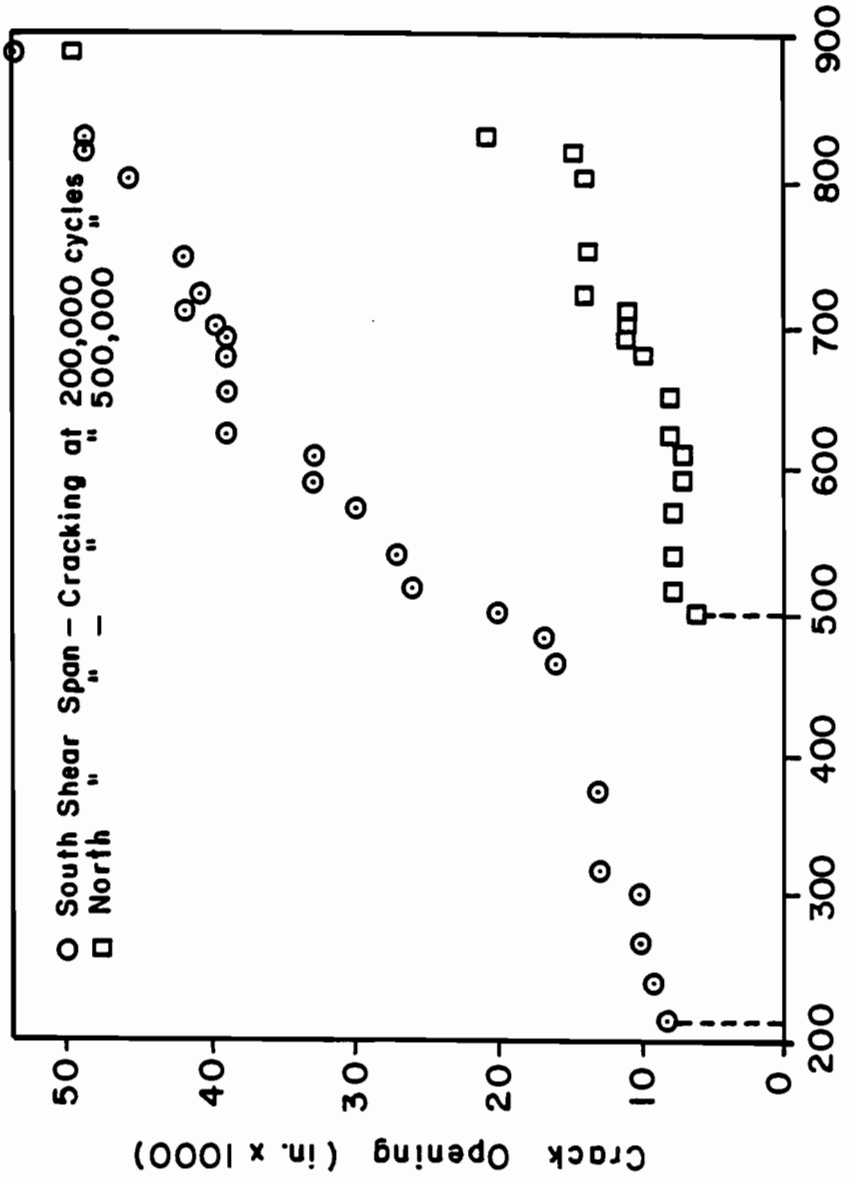

Fig. 4.14 Maximum crack width during fatigue loading over the life of Beam 2

during fatigue loading. As shown in Figs. 4.15 and 4.16, stirrup stress ranges also increased rapidly throughout the life of the specimen. The increase in stress range on gage S8B (for location see Fig. 4.13) was approximately linear until the stirrup fractured at 485,000 cycles. The increase in stress range for gage N6C (for location see Fig. 4.12) followed more of a parabolic shape. This agrees qualitatively with the distribution of crack-width data for the north shear span (Fig. 4.14).

The approximately linear relationship between stirrup stress range and crack opening seemed to hold throughout the life of the specimen. This is important because it implies that there was little debonding of stirrups along their length once a crack had formed. This observation is also supported by the fact that very low stress ranges were measured on gages more than a few inches away from a crack.

Figure 4.17 illustrates the general shape of the load-stress range curve for electrical strain gage S6A (for location see Fig. 4.13). Most of the strain gages exhibited this type of bilinear behavior with the first portion of the curve being nearly vertical. This portion of the curve could be considered the concrete contribution to shear strength and represents the load necessary to overcome the prestress force and initiate widening of the inclined crack. It should be noted that as the number of fatigue load cycles increased, the vertical portion of the curve became shorter and the inclined portion became less steep, resulting in an increase in stirrup stress range. Figure 4.18 illustrates the general shape of the load-crack opening curve for the south shear span as measured at the location of the LVDT (for location see Fig. 4.13). This curve also exhibits some bilinear behavior that became less pronounced as the number of fatigue cycles progressed.

Mechanical strain gages were mounted across the three major inclined cracks on the north and south shear spans (for location see Figs. 4.12 and 4.13 respectively). They were positioned so that vertical and horizontal components of residual crack widths, and change in crack width with load, could be measured. Throughout this discussion, a crack and its associated mechanical strain gage will be referred to by the same number (crack S3 is the crack monitored by mechanical strain gage S3). All crack and mechanical strain gage positions are shown in Figs. 4.12 and 4.13 for the north and south shear spans, respectively. Figure 4.19 illustrates that the change in vertical crack opening did not increase for all cracks in the south shear span. Instead, the size of crack S2 decreased as the test progressed.

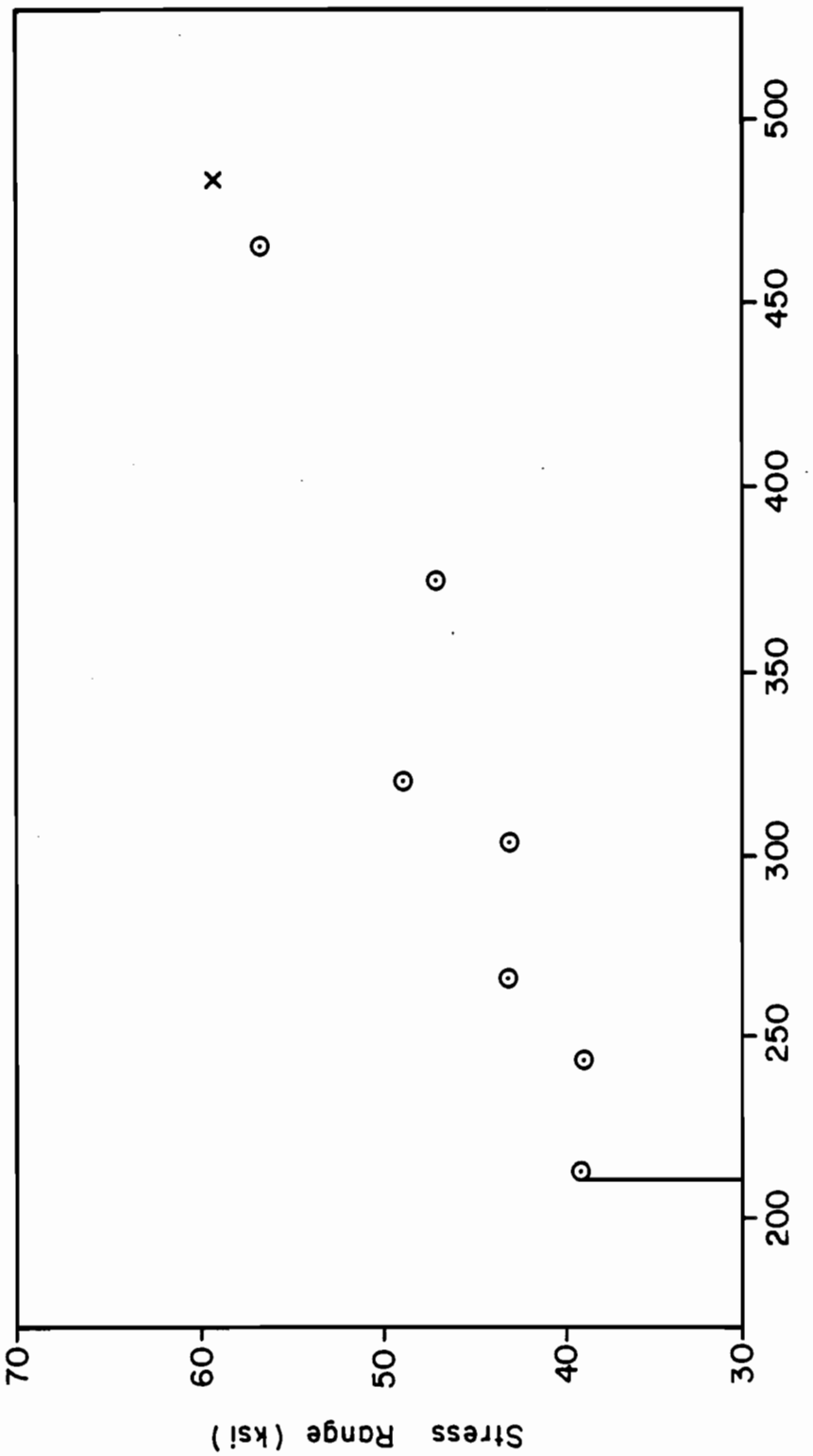

Fig. 4.15 Electrical strain gage S8B monitored with electronic signal peak detector

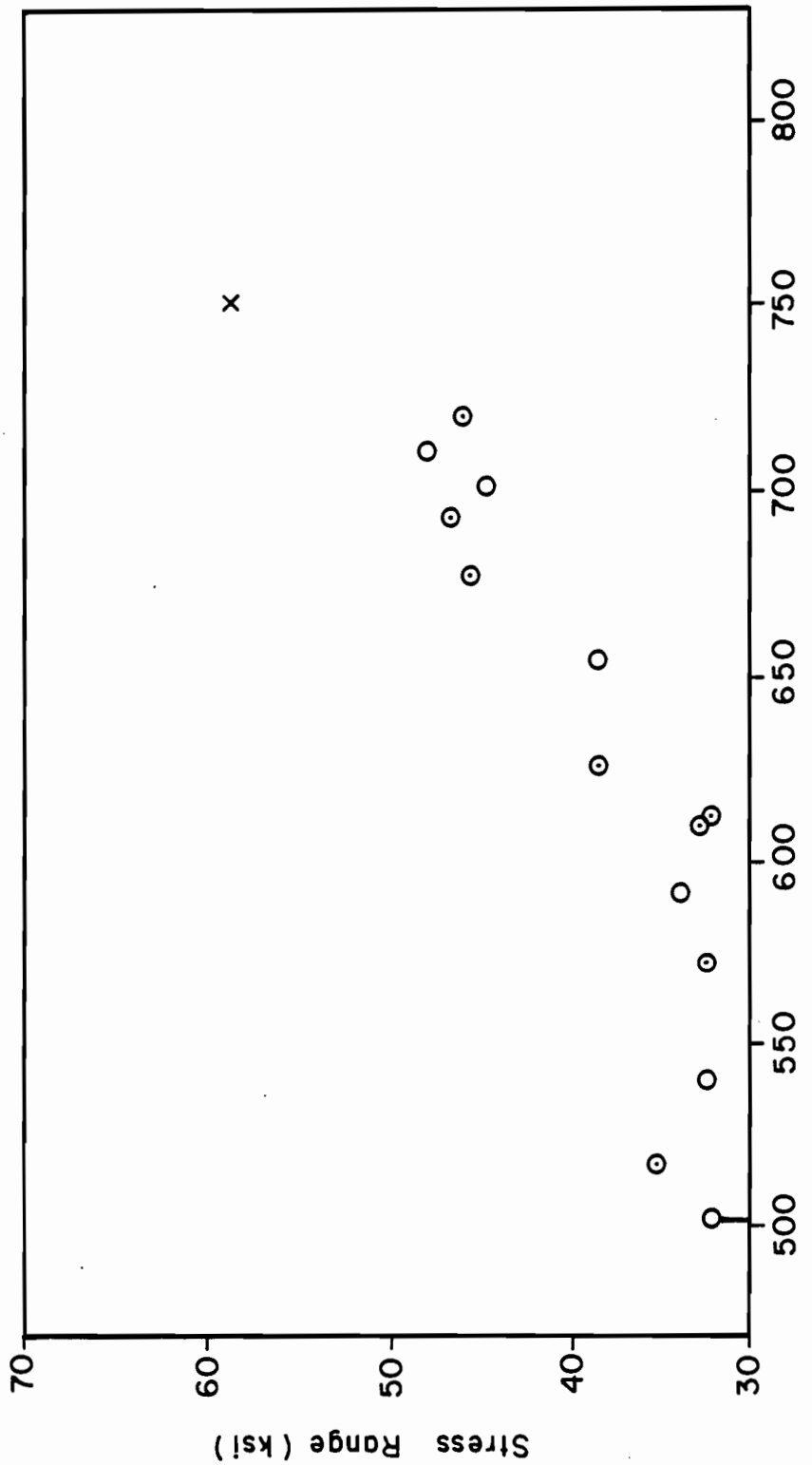

Fig. 4.16 Electrical strain gage N6C monitored with electronic signal peak detector

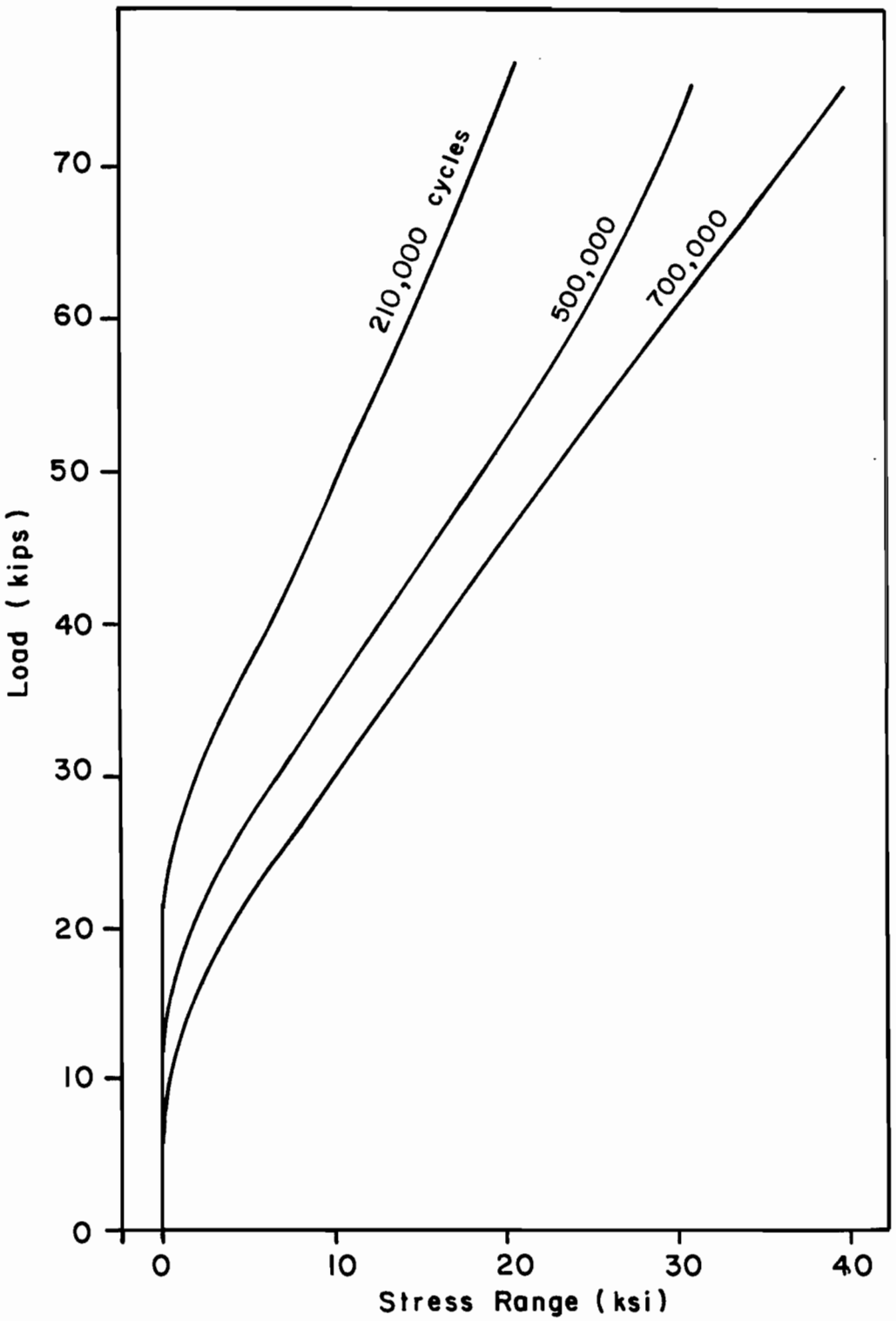

Fig. 4.17 Load versus stirrup stress range over the life of Beam 2 for electrical strain gage S6A.

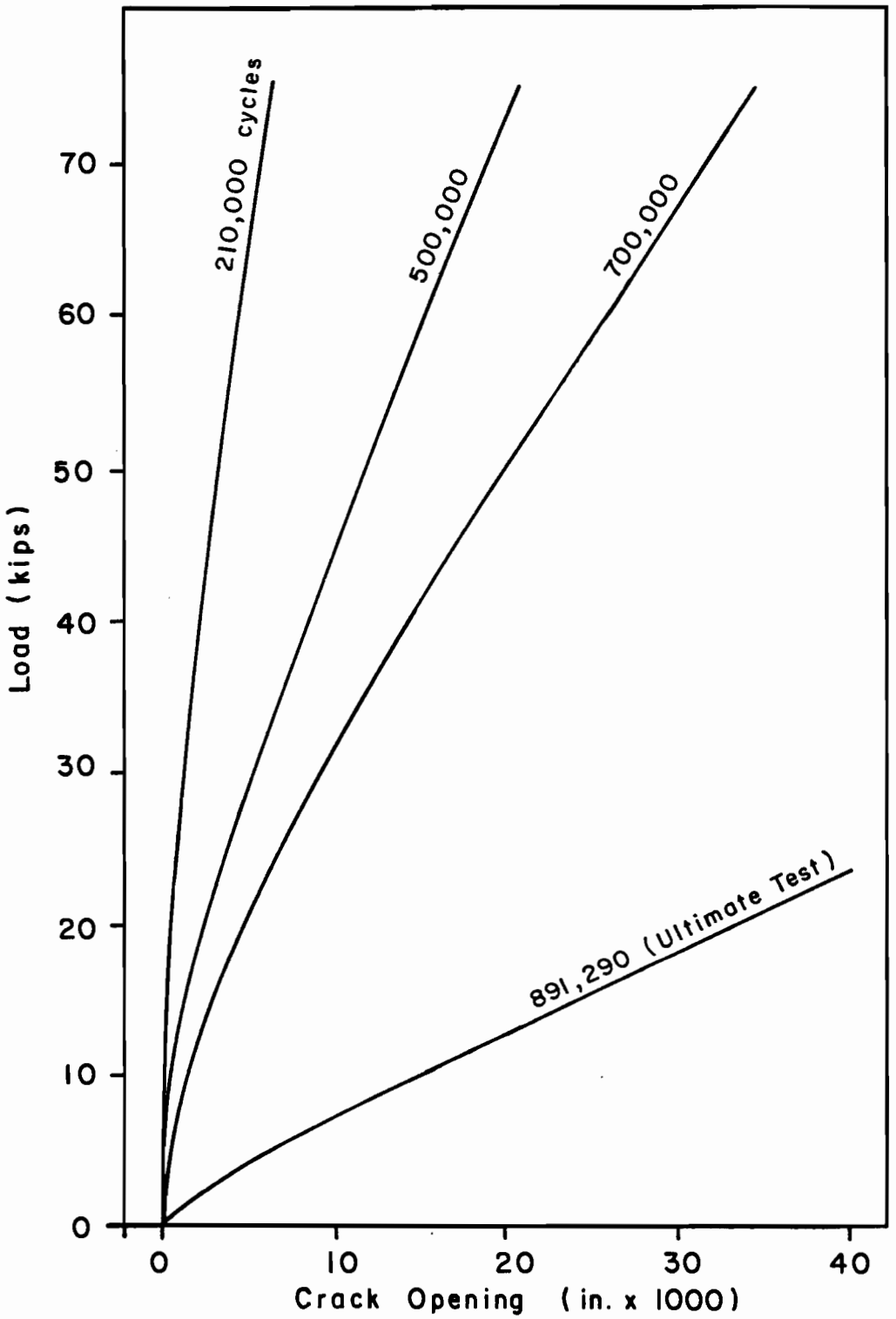

Fig. 4.18 Load versus crack opening for the south shear span over the life of Beam 2

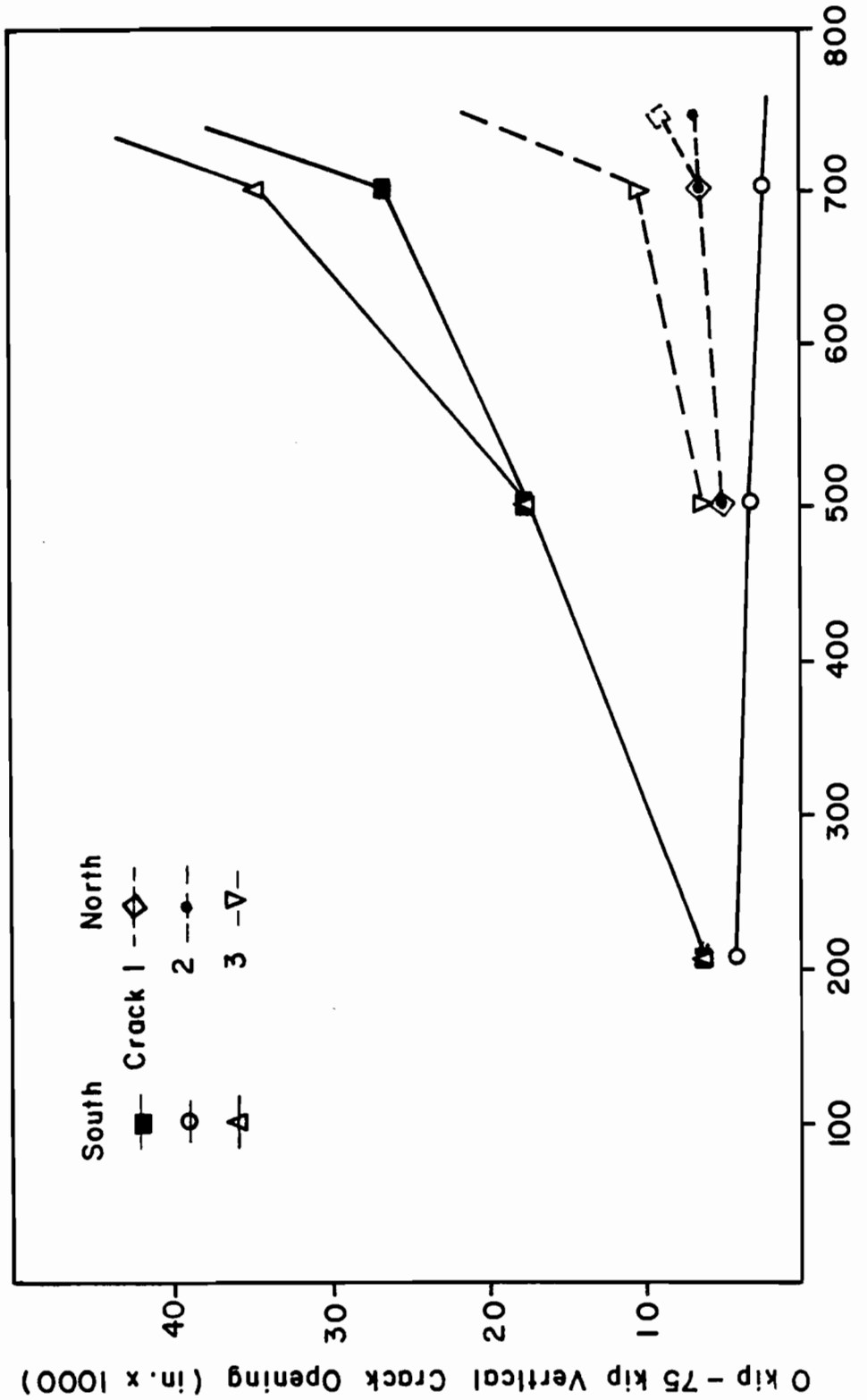

Fig. 4.19 Beam 2, history of vertical crack opening

This was confirmed by the fact that no stirrups fractured across crack S2. In the north shear span, crack N3 was dominant as reflected by the crack width-load cycles plot and five of six fractures in the north shear span along crack N3. Figure 4.20 illustrates that the change in horizontal crack opening did not increase as rapidly as the change in vertical crack opening. However, the same trends are present in the plot of horizontal crack opening as for the plot of vertical crack opening. A change in horizontal crack opening would impose bending and shear stresses on the stirrups. Figure 4.21 illustrates the relationship between vertical and horizontal crack opening. Clearly, the change in vertical crack opening increased much faster than the change in horizontal crack opening, especially as the fatigue history of the specimen progressed. Figure 4.22 illustrates the residual vertical crack opening (crack opening which remains after unloading the specimen) for the south shear span. This behavior reflects the gradual debonding of stirrups along their length near the crack. Figure 4.23 shows the residual horizontal crack opening for the south shear span. This crack opening remained very small until the end of the test when several stirrups fractured, indicating that there was very little permanent deformation in the horizontal direction.

After Beam 2 cracked and a shear truss mechanism formed, the shear fatigue deterioration was rapid and changes in behavior of the specimen were apparent almost every time data was recorded (approximately every two hours or 20,000 cycles during working hours). Changes in the specimen included visible widening of the inclined cracks and a steady change in the strain range for the stirrups that were monitored continuously during fatigue loading (Figs. 4.15 and 4.16). Figure 4.24 shows stress range versus number of cycles to failure for stirrups which had electrical strain gages near fractures. Some of the data are plotted as a vertical line because the stress range was not constant throughout the life of the specimen.

The first stirrup to fracture was S8 in the south shear span at 485,000 cycles. The failure was first detected by erratic readings on the electronic signal peak detector while fatigue loading was in progress. The following day the concrete cover was removed in the area of the stirrup fracture to check for corrosion around the fracture surface (Fig. 4.25). Although it cannot be seen on a black-and-white photograph, corrosion was present, which indicates fretting may have occurred.

At 750,000 cycles stirrups S2 through S10 in the south shear span had fractured and an additional inclined crack had

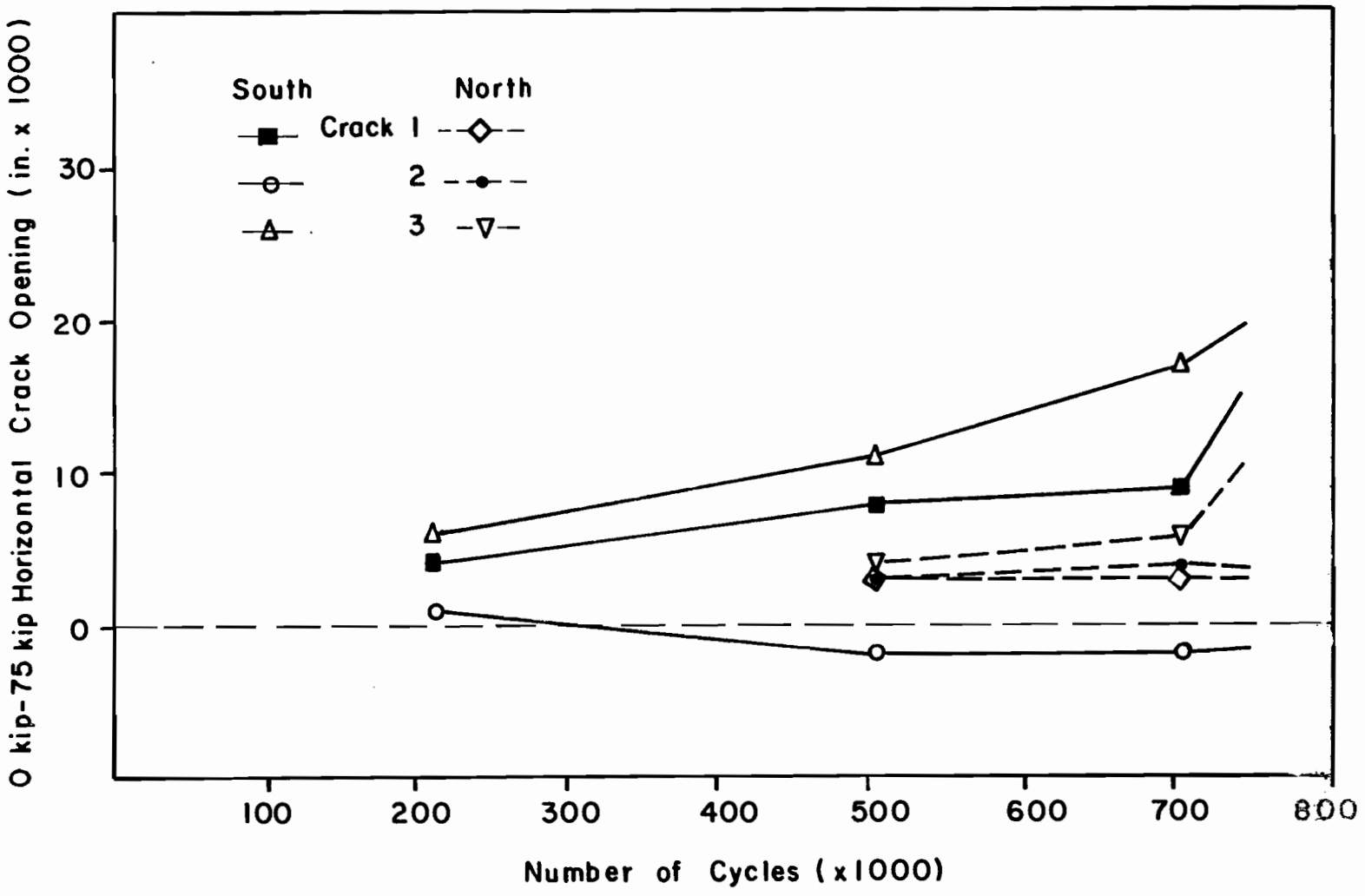

Fig. 4.20 Beam 2, history of horizontal crack opening

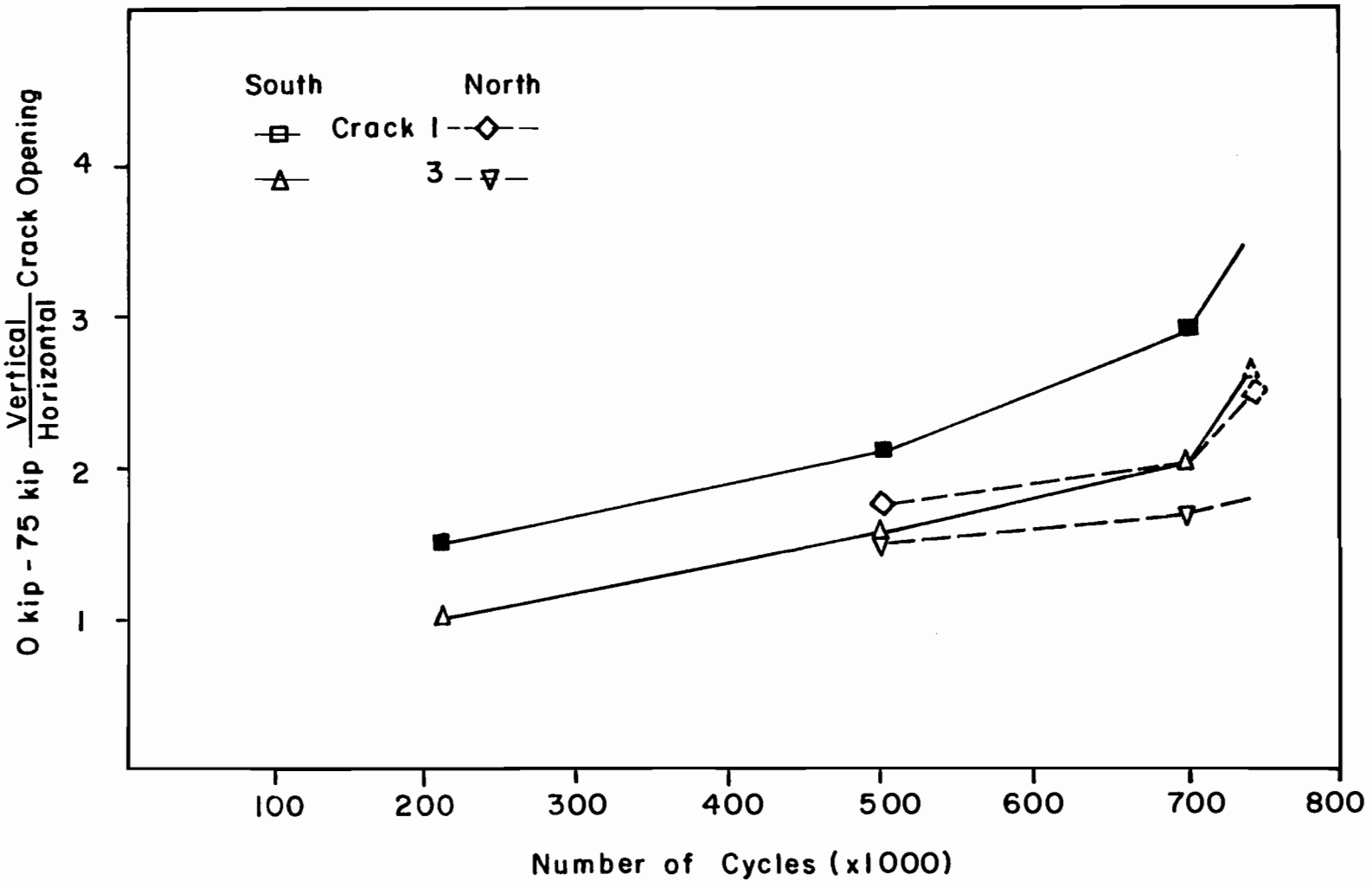

Fig. 4.21 Beam 2, relationship between horizontal and vertical crack opening with progressive load cycles

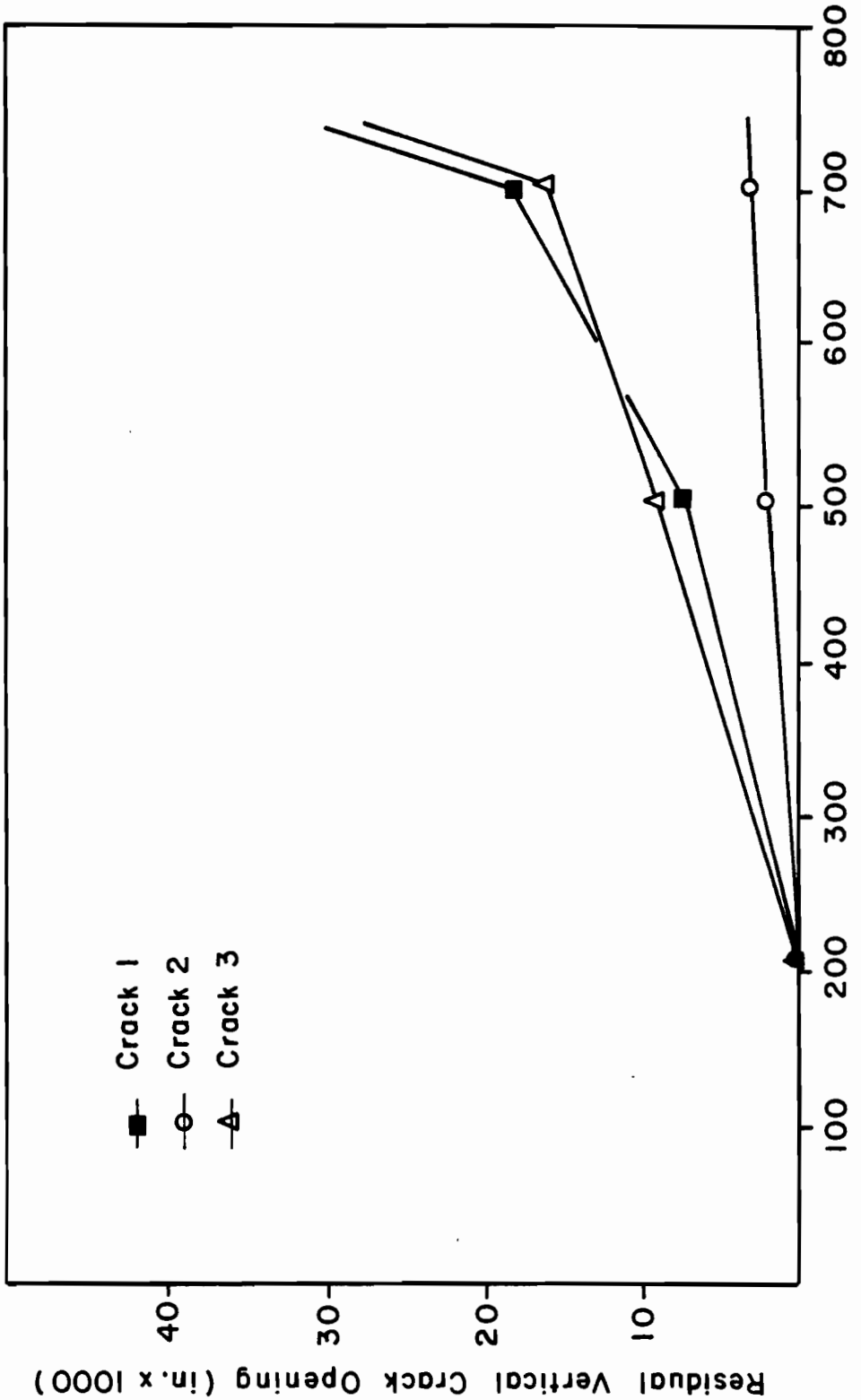

Fig. 4.22 Beam 2, south shear span, residual vertical crack opening with progressive load cycles

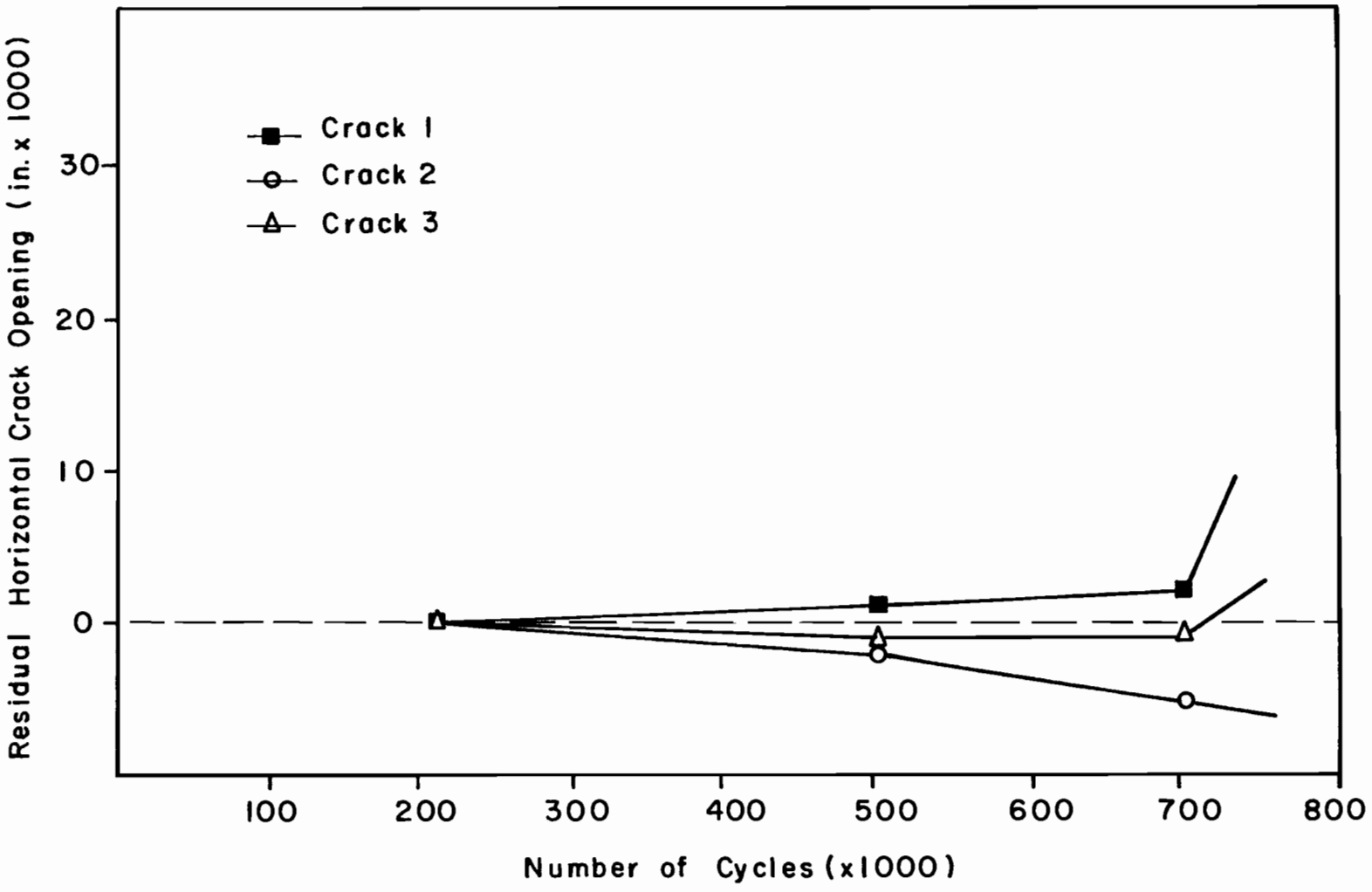

Fig. 4.23 Beam 2, south shear span, residual horizontal crack opening with progressive cycles

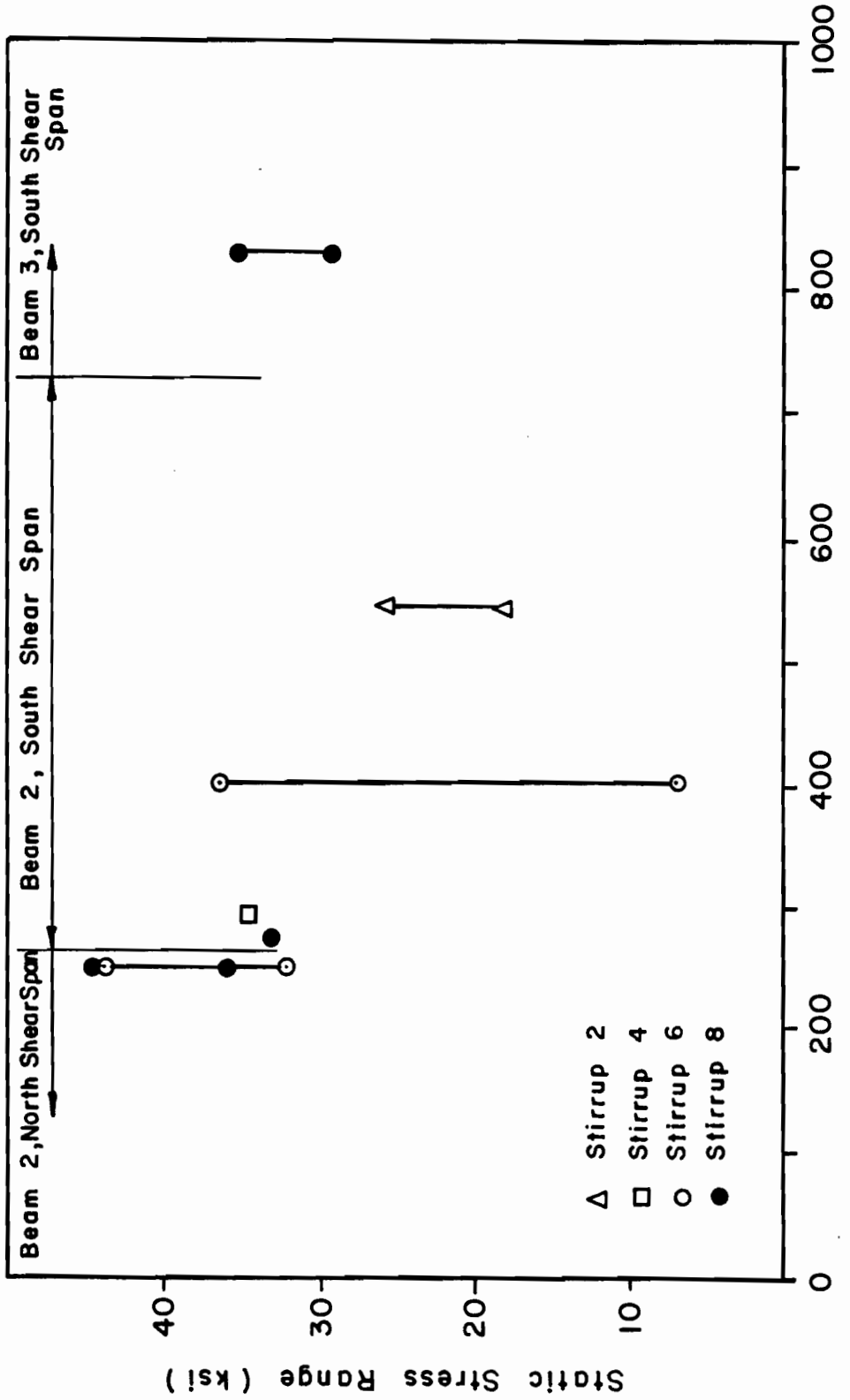

Fig. 4.24 S-N data for selected stirrups in Beam 2 and Beam 3

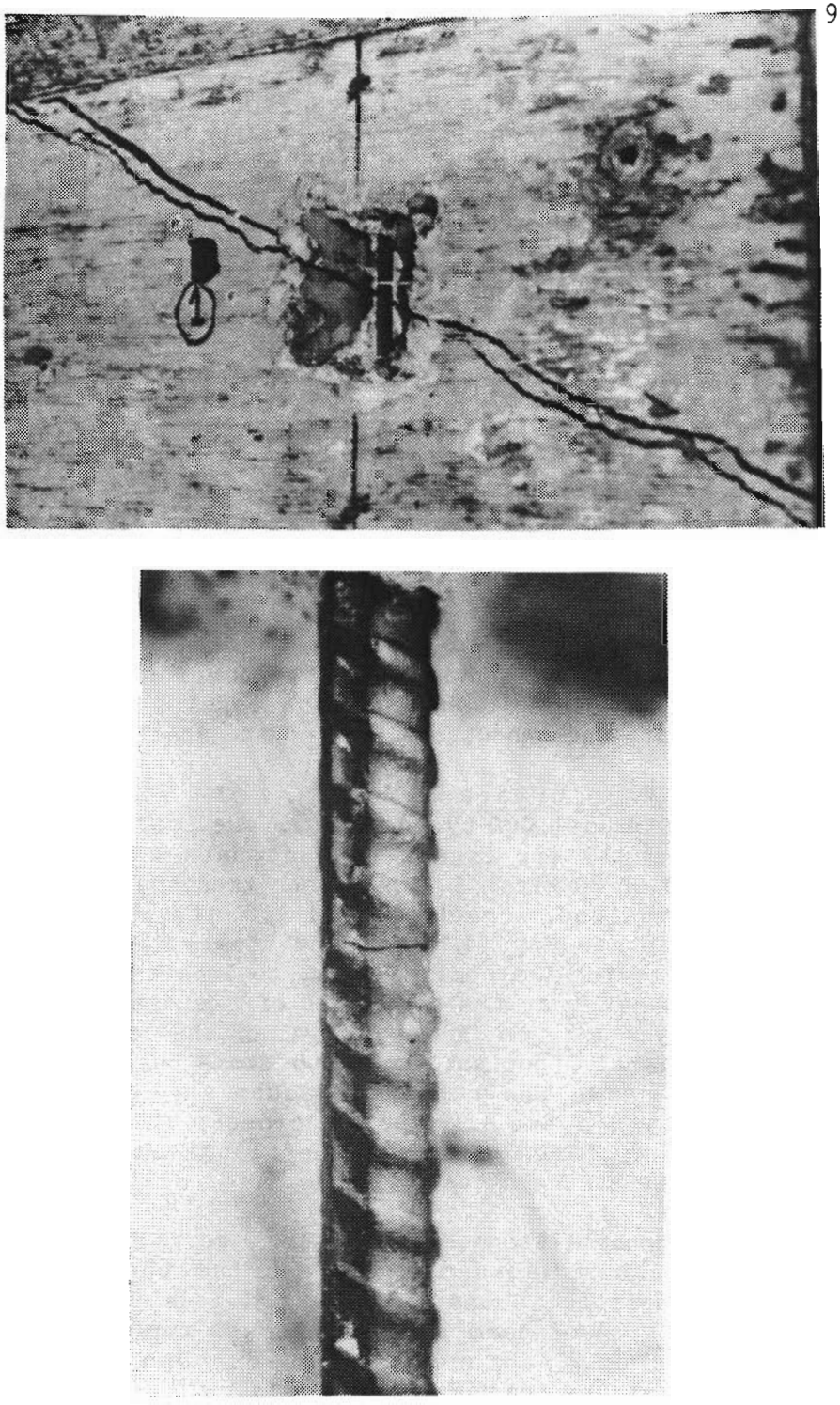

Fig. 4.25 First stirrup fracture in south shear span (concrete cover removed to expose fracture)

formed in the top of the web, near the support, through the heavily reinforced anchorage zone (for location see Fig. 4.13). Stirrups S6 and S7 had actually fractured in two locations. In addition, the top two prestressing strands in the south shear span had slipped approximately 0.01 in. in a similar manner as shown in Fig. 4.7 for Beam 1. The shear-truss mechanism was no longer possible after the stirrups had failed. Shear forces were developed through a system that resembled a tied arch. The load pulsator stopped at 891,000 cycles because of a sudden increase in deflection. The inclined crack monitored by mechanical strain gage S1 had progressed through the bottom flange at the south end of the girder. Figure 4.26 shows the net change in deflection of Beam 2 along its length from 10,000 to 500,000 cycles and from 10,000 to 700,000 cycles. It can be seen that most of the change in deflection was concentrated in the south quarter of the beam where the shear failure finally occurred. Figure 4.27 shows that the centerline deflection of Beam 2 remained fairly constant throughout the life of the specimen. In fact, during the ultimate strength test the maximum centerline deflection was approximately 1/2 in., indicating the portion of the specimen dominated by flexural behavior (the constant moment region) remained intact throughout the life of the specimen.

4.3.4 Ultimate Behavior. The strength test was performed after 891,000 cycles of fatigue loading. The girder was loaded in 10 kip increments and data were recorded. A maximum load of 80 kips, 5 kips higher than the maximum fatigue load, was attained. Cracks S1 and S3 in the south shear span (for location see Fig. 4.13) opened to greater than 1 in. at ultimate, allowing the research team to look through the web of the beam. Strands at the south end of the beam were recessed approximately 1-1/8 in. After removal of the load, the specimen recovered slightly, but not enough to close the inclined cracks. Figure 4.28 shows the north and south shear span after the strength test. Figure 4.29 shows a closeup view of the failure region and the offset of the bottom flange in the south shear span after the strength test.

Upon completion of the strength test, the stirrups were uncovered with a jackhammer to examine the fractures and determine their locations. Figure 4.30 is a photograph of the north shear span of Beam 13 with the web concrete removed to expose stirrup fractures. The stirrups are separated horizontally at the fracture for clarity.

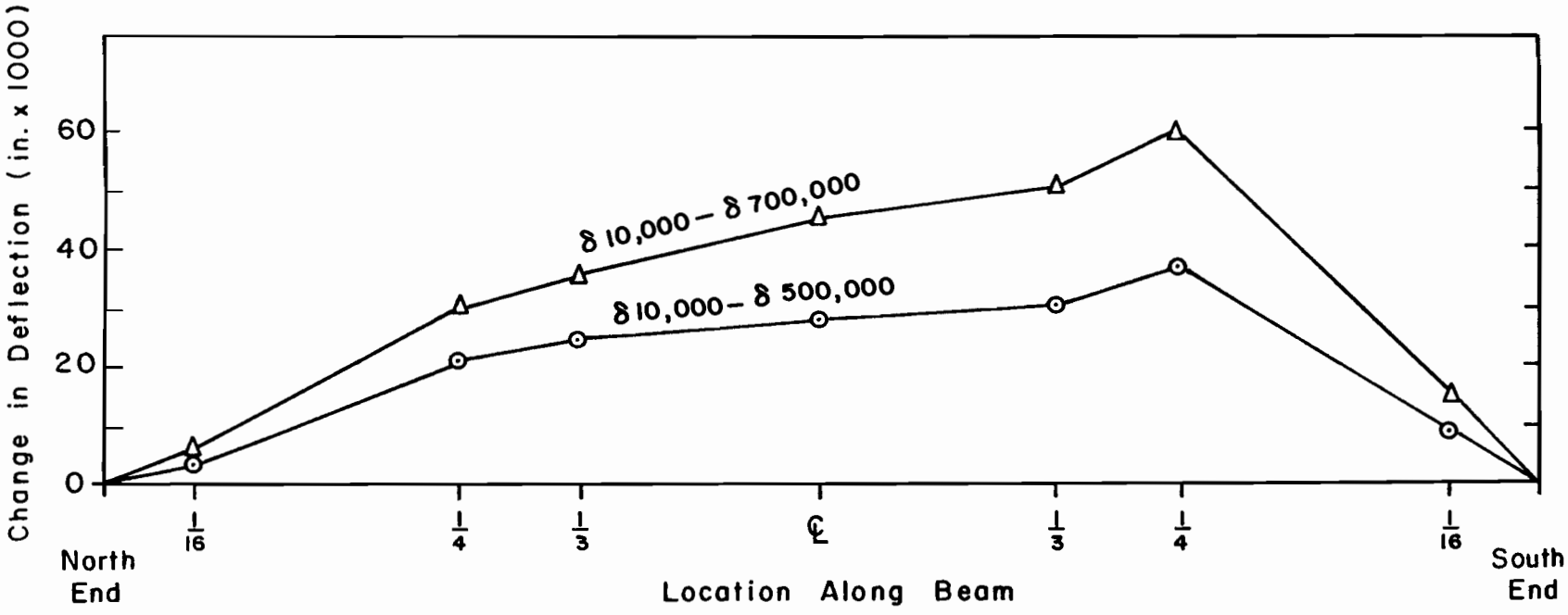

Fig. 4.26 Change in deflection along Beam 2 from 10,000 to 500,000 cycles and from 10,000 to 700,000 cycles

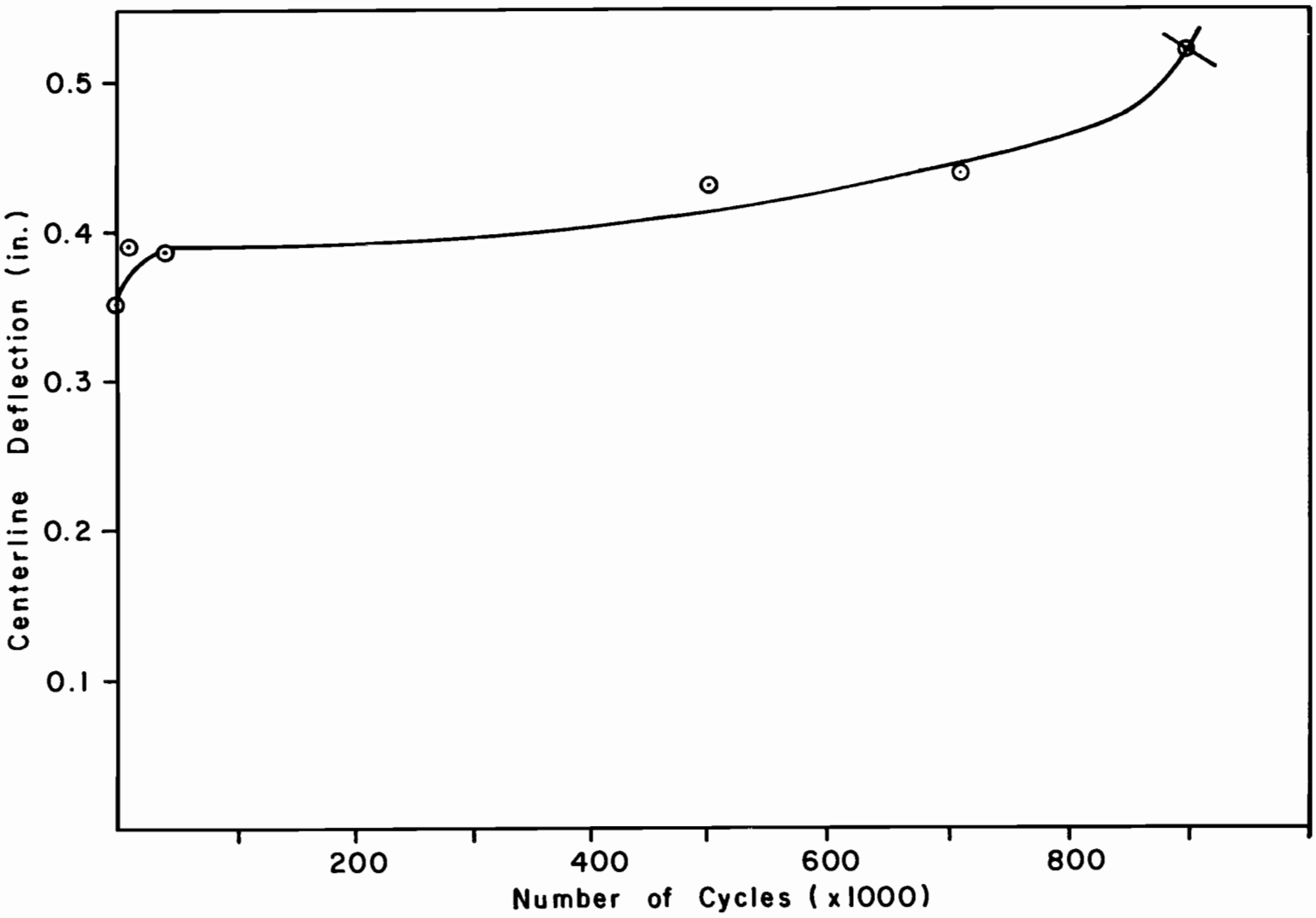

Fig. 4.27 Centerline deflection versus number of load cycles for Beam 2

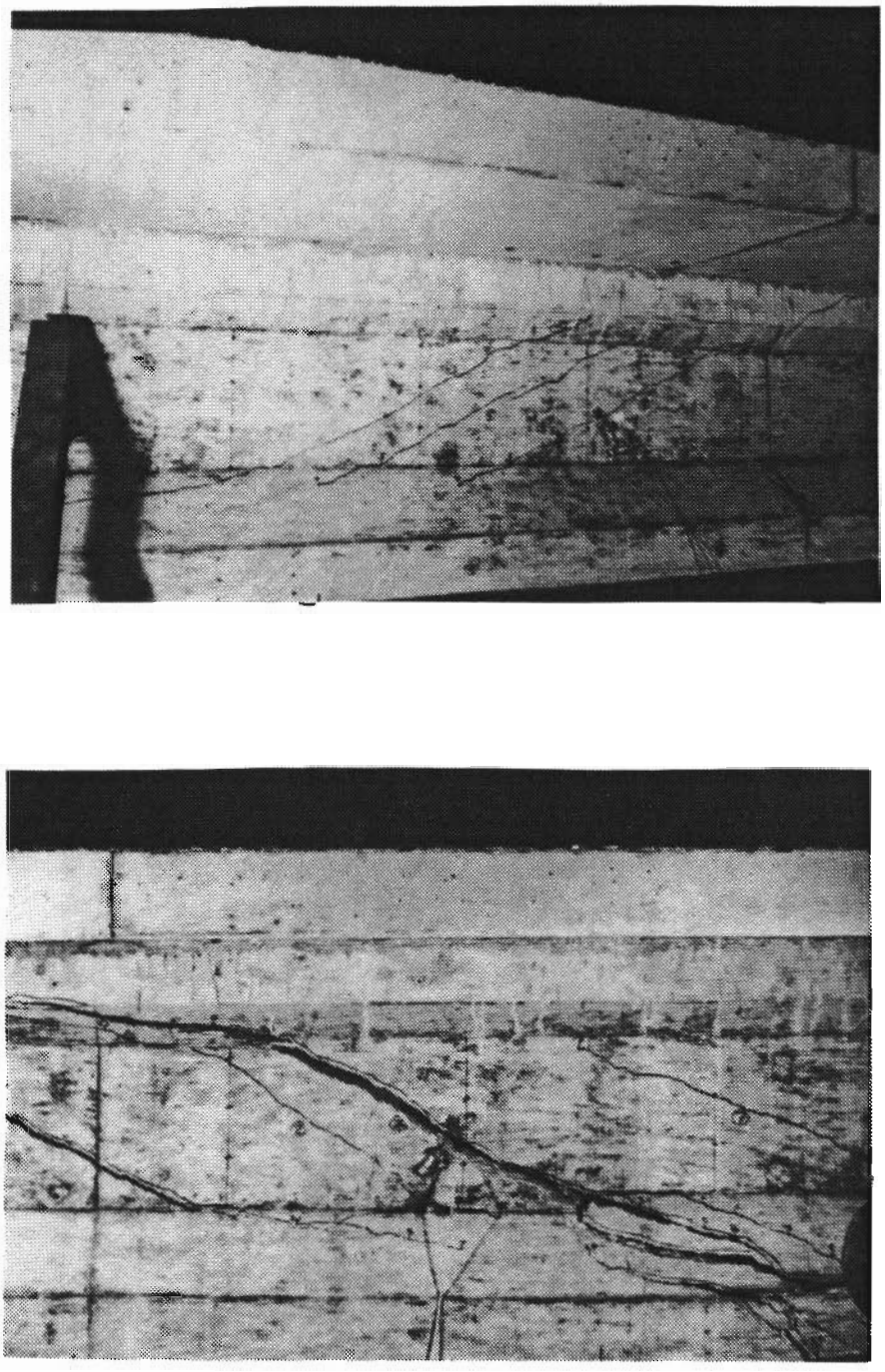

Fig. 4.28 Inclined crack pattern in north (top) and south (bottom) shear spans after the strength test

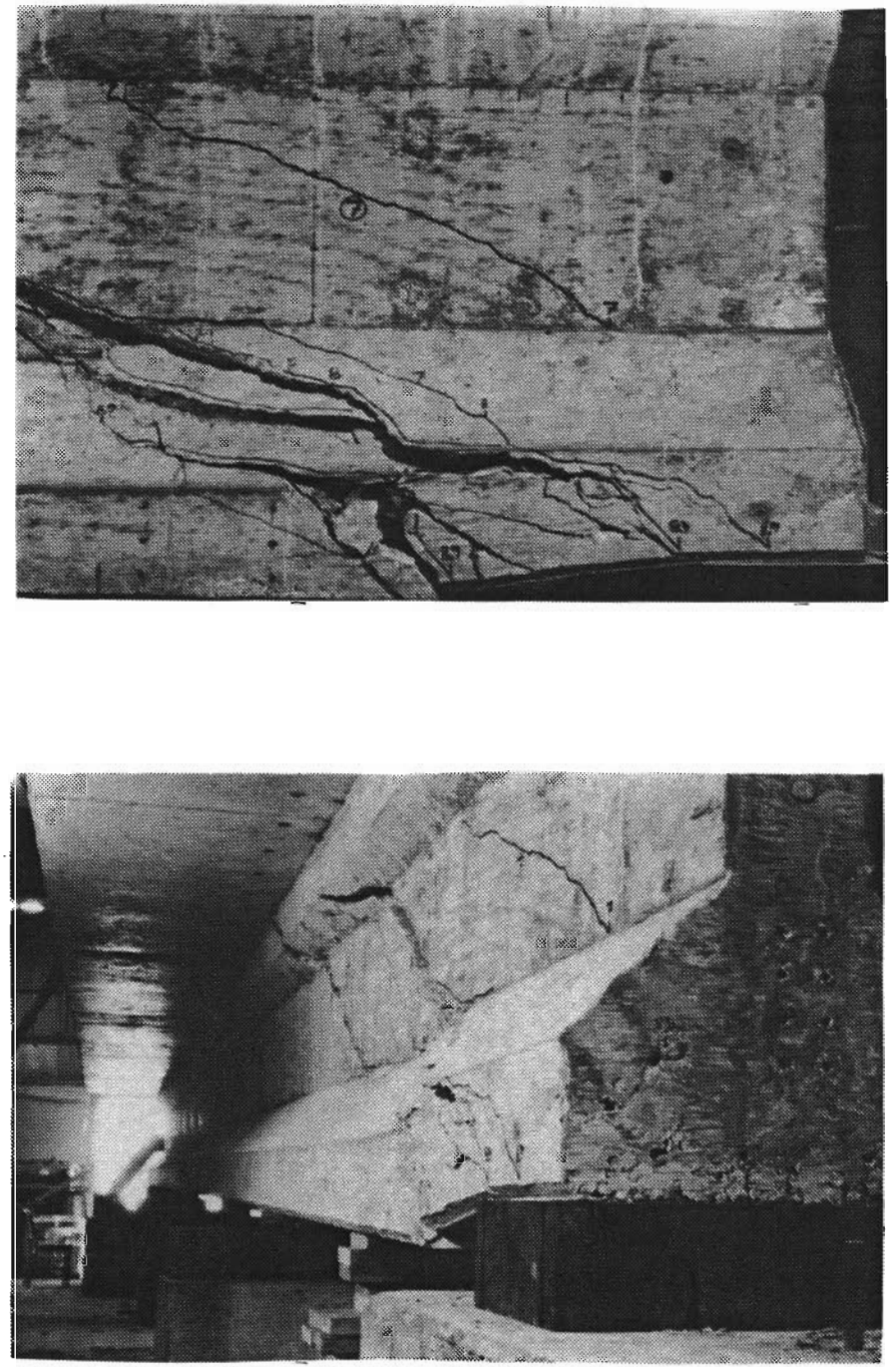

Fig. 4.29 Closeup view of failure region (top) and offset of the bottom flange after the strength test (bottom)

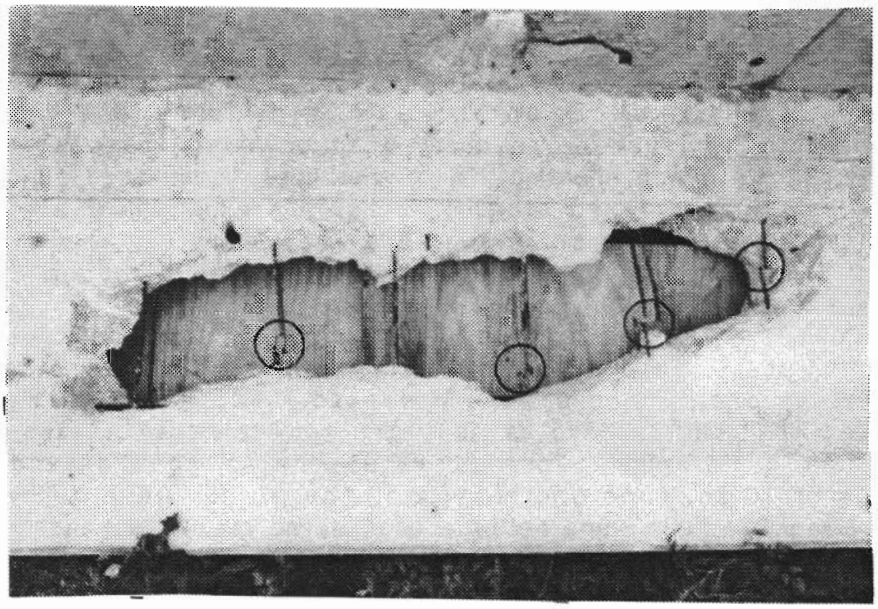

Fig. 4.30 Beam 2, north shear span, web concrete removed to expose fractures (stirrups separated horizontally for clarity)

4.4 Description of the Behavior of Beam 3

4.4.1 General. Testing was started 25 days after the girder was cast. The specimen was not precracked in flexure or shear. A schedule of static and fatigue testing over the life of the girder is shown in Fig. 4.31. An illustration showing instrumentation, crack pattern at ultimate, and fatigue fractures for the south shear span is shown in Fig. 4.32. As with Beam 2, the pickup loops were placed 1 ft from each end of the specimen so that they would not contribute to the shear strength in the center of the shear span. The data acquisition system for reading electrical strain gages was strain indicators with switch-and-balance boxes.

4.4.2 Uncracked Behavior. To begin testing of Beam 3, two initial static load cycles to 67.5 kips were performed to obtain initial data and check data acquisition and instrumentation systems. An upper load of 67.5 kips was chosen for Beam 3. This represented 90% of the upper load used for Beam 2. The maximum computed diagonal tension stress was 299 psi or $3.97\sqrt{f'_c}$ at a section at the top of the web, 24 in. (h/2) from the face of the support. The corresponding maximum bottom fiber tensile stress at midspan was 414 psi or $5.49\sqrt{f'_c}$

A static load test was performed at 38,000 cycles and no flexural or shear cracks were observed. Fatigue loading was continued to 1,000,000 cycles at which time another static load cycle was performed. Four flexural cracks that extended a maximum of 10 in. from the bottom of the girder were detected. As for Beam 2, these were fatigue cracks; no cracks were detected during the initial load cycles. The flexural cracks were detected on one side of the member only, indicating possible substantially different forces in the prestressing strands. No shear cracks were detected.

At this time the maximum fatigue load was increased to 71.3 kips or 95% of the upper load for Beam 2. Fatigue loading was continued to 3,133,000 cycles when testing was stopped because the girder was showing signs of flexural distress, such as an increase in centerline deflection, light spalling along the bottom of the section (no strands exposed), and a large increase in crack opening at the spalled section. No shear cracks had developed yet, so the specimen was loaded statically to produce inclined cracks. At an applied load of 90 kips, four inclined cracks developed in the south shear span (for location see Fig. 4.32) resulting in an immediate increase in the stress levels of stirrups. Stirrup stresses for stirrups located near inclined

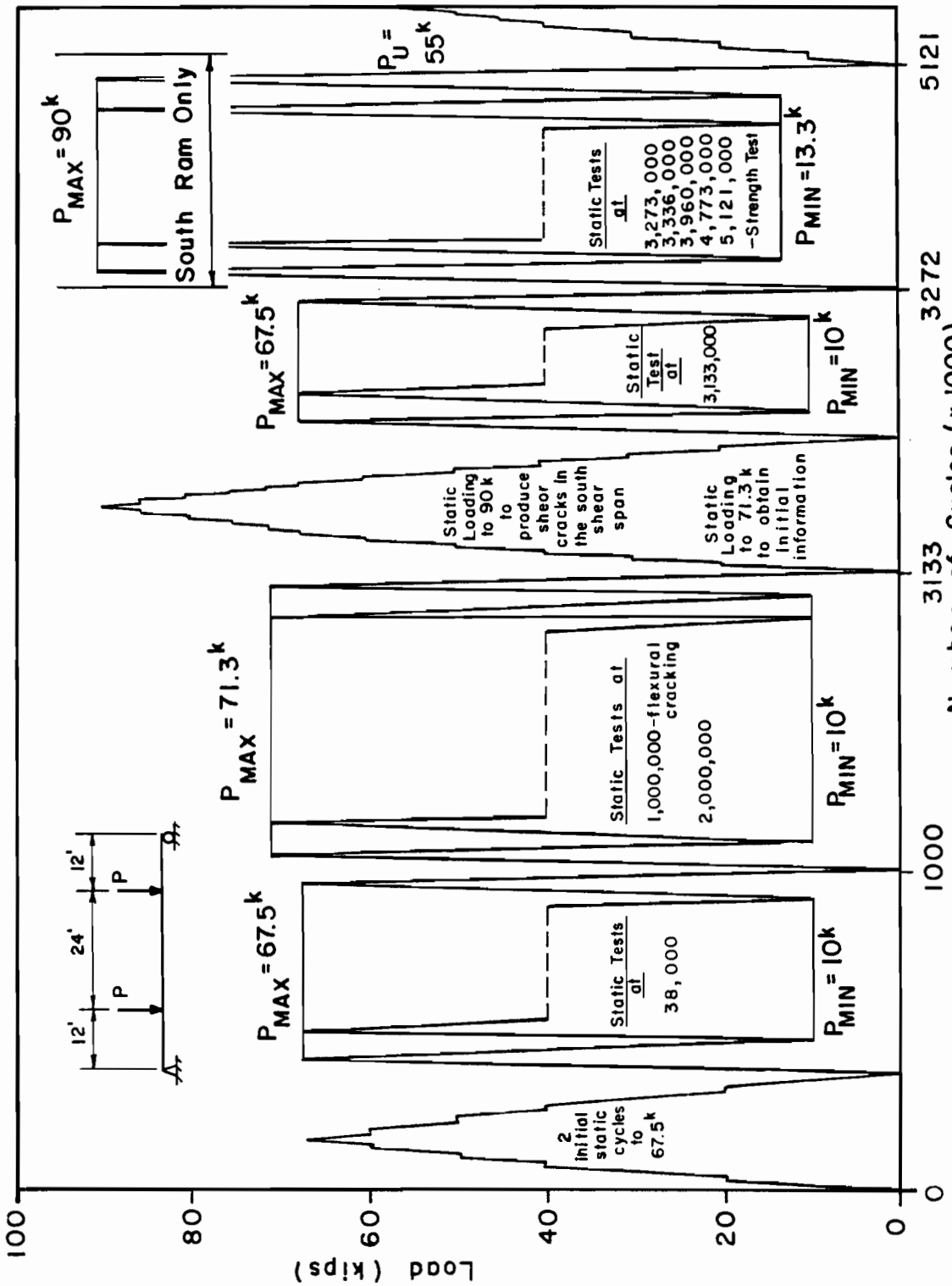

Fig. 4.31 Load program for Beam 3

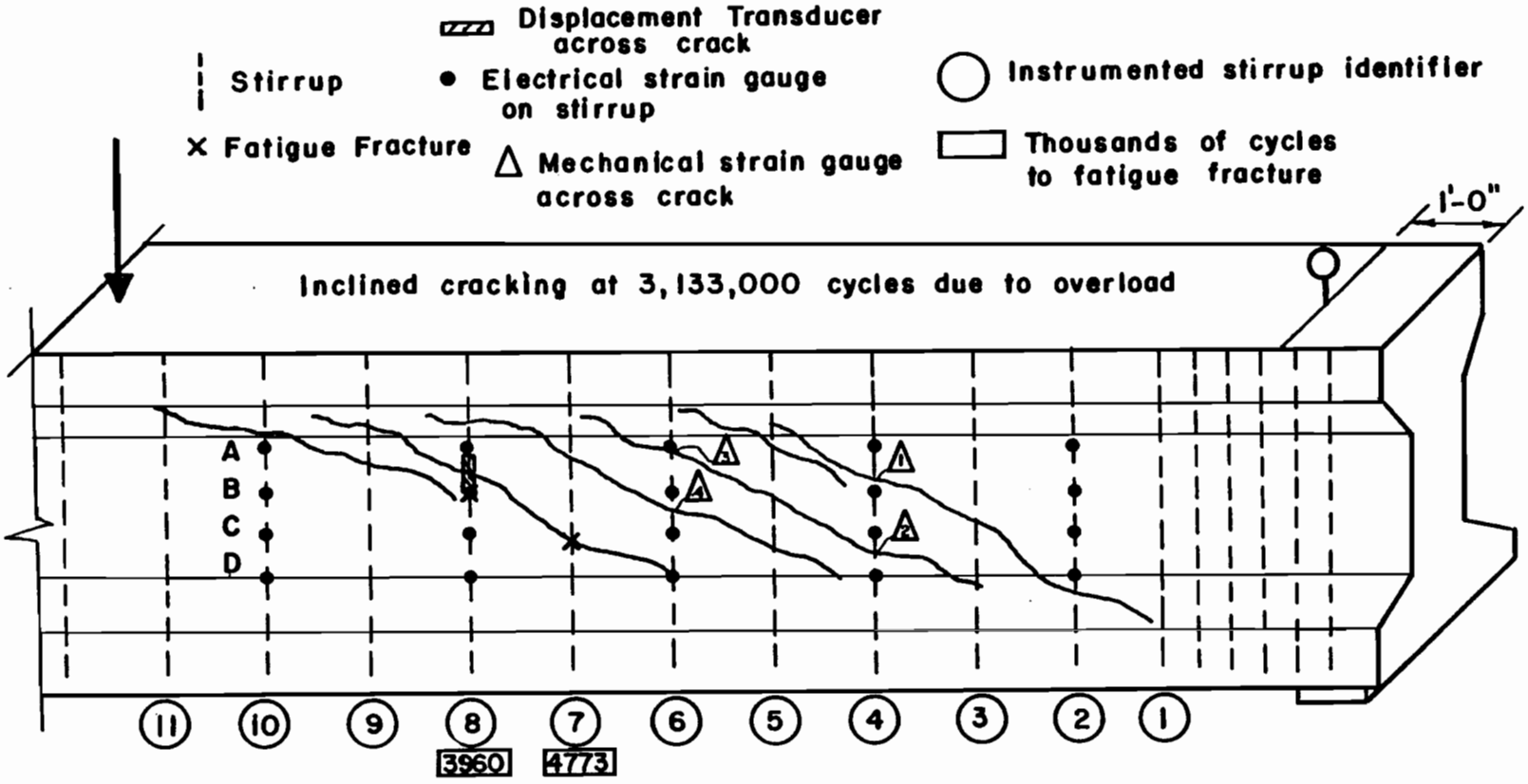

Fig. 4.32 Beam 3, south shear span; instrumentation, crack pattern, and fatigue fractures

cracks are shown as a function of the distance from respective cracks in Fig. 4.33. The stresses in the stirrups did not return to their uncracked values after the load was removed as shown in Fig. 4.33 and as evidenced by the fact that cracks did not close completely upon unloading. This was probably due to the stirrups carrying the dead load of the concrete and/or plastic strains in the stirrups or surrounding concrete. Mechanical strain gage targets were mounted on each side of the inclined cracks at points where the cracks intersected stirrups that were instrumented with electrical strain gages. An LVDT was also mounted across the diagonal crack at the location of stirrup S8 (for location see Fig. 4.32) so that the crack opening could be recorded while fatigue loading was in progress. An additional static load cycle to 71.3 kips was performed to obtain initial stress ranges for the stirrups and widths of inclined crack openings.

The load level of 71.3 kips was a lower bound for concrete fatigue inclined cracking because no inclined cracks developed in more than three million cycles. It should also be noted that the load required to produce inclined cracking was 90 kips, indicating that inclined fatigue cracking was not impending.

4.4.3 Post-Cracking Behavior. After inclined cracks developed in the south shear span, the maximum fatigue load was decreased to 67.5 kips, the original maximum fatigue load for this specimen. Fatigue loading was continued to 3,272,000 cycles when the load pulsator turned off due to a large increase in centerline deflection (Fig. 4.34). Severe flexural fatigue damage was evident with two visible broken strands as shown in Fig. 4.35. This was considered a complete flexural fatigue failure.

Fatigue loading was continued only the south ram at a maximum load of 90 kips and a minimum load of 13.3 kips. This represented 1-1/3 of the previous maximum and minimum load and produced the same shear and bending moment distribution in the south shear span as for the previous maximum load of 67.5 kips and minimum load of 10 kips. Bending moment at the point of the flexural fatigue failure was decreased by 48%. With this loading some shear fatigue data were obtained from a specimen that had inadvertently failed in flexural fatigue.

Shear truss action was evident in the south shear span after inclined cracking. However, shear deterioration was much less pronounced than that of Beam 2. Stirrup stress ranges and

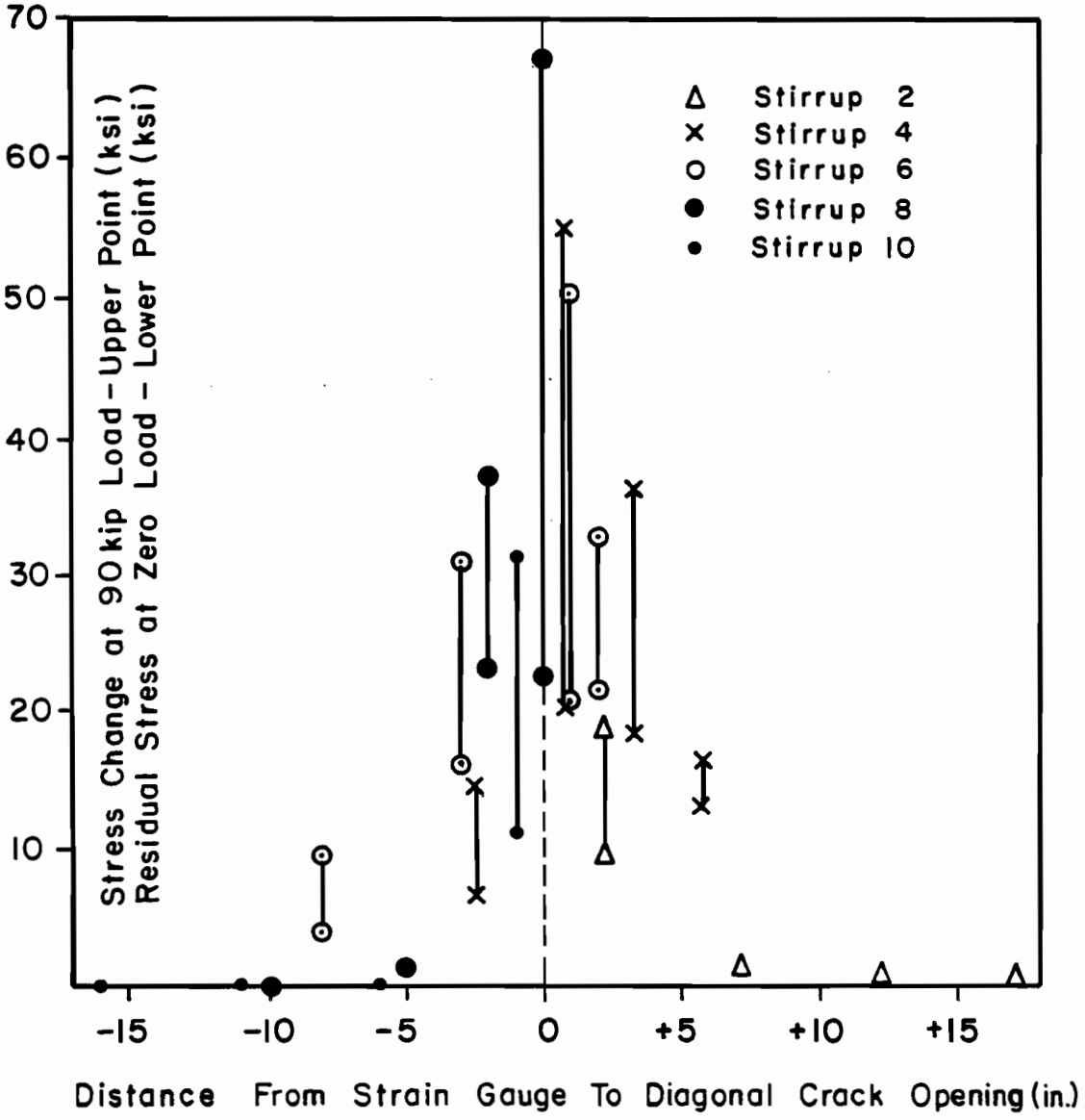

Fig. 4.33 Beam 3, stirrup stresses at cracking and after unloading

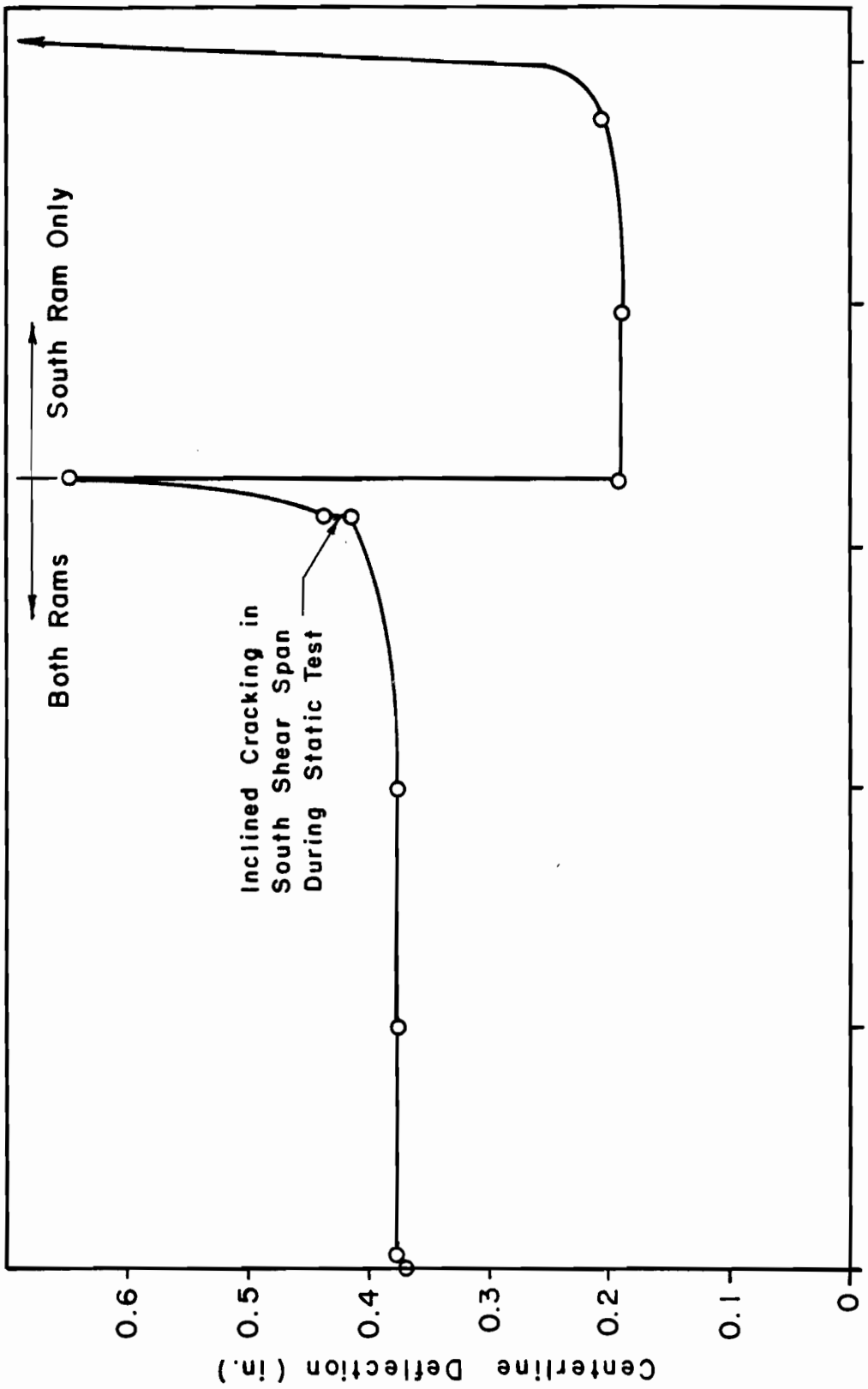

Fig. 4.34 Centerline deflection versus number of cycles for Beam 3

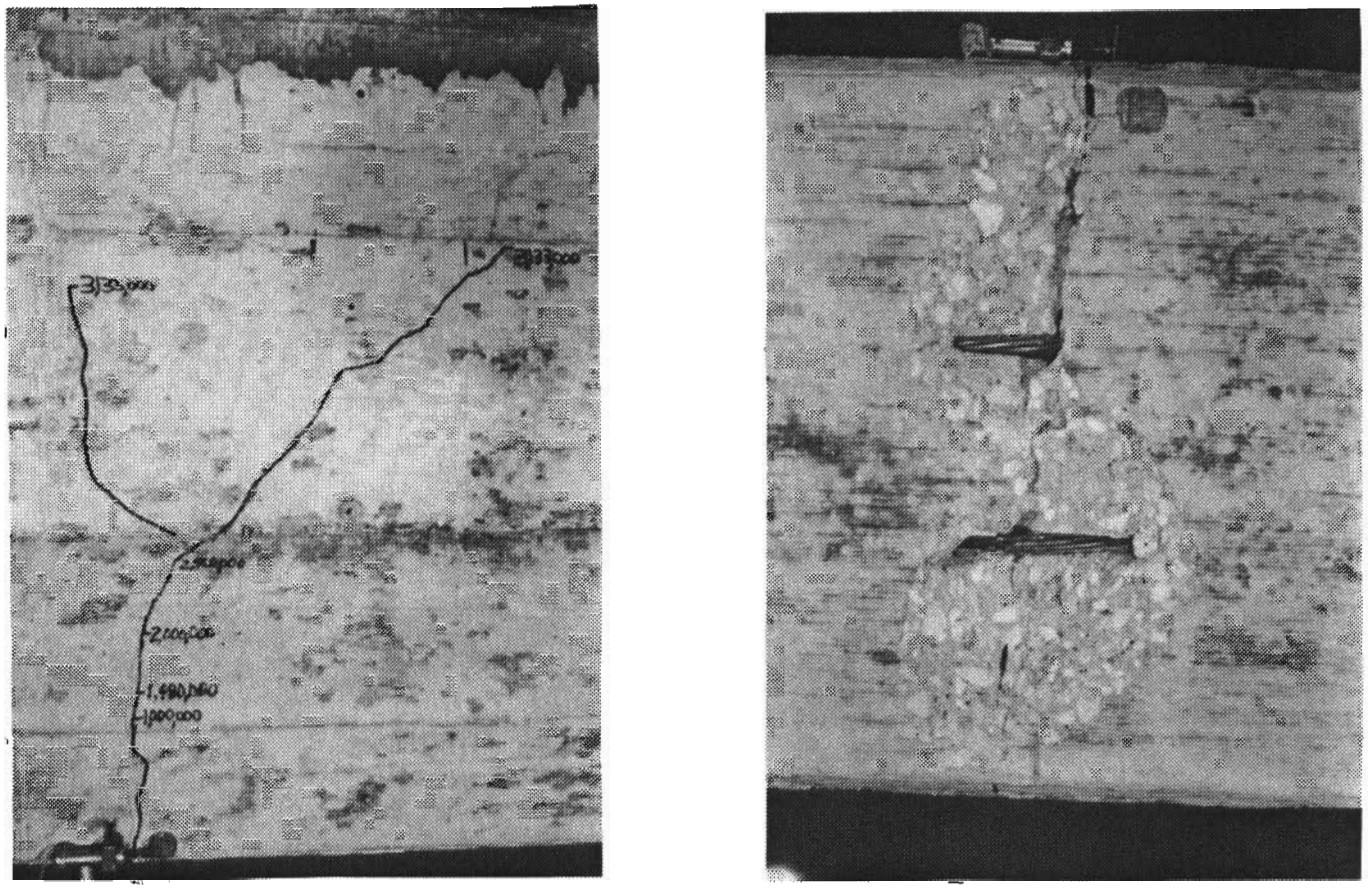

Fig. 4.35 Flexural fatigue failure at 3,272,000 cycles; side view of crack pattern (left) and bottom view of spalled concrete and fractured strand wires (right)

inclined crack widths were increasing at a slower rate. Figure 4.36 shows the change in vertical crack width over the fatigue history of the specimen at the location of stirrup S8 (for location see Fig. 4.32). The crack opening remained constant until approximately 4,000,000 cycles when truss action began to degrade. The other four cracks, which were instrumented with mechanical strain gages, remained constant at approximately 0.003 in. vertical crack opening throughout the fatigue history of the specimen. This is consistent with the fact that no stirrups were fractured at these cracks.

Figure 4.37 illustrates the relationship between vertical crack opening and stirrup stress change for electrical strain gage S8B (for location see Fig. 4.32). This plot was made after inclined cracks were produced at 3,133,000 cycles. It can be seen that the relationship is nearly proportional. Stirrup stress increased at a slightly higher rate than crack width. From this relationship it can be determined that the development length of stirrup S8 was approximately 6 in. which agrees with the data shown in Fig. 4.33. As for Beam 2, bilinear behavior was observed for both stirrup strains and crack opening versus applied load.

The first stirrup to fracture was S8 at the location of electrical strain gage S8B at 3,960,000 cycles. This data point is plotted on Fig. 4.24. A static load cycle was performed at 4,773,000 cycles and it was determined that stirrup S7 had fractured (for location see Fig. 4.32). In addition, flexural failure appeared to be imminent; flexural crack width was increasing rapidly and the flexural crack pattern had expanded dramatically. The crack pattern observed was indicative of torsional response; cracks on each side of the beam propagated in opposing directions. This supports an interpretation of observed behavior mentioned previously (Sec. 4.4.2) that substantially different forces were present in the prestressing strand. The torsional crack pattern is shown in Fig. 4.38. Figure 4.39 illustrates the net change in deflection of Beam 3 along its length from 1,000,000 to 3,133,000 cycles. It can be seen that the maximum change in deflection occurs near the flexural failure. Also note the jump in deflection change at the south quarter point where inclined cracking had occurred.

Fatigue loading was continued until 5,121,000 cycles when the load pulsator turned off due to a large increase in deflection. The strength test was performed at this time.

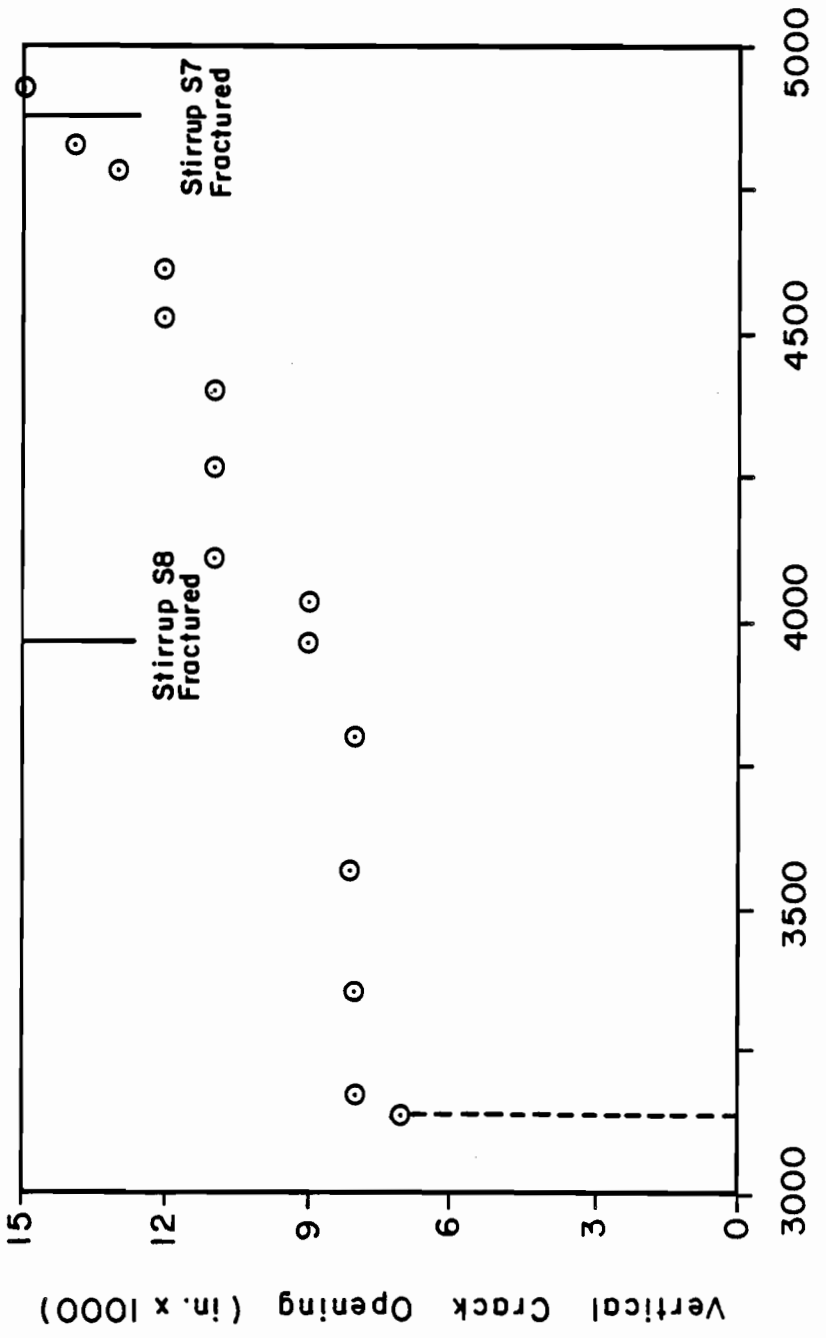

Fig. 4.36 Vertical crack width versus number of load cycles for Beam 3

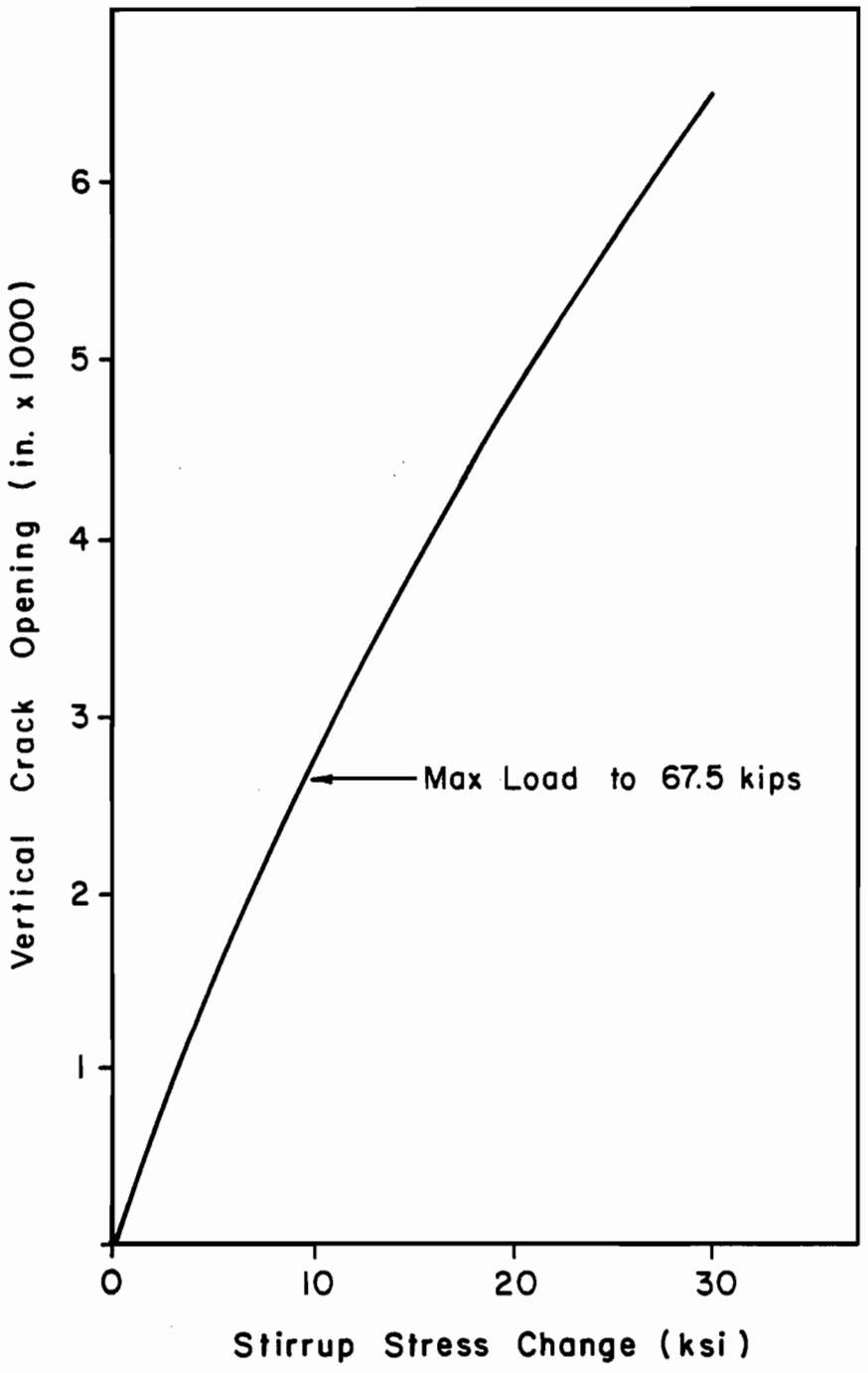

Fig. 4.37 Crack opening versus stirrup stress change at location of gage S8B

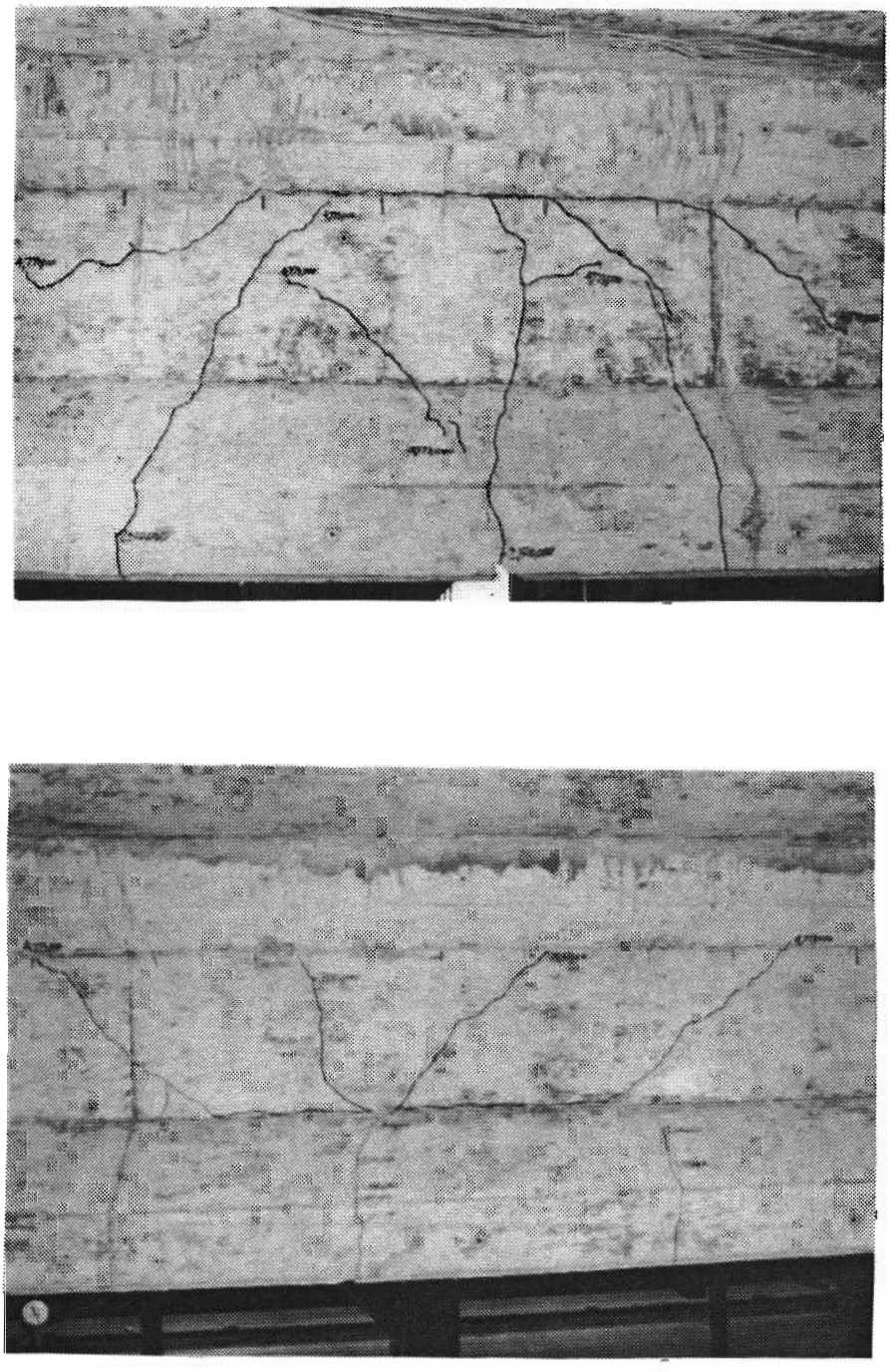

Fig. 4.38 East side (top) and west side (bottom) torsional cracking observed in the flexural failure zone

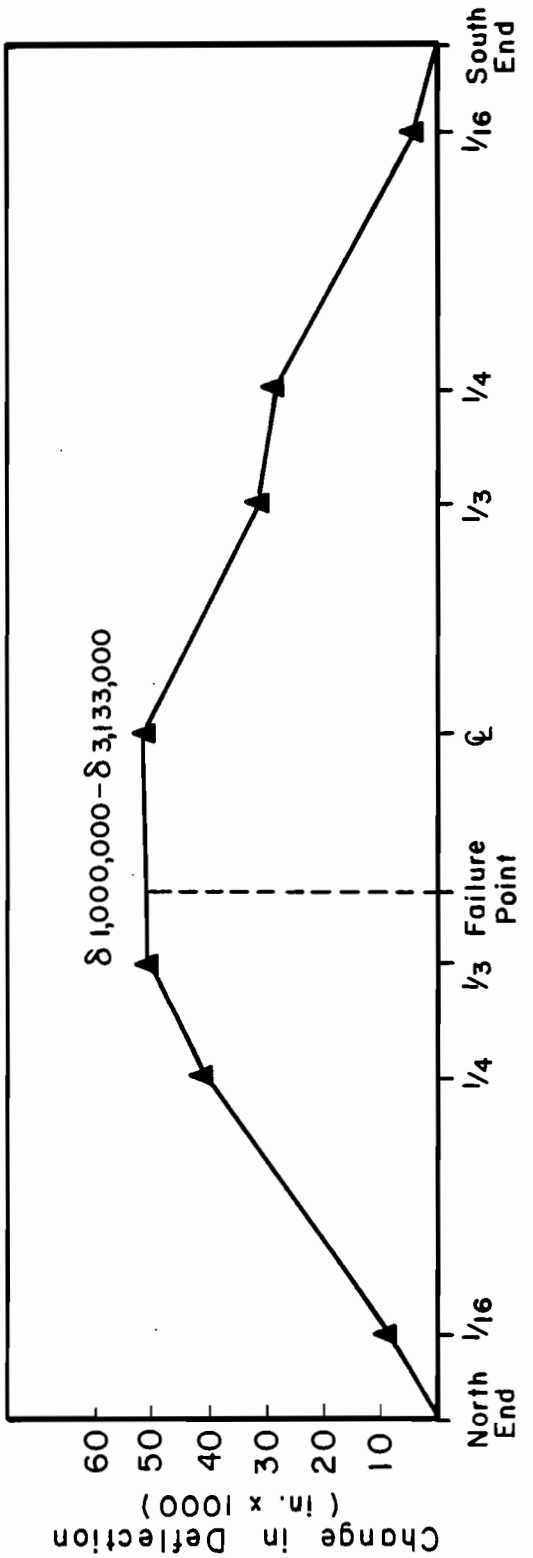

Fig. 4.39 Change in deflection of Beam 3 from 1,000,000 to 3,133,000 cycles

4.4.4 Ultimate Behavior. The strength test was performed with both loading rams. The specimen reached a load of 55 kips before failing in flexure. This was 35% of the calculated ultimate flexural capacity of 157 kips. Figure 4.40 shows the flexural failure.

After the strength test, stirrups in the south shear span were uncovered to confirm fatigue fractures and locations. Figure 4.41 shows the inclined crack pattern in the south shear span at the end of the strength test.

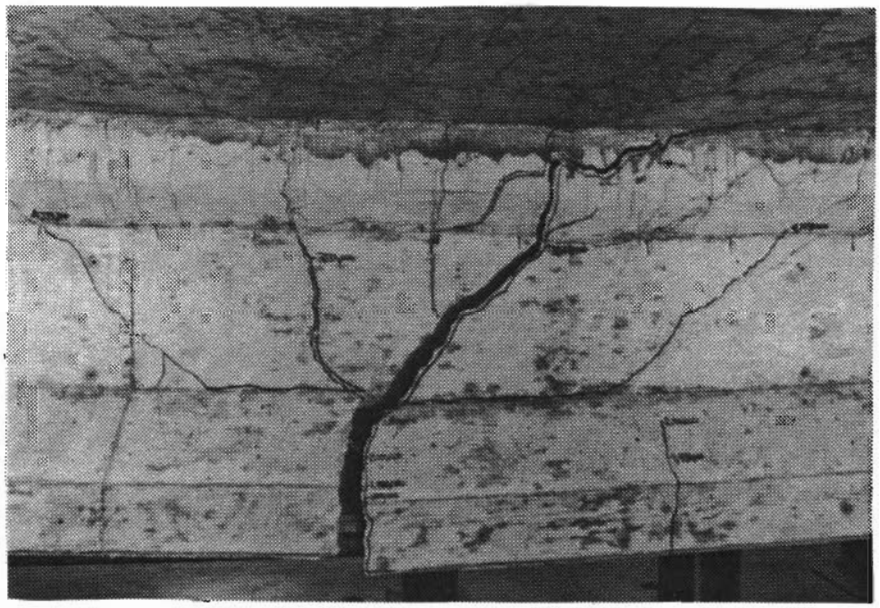

Fig. 4.40 Photograph of flexural failure

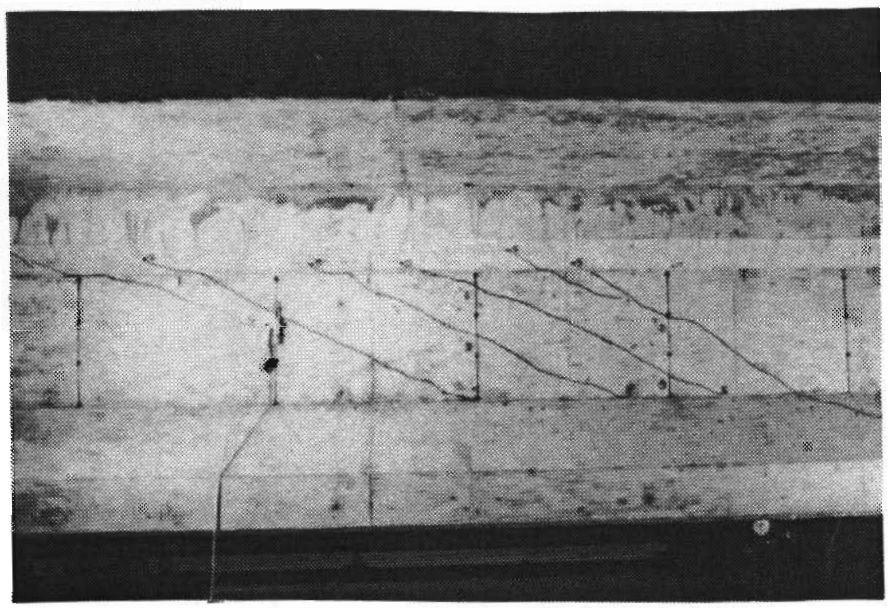

Fig. 4.41 Inclined crack pattern in south shear span at ultimate

CHAPTER 5

EVALUATION OF TEST RESULTS

The experimental results from the three shear fatigue specimens reported in Chapter 4 will be evaluated and compared in this chapter. In the first section, comparison is made between applied fatigue loads for the specimens and design service loads. It is shown that actual bridges can be designed for shears similar to those applied in this series of tests. In subsequent sections comparison is made between experimental results for the three specimens in this study and results of previous prestressed beam studies, results of recent reinforced concrete beam studies performed by the Japanese, and results of data obtained from a companion study on fatigue tests of deformed reinforcing bars in air. Finally, comparisons and evaluation of the test results are made with ACI and AASHTO Code and committee provisions.

5.1 Comparison of Applied Loads with AASHTO Service Loads

In this section applied maximum shears and shear ranges for the test specimens will be compared with shears resulting from AASHTO provisions for live-plus-impact service loads. An HS20-44 standard truck loading is used with the minimum distance of 14 ft between the rear two sets of axles to provide the critical loading condition for shear.

In Ref. 23 Overman designed a hypothetical Texas Type C bridge girder to compare the applied loads used in that series of tests with AASHTO service loads. A spacing of 9.80 ft was determined based on flexural stresses at midspan of the section. The same spacing will be used in this analysis.

The maximum live load shear for the HS20-44 truck loading is expressed by the following equation:

$$V_{LL} \text{ (kips)} = 58 - 1.5x$$

where x = distance from face of support (ft).

At a distance h/2 from the face of support the live load shear is 55 kips. The impact factor for a 48 ft span is 29%, which yields a shear due to live-plus-impact load of 71 kips. The AASHTO Code specifies that the standard truck loading shall be considered to act on a 10-ft wide section of the bridge.

The girder spacing for the hypothetical design is 9.80 ft; therefore, it is consistent with AASHTO recommendations to assume a full truck load on one girder. The maximum shear resulting from the applied fatigue load for the three specimens varied from 67.5 kips to 80 kips, while the shear range varied from 57.5 kips to 70 kips. These shears are similar to shears resulting from live-plus-impact service loads recommended by the AASHTO Code.

5.2 Comparison of Test Results with Results of Previous Prestressed Concrete Beam Studies

Comparison of test results with those of three previous studies will be made in this section. The first comparison will be with results from a study performed in the 1960's by Hanson and Hulsbos [10]. The second comparison is made with results from a study performed a few years later by Hanson, Hulsbos and Van Horn [12]. The third comparison considers a study concluded in 1970 by Price and Edwards [26]. All tests were on simply supported I-beams with no composite slab. Comparisons will be based primarily on observations and limited test data because very few relationships were developed in these studies.

Hanson and Hulsbos tested two prestressed concrete beams [10] with the intent of determining if a beam controlled by flexural behavior for monotonically applied loads could fail in shear as a result of an applied fatigue loading if diagonal cracks were present. Details of that testing program were presented in Chapter 2. Both beams were precracked in shear. The web reinforcement provided was approximately half that required by AASHTO to ensure development of flexural capacity. However, the authors knew that the provided reinforcement could develop the monotonic flexural capacity because they had loaded identical specimens to ultimate and a flexural failure had occurred.

The second beam of the series failed in shear at a fatigue load of approximately 59% of the flexural strength. This demonstrated that a shear fatigue failure could occur at a section which would fail in flexure under static conditions. This agrees with results of tests reported here; Beam 2 failed in shear under a fatigue load of 56% of the computed static flexural strength. The shear strength was not known precisely but it was at least as high as the flexural strength. In addition, in the tests reported here, the beam was not precracked in shear, but developed inclined cracks during fatigue loading. In the shear

fatigue study reported by Hanson and Hulsbos they noted that near the end of the fatigue test the main diagonal crack was approximately 3/16-in. wide and one could see through the web. This was also true for Beam 2. The failure of the Hanson and Hulsbos beam occurred when a diagonal crack extended through the compression flange, while a diagonal crack extended through the tension flange in Beam 2. This was predictable because in the tests reported here there was a composite slab. It was noted that the critical crack in Beam 2 extended through the precast section, and during the strength test the composite slab separated from the precast section. Hanson and Hulsbos speculated that the failure of their girder would have been catastrophic under gravity loading conditions. This was not true for Beam 2 because during the strength test the beam carried greater than the maximum fatigue load. Hanson and Hulsbos reported that the diagonal cracks did not open until a shear of 10 kips was applied. Following crack opening, the crack width was linearly related to the applied load. The same behavior was observed for Beam 2 except that the load at which the crack opened decreased with the number of applied load cycles.

Hanson and Hulsbos suggested a criterion based on the load-deflection curve for judging whether fatigue may be critical in a prestressed concrete beam with inclined cracks:

> If the repeated loadings are within the range which permits the deflection of the member to remain essentially linear, the probability of a fatigue failure within the normal life of the member is small.

This was not true in this series of tests. The load-deflection response was essentially linear in the fatigue load range for all three beams. For Beam 2 the centerline load-deflection response remained nearly linear even after stirrup fractures had occurred (Fig. 5.1). However, it should be noted that the maximum fatigue load was greater than the decompression load, which is the theoretical beginning of nonlinearity.

Hanson, Hulsbos and Van Horn tested six prestressed concrete beams to aid in interpreting the results of the first series of tests [12]. Details for this series of tests were presented in Chapter 2. The beams were designed with just enough web reinforcement according to AASHTO requirements to develop the static flexural strength. All specimens were precracked in flexure and shear.

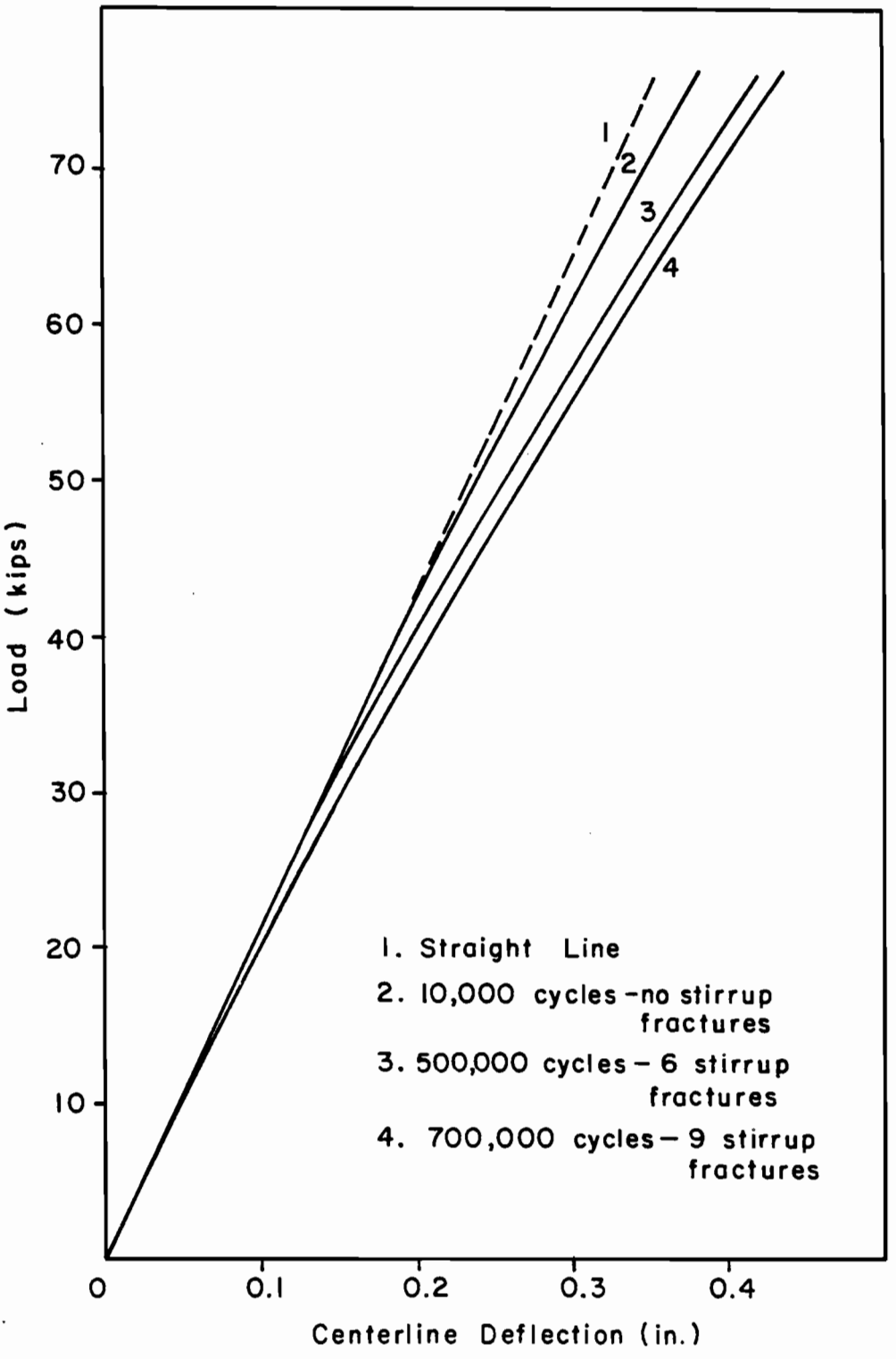

Fig. 5.1 Load-deflection curve for Beam 2 showing approximate linearity

Two of the six beams experienced fractured stirrups during testing, and one of those developed a shear fatigue failure. Hanson, Hulsbos, and Van Horn estimated the axial stress range in the stirrups was probably less than 10 ksi and, based on data obtained from crack widths, proposed that the stirrups were subjected to transverse shear and bending of sufficient magnitude to produce the stirrup fatigue failures. Results of the investigation reported here showed axial stress range in stirrups that fractured exceeded 10 ksi and was as high as 50 ksi before fracture. The results also showed that inclined cracks opened horizontally as well as vertically at the stirrup locations. Hanson, Hulsbos and Van Horn noted that inclined cracks must be present for stirrup fractures to occur. It was observed during this investigation that stirrup stress ranges were less than 2 ksi unless diagonal cracks were present.

Hanson, Hulsbos and Van Horn proposed that prestressed concrete beams have a remarkable shear fatigue resistance after the first stirrup fracture. This was observed for all tests reported here, especially for Beam 2 where all stirrups in the south shear span were fractured and yet load was sustained through apparent tied-arch action.

The last comparison to be made is with results of tests performed by Price and Edwards at the University of London [26]. They performed the tests to determine the effect of fatigue on diagonal cracking strength and shear failure. Additional details related to these tests were presnted in Chapter 2. The following conclusions, which are similar to some of those discussed previously, were reached:

1. Stirrup strains were negligible until diagonal cracking occurred.

2. Final shear fatigue failure occurred when the diagonal crack propagated through the top flange.

3. Specimens were able to sustain load for many cycles after the first stirrup fracture.

Price and Edwards also discussed their observation that diagonal cracks did not close completely upon unloading. This was observed in all three tests reported here. Price and Edwards observed very little change in stirrup strains with additional load cycles, even though diagonal crack widths increased with additional cycles. They attributed this to progressive bond breakdown between stirrups and surrounding concrete. Their

findings were supported by the fact that stirrup fractures were located as far as 8 in. away from the diagonal crack. It is possible that bond breakdown occurred because of limited confinement as a result of the thinness of the web (1.5 in.). This behavior was not observed in Beams 1 through 3. In fact, stirrups clearly exhibited increasing stress range with progressive number of load cycles, and the greatest distance between a stirrup fracture and a diagonal crack was approximately 3 in. Price and Edwards observed fretting of the reinforcing bars when the stirrups were exposed. This was observed in Beam 2. A stirrup was uncovered shortly after fracture was detected and the presence of corrosion confirmed that fretting had occurred.

5.3 Comparison of Test Results with Results of Japanese Reinforced Concrete Beam Studies

Extensive research has been performed in recent years on the shear fatigue behavior of reinforced concrete beams at the University of Tokyo in Japan under the supervision of Hajiime Okamura [14,19,21,22]. Tests were performed on reinforced rather than prestressed concrete beams. However, many of the observations and conclusions drawn from the research appear to apply to prestressed concrete also. In addition, a serious attempt was made to develop equations to predict the fatigue life of a beam considering all stages of behavior, including uncracked elastic behavior, post-cracked truss behavior, and finally the limit state for design of first stirrup fracture. The equations are applied in this discussion to test their limitations and to see how they might be modified to account for prestressed behavior.

The Japanese model for development of shear under fatigue loading conditions is similar to the ACI-AASHTO model for static load applications. The total resistance is made up of a concrete contribution and a web reinforcement contribution. The important difference in the Japanese model is the concrete contribution decreases logarithmically throughout the fatigue history of the beam. As the concrete contribution decreases, the web reinforcement contribution increases until a sufficient number of cycles has elapsed for the web reinforcement to reach its fatigue limit (Fig. 5.2) The Japanese model considers first stirrup fracture as a design limit state. This concept seems appropriate for prestressed concrete as well as reinforced concrete. In all three beams tested in the series reported here, the stirrup stress ranges increased with progressive cycles

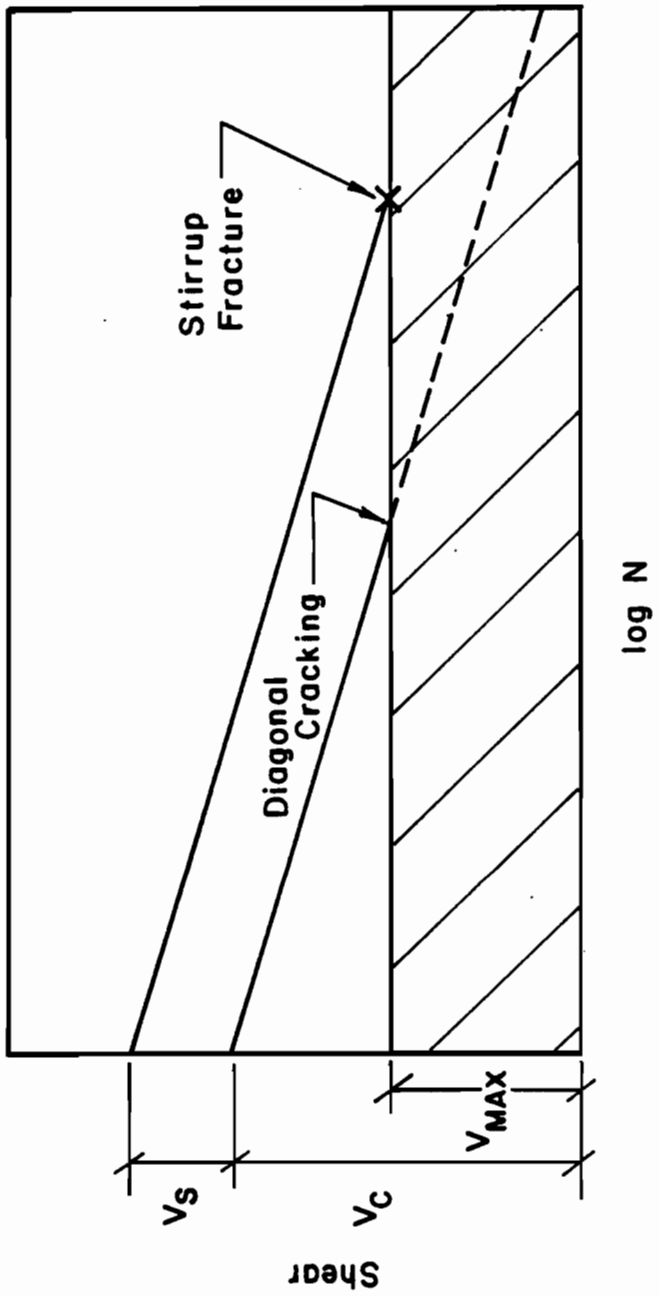

Fig. 5.2 Proposed Japanese model of shear-fatigue behavior for reinforced concrete

indicating a deterioration of the concrete contribution to shear strength.

Several tests were performed to investigate the effect of shear span-to-depth ratio. They discovered that a small shear span-to-depth ratio increased the shear strength of the section. They also learned that shear strength of a section was higher near a reaction or concentrated load point if vertical compression was induced in the member. These effects have been documented by other researchers, and have been attributed to the presence of σ_y stresses lowering the principal tensile stress, and/or the effects of arch action. The latest proposal is to consider a reduction of shear force instead of considering the increase in shear strength near concentrated forces. This reduction is to be applied only to the portion of the shear assumed to be carried by the truss mechanism. An example of the application of this reduction to a particular loading condition is shown in Fig. 5.3.

In the Japanese tests it was observed that after the initial diagonal crack pattern formed, very few new diagonal cracks appeared. Instead, the initial cracks widened and extended with progressive cycles. This behavior was noted for all three beam tests reported here. The researchers noted that the first stirrup to fracture was the one that developed the highest initial strain after diagonal cracking. This was also true for the three girders tested at the University of Texas (UT). The Japanese researchers found that reinforcing bars tested in the beams had between 50% and 100% of the fatigue life of the same reinforcing bars tested in air. They attributed this to the fact that many of the fractures occurred at bends where a reinforcing bar has approximately one-half the fatigue life of a straight reinforcing bar. Results of the recent UT study indicate that the fatigue life in air is greater than the fatigue life in a prestressed beam, even though the fractures did not occur at bends.

The first relationship to be evaluated here is an equation to predict the number of cycles until formation of inclined cracks in the web of the beam. The equation was originally developed for beams with no web reinforcement, but has been extended to be applicable to beams with web reinforcement. The equation is:

$$\log (V_{max}/V_{co}) = -0.036 (1-r^2) \log N_f \qquad (5.1)$$

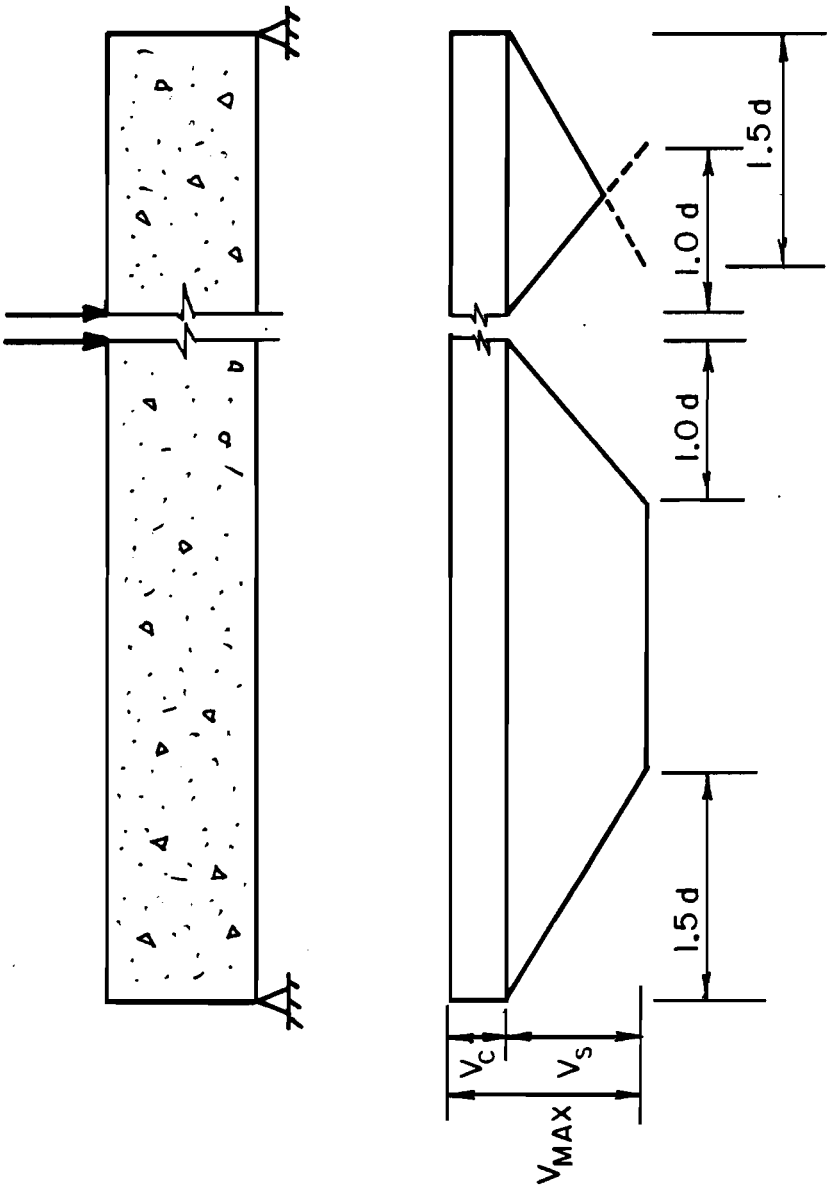

Fig. 5.3 Proposed Japanese reduction of shear force carried by truss mechanism in vicinity of supports and concentrated load points (from Ref. 22)

where V_{max} = maximum applied shear force

V_{min} = minimum applied shear force

$r = V_{min}/V_{max}$

V_{co} = concrete shear strength at start of fatigue life

N_f = number of cycles to inclined cracking

Okamura et al. claim that the equation fits their test data and other previous test data very well. The equation is consistent for any set of units. The equation considers load range, maximum load, and initial concrete shear strength as the variables. In the UT test data, all of the variables were known except V_{co}. The equation was rearranged in the form

$$V_{co} = V_{max}\ 10^{0.036(1-r^2)\log N_f}$$

so that it could be used to predict V_{co} for our test specimens. Beam 3 was excluded from the analysis because inclined cracks did not form in fatigue. V_{max} and V_{min} were calculated at h/2 from the face of the support. Table 5.1 lists the results with the mean value of V_{co} from three data points being 152 kips. This value is higher than that calculated using the principal tensile stress concept. However, it was demonstrated that V_{co} was at least 115 kips. This was the load at which inclined cracks developed in Beam 3 under static loading after 3,133,000 cycles of fatigue loading. These values will be used in a subsequent equation to predict stress range.

Equation 5.1 would normally be used to predict the number of cycles to develop inclined cracking in which case V_{co} would have to be known. The equation proposed by Okamura et al. is

$$V_{co} = 0.20 f_c'^{1/3}\ (0.75+1.40\ d/a)\ (1+\beta_p+\beta_d) b_w d \qquad (5.2)$$

where f_c' = compressive strength of concrete (MPa)

d/a = effective depth to shear span ratio

TABLE 5.1 Initial Concrete Shear Strength as Predicted by Japanese Equations for Reinforced Concrete

$$V_{co} = V_{max}\ 10^{0.036(1-r^2)\ \log N_f}$$

Beam No.	V_{min} (kip)	V_{max} (kip)	r	N_f x 1000	V_{co} (kip)
1	35	105	0.333	300	157
2S	35	100	0.350	210	147
2N	35	100	0.350	500	151

$\beta\rho = \rho_w^{1/2} - 1$ (ρ_w in %)

$\rho_w = (A_s/b_w d)\ 100$

$\beta_d = d^{-1/4} - 1$ (d in meters)

b_w = web width

d = effective depth

Again, the authors claim the equation fits available test data very well. It is intended for beams with no axial force and a shear span-to-depth ratio greater than three. It is interesting to note that the influence of compressive strength in this equation is less than that of the ACI Code because it is raised to the 1/3 power rather than the 1/2 power.

Equation 5.1 is used as a basis for developing an equation to predict stirrup stress range. Following is an abbreviated development. For further information see Ref. 22. The total shear force is assumed to be carried by a concrete component and a web reinforcement truss component:

$$V_{max} = V_s + V_c$$

or

$$V_s = V_{max} - V_c$$

where V_{max} = maximum applied shear

V_s = truss component

V_c = concrete component.

The truss component of shear is assumed to be reduced near supports or concentrated loads (when those forces induce vertical compression in the web) by the factor β_x as discussed previously (see Fig. 5.3).

$$V_s = \beta_x\ (V_{max} - V_c)$$

where $\beta_x = x/1.5d \leq 1.0$ at supports

$\beta_x = x/1.0d \leq 1.0$ at concentrated loads

$\beta_x = 1.0$ elsewhere.

The factor V_c is assumed to decrease logarithmically in the same manner as it did before inclined cracking so that Eq. 1 may be used in the form:

$$V_c = V_{co}\ 10^{-0.036(1-r^2)}\ \log N$$

where V_c = concrete contribution at N cycles

V_{co} = concrete shear strength at start of fatigue life

$r = V_{min}/V_{max}$

N = number of cycles from initial loading.

Examination of this equation reveals that at N_f cycles (inclined cracking), $V_c = V_{max}$. The authors suggest the use of this equation before and after inclined cracking. This assumes that the shear strength of concrete declines along the same path after inclined cracking with no sudden loss. The maximum stirrup stress is derived from the 45 degree truss model as:

$$f_{wmax} = V_s/(A_w z/s)$$

where A_w = area of web reinforcement in a distance "s"

z = Distance between centroid of compression chord and centroid of tension chord = d/1.15

s = stirrup spacing.

Collecting the terms yields:

$$f_{wmax} = \beta_x\ [V_{max}-V_{co}\ 10^{-0.036(1-r^2)\log N}]/(A_w z/s) \geq 0 \qquad (5.3)$$

To obtain an equation for the stress range, the authors made some assumptions about the geometry of the shear force-stirrup stress curve as shown in Fig. 5.4. By assuming the projection of the straight portion of the curve intersects the shear force axis at $-V_{co}$ they obtained:

$$f_{wr} = f_{wmax}\ (V_{max}-V_{min})/(V_{max}+V_{co}) \qquad (5.4)$$

where f_{wr} = stress range.

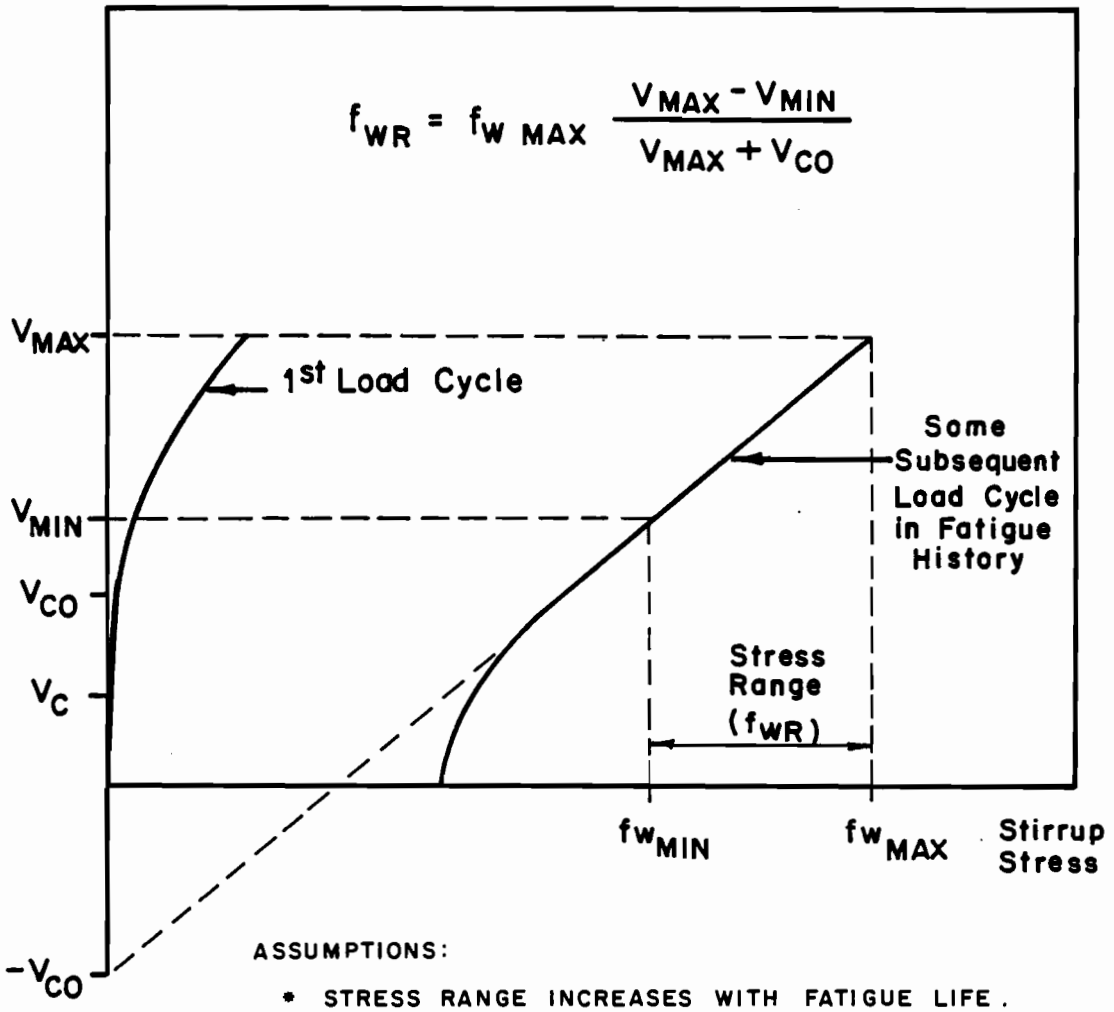

ASSUMPTIONS:

* STRESS RANGE INCREASES WITH FATIGUE LIFE.
* RESIDUAL STRESS INCREASES WITH FATIGUE LIFE.
* STRESS RANGE AND RESIDUAL STRESS INCREASE THROUGHOUT FATIGUE LIFE IN SUCH A MANNER THAT A PROJECTION OF THE SHEAR FORCE VS. STIRRUP STRESS LINE WILL ALWAYS INTERSECT THE SHEAR FORCE AXIS AT $-V_{CO}$.
* V_{MIN} IS GREATER THAN V_C.

Fig. 5.4 Interpretation of Japanese equation for stress range

Equations 5.3 and 5.4 were used to predict the stress range at the first stirrup fracture in the south and north shear spans of Beam 2. V_{min} and V_{max} were calculated at h/2 from the face of support as before and the value of β_x was taken as 1.0 since both stirrups were greater than "d" from the concentrated load. The value of V_{co} calculated from Eq. 5.1 was used. The results are shown in Table 5.2. These equations predicted a very small stress range at the time of first fracture. This was not true for the recent UT tests. One reason is that the fatigue equation does not model the sudden drop in V_c at the onset of inclined cracking (see Fig. 5.2).

The Japanese reinforced concrete fatigue model may hold promise for future adaptation to prestressed concrete. Some aspects which need to be considered in the model are:

1. Influence of axial force in the equation for initial concrete shear strength.

2. Sudden drop in concrete contribution at the onset of inclined cracking.

3. Reevaluation of the constant in the logarithmic equation for V_c.

4. Change in inclination of the web reinforcement "truss".

5. Examination of the stress range equation as related to prestressed concrete.

5.4 Comparison of Test Results with Companion Study

A companion study was performed to investigate the fatigue behavior of reinforcing bars in air and to compare the behavior in air with the fatigue response of stirrups in prestressed concrete beams. Tests were performed on 30 specimens with nine different magnitudes of constant amplitude sinusoidal cyclic loading. The specimens were loaded at 600 cycles per minute (cpm) with a constant lower stress of 6 ksi. See Table 2.4 for a summary of test results.

A linear regression analysis was performed on the data, excluding the run-out values. A run-out was considered as 5,000,000 cycles. Comparison will be made with the regression equation. For detailed information concerning development of the equation, see Ref. 18. The equation is:

TABLE 5.2 Maximum Stress and Stress Range for First Stirrup Fracture as Predicted by Japanese Equations for Reinforced Concrete

$$f_{wmax} = \beta_x \{V_{max} - V_{co}\ 10^{-0.036(1-r^2)\log N}\} / (A_w z/s)$$

$$f_{wr} = f_{wmax}\ (V_{max} - V_{min}) / (V_{max} + V_{co})$$

Beam No.	β_x	V_{min} (kip)	V_{max} (kip)	r	V_{co} (kip)	N x 1000	$A_w z/s$ ($in.^2$)	f_{wmax} (ksi)	f_{wr} (ksi)
2S	1.0	35	100	0.350	147	485	0.662	4.22	1.11
2N	1.0	35	100	0.350	151	750	0.662	2.29	0.26

$$\log N = 14.8 - 5.65 \log SR \qquad (5.5)$$

The equation with its 95% and 5% survival bounds is plotted in Fig. 5.5. Data points from the static beam tests are shown on the plot for those bars which experienced fatigue fractures and for which accurate data were available. Some of the points are shown as vertical lines which indicate the variation in stress range over the life of the test. All data shown are based on stress ranges measured during static tests, which means the bars had not fractured at the time of the measurement. In general, the stress range was probably higher at the actual time of fracture because it was observed that stress ranges increased throughout the life of the specimen.

From the data it is apparent that for this series of in-air and beam tests, the reinforcing bars embedded in concrete failed at lower stress ranges than the same reinforcing bars tested in air. Some of the probable reasons are listed below:

1. The in-air tests subjected each bar to constant amplitude fluctuating stress, while bars embedded in concrete were subjected to slowly increasing fluctuating stress with increasing concrete crack growth. Tests reported here indicate that increases in stress range during a fatigue test reduce the fatigue life.

2. The in-air tests subjected each bar to pure axial tension, while the bar embedded in concrete may have been subjected to axial tension plus bending stresses. This was documented by horizontal movements in the inclined crack for this series of tests.

3. In the air tests, the stress range was measured precisely with load cells attached to the loading rams. In beam tests, the stress range was measured through a strain gage. It is uncertain whether the strain gage was precisely at the point of maximum stress range. Also, the surface treatment for strain gage placement may have disrupted the surface and provided a trigger for fatigue crack initiation.

Some of the stirrup stress ranges were measured continuously with an electronic signal peak detector. Gages S8B and N6C in Beam 2 (for location see Figs. 4.12 and 4.13) were monitored continuously and both approached 60 ksi stress range before fatigue fracture. Matsumoto [18] applied Minor's Law of Cumulative Damage to these gages in an attempt to determine if

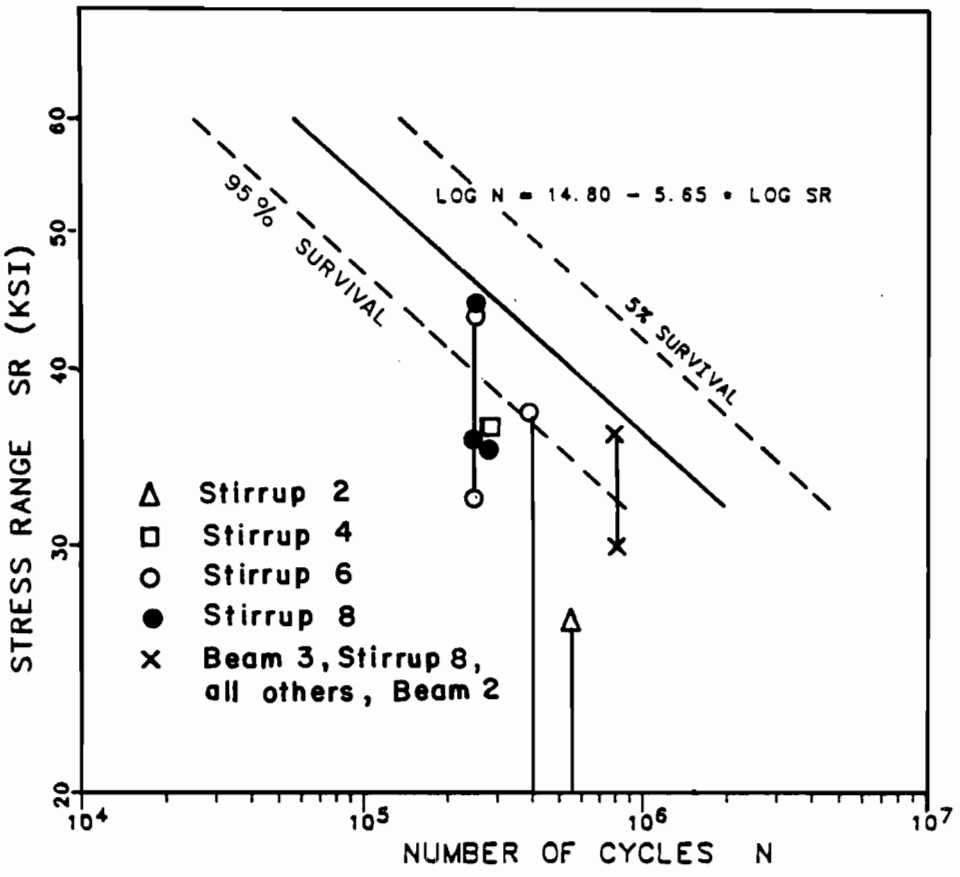

Fig. 5.5 Comparison of beam tests with Eq. 5.5

the beam tests could be correlated with the air tests. He considered that the fatigue history started at the initiation of inclined cracking and used linear approximations of the stress range for different regions of the fatigue history as shown in Figs. 5.6 and 5.7. In this manner he determined a cumulative damage index of 1.682 for gage S8B and 0.756 for gage N6C. Minor's Law would predict a value of 1.000. However, both values obtained by Matsumoto fell within the 95% confidence interval of Eq. 5.5. Matsumoto concluded that the behavior of stirrups in prestressed concrete beams is primarily governed by axial stresses produced by shear forces in the span, and that stirrups in concrete beams will be subjected to a sudden increase in stress range just before fracture.

The length of the specimens in the in-air tests was approximately the same as the length of the specimens in the beam tests. This is significant because size-effect is very important in fatigue considerations. In general, when specimens of different length are tested and if all other variables are equal, the longer specimen will fail first and result in a lower bound for the shorter specimens. This effect did not influence the comparison.

5.5 Evaluation of Current Design Procedures for Shear

5.5.1 ACI and AASHTO Codes. This discussion will be limited to ACI 318-83, "Building Code Requirements for Reinforced Concrete", because at present the AASHTO Code equations and recommendations for strength of sections are modeled after the ACI Code. Load resistance factors are different for ACI and AASHTO. However, this will not affect the discussion because loads on the test specimens were known.

There are limited references to fatigue in the ACI Code. Section 18.19.4 warns of the possibility of fatigue failure in anchorages and couplers when unbonded construction is used. The Commentary in this section refers one to the ACI Committee 215 Report. Section 11.5.5.2 ("Minimum Shear Reinforcement") of the Commentary offers the following:

> When repetitive loading might occur on flexural members, the possibility of inclined diagonal tension cracks forming at appreciably smaller stresses than under static loading should be taken into account in the design. In these instances, it would be prudent to use at least the minimum shear reinforcement expressed by

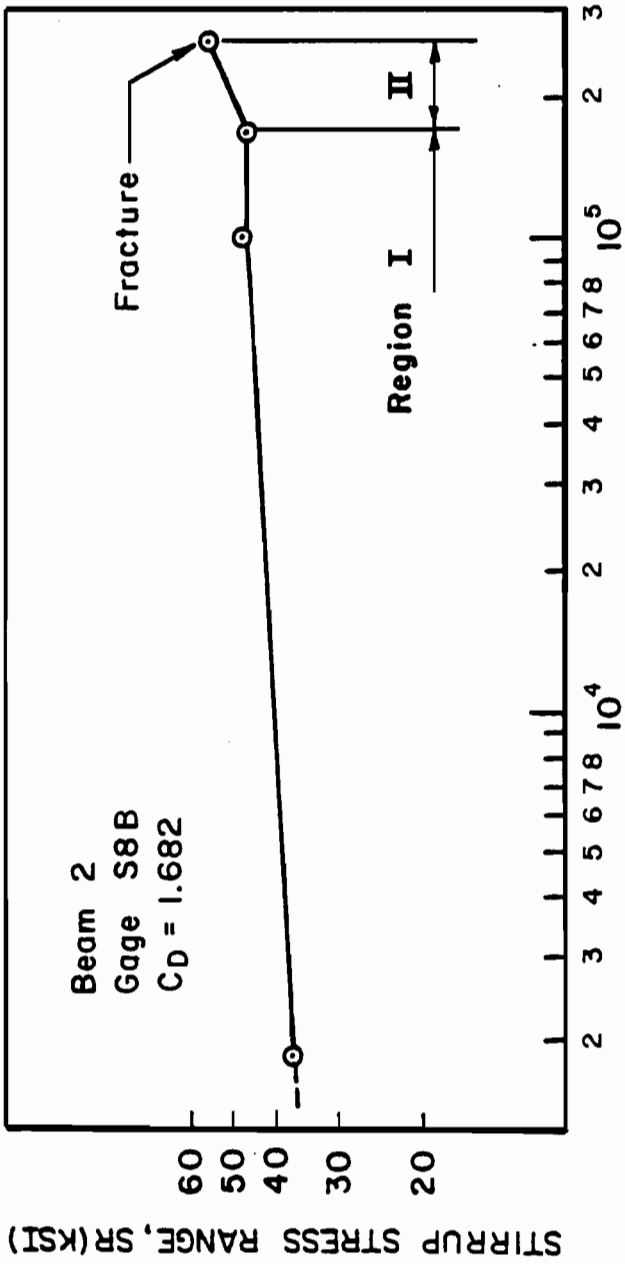

Fig. 5.6 Stress range history for gage S8B
(for location see Fig. 4.13)

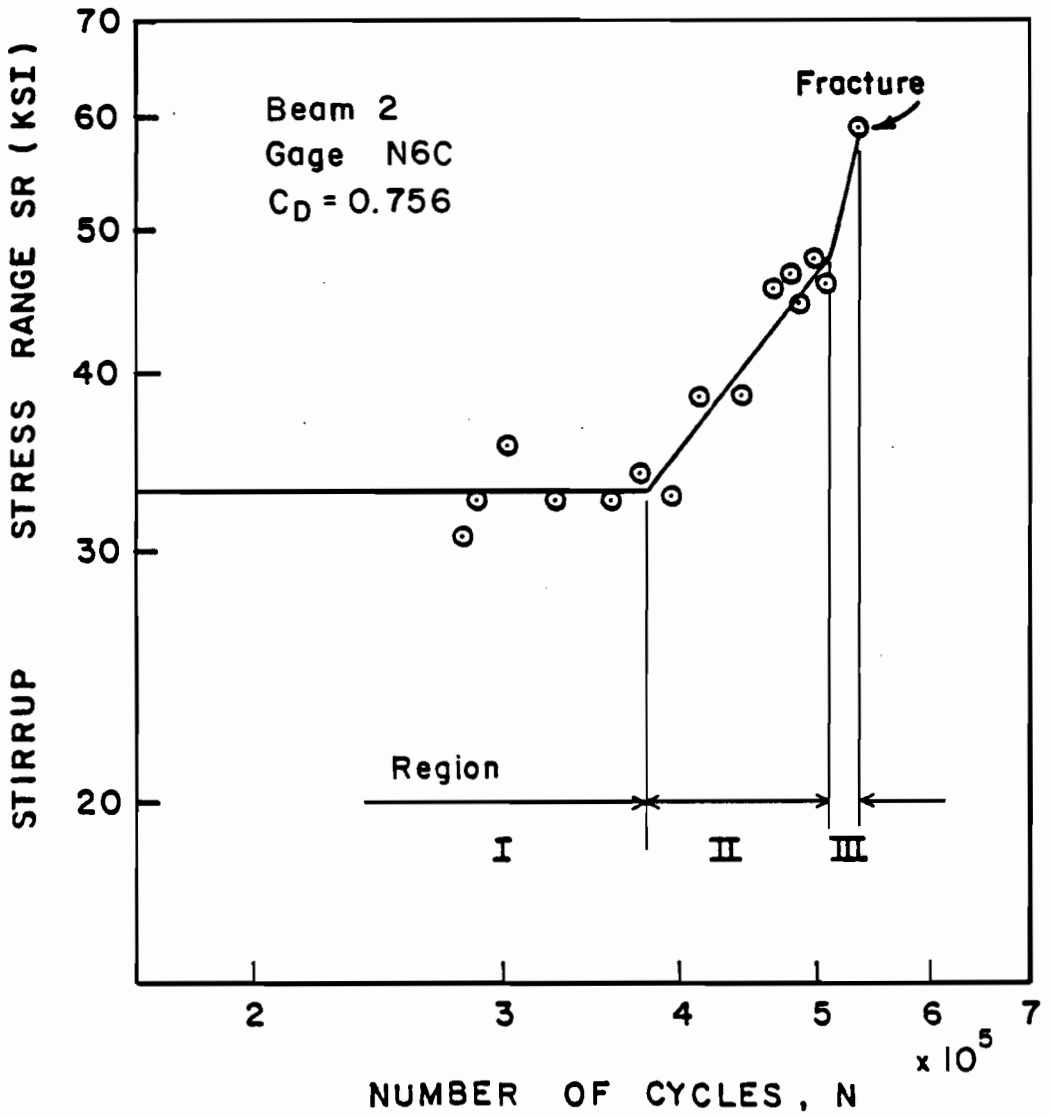

Fig. 5.7 Stress range history for gage N6C
(for location see Fig. 4.12)

Eq. (11-14) or (11-15), even though tests or calculations based on static loads show that shear reinforcement is not required.

It should be noted that there is no reference to fatigue in Chapter 9, Strength and Serviceability Requirements, or Appendix B, Service Load Design.

Design for shear in reinforced and prestressed concrete beams is based on a hybrid model which considers that shear is carried by two phenomena:

1. Concrete as a homogeneous material carrying shear according to the theory of elasticity.

2. Truss action after inclined cracking develops, with concrete compression diagonals and stirrup vertical tension members. The inclination of the compression diagonals is assumed as 45 degrees, because this is the angle of principal tensile stress predicted by elastic theory for a reinforced concrete beam.

Design strength of a beam is the sum of the two contributions with the concrete term considered to be the shear carried by the web section before inclined cracking develops and the shear carried by the compression zone after inclined cracking develops. The ACI Code value is based on the web section, whether the section is or is not cracked.

In prestressed concrete two types of shear cracking are considered as shown in Fig. 5.8:

1. V_{cw}--Web-shear cracking is produced by principal tensile stresses at the centroid of the section.

2. V_{ci}--Flexure-shear cracking is produced when a crack that has been initiated by flexural stresses propagates into the web and becomes a diagonal crack under the state of stress existing in the web.

For prestressed concrete design, the concrete contribution of shear strength at a section along the beam is considered as the least load to produce either of the above types of cracking. In general, the concrete contribution for prestressed concrete is higher than that for reinforced concrete, because of the beneficial effect that prestressing has on shear behavior.

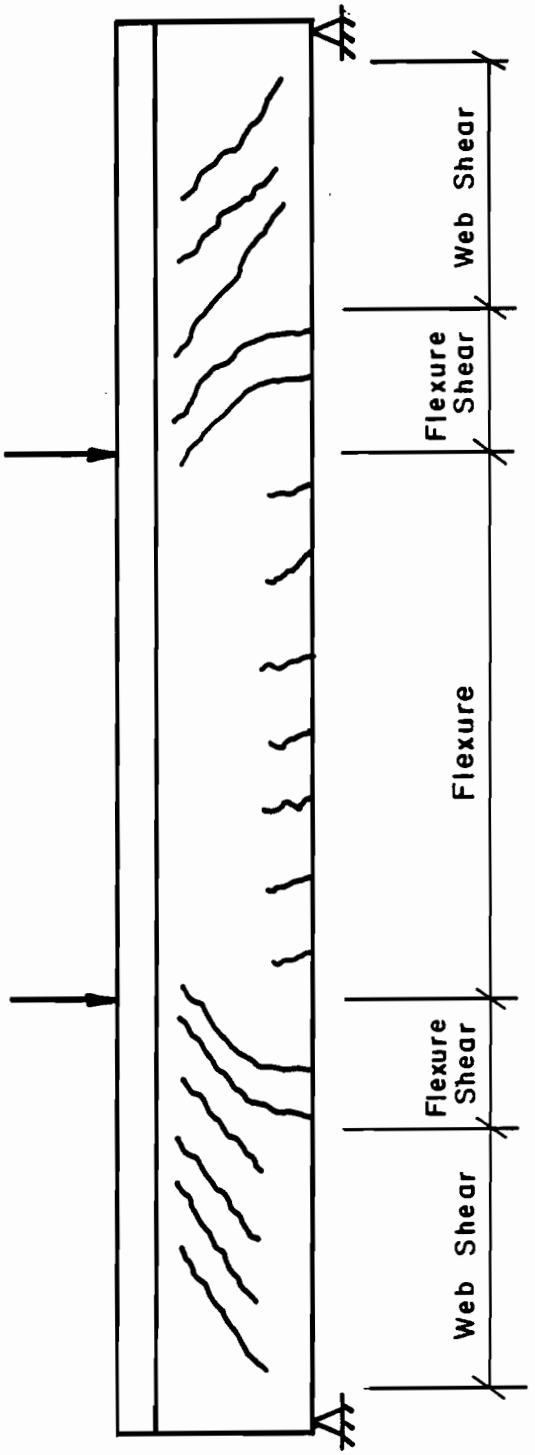

Fig. 5.8 Possible types of cracking in prestressed beams

When flexure cracks develop, the fatigue behavior is dominated by flexure with the primary limit state being fatigue of the prestressing strands. When web shear cracks develop, fatigue behavior is generally dominated by shear with the primary limit state being fatigue of the stirrups. The intent of this test program was to study fatigue of stirrups. Therefore, all three specimens were loaded with the intent that web shear cracking would dominate. A plot of V_{cw} and V_{ci} along the length of the shear span is shown in Fig. 5.9 for Beam 2. Beams 1 and 3 were similar. No flexure-shear cracks developed in any of the three specimens. This supports the validity of the ACI equations. It can be seen in the illustration that flexure-shear is dominant at the load point. However, it is documented that shear strength is significantly higher at locations of concentrated forces (reactions and concentrated loads). This is why the ACI Code permits computation of shear forces at a distance h/2 from the face of the support. The ACI concept of adding the concrete term and the steel term is not rational based on the fact that the concrete term should be reduced considerably after inclined cracking develops. Nevertheless, this empirical relationship has produced safe designs for many years and has been shown through test results to accurately predict shear strength under monotonic loading conditions. No contribution for aggregate interlock and dowel action are present in the equations and this helps make up for the extra contribution of concrete strength afforded by the present equations.

Although the equations seem to be satisfactory for ultimate strength considerations, they are not satisfactory for fatigue loading. Under fatigue loading, the concrete contribution is reduced with progressive cycles, probably because of breakdown in aggregate interlock resulting from abrasion along the crack interface and debonding of the stirrups near the diagonal crack. As this happens, the force carried by the stirrups increases. The commentary for design of shear reinforcement (Section 11.5.6) states:

> Design of shear reinforcement is based on a modified form of the truss analogy. The truss analogy assumes that the total shear is carried by shear reinforcement. However, considerable research on both nonprestressed and prestressed members has indicated that shear reinforcement needs to be designed to carry only the shear exceeding that which causes inclined cracking.

A plot of the ratio of applied shear to Code values for V_s, V_{cw}, and V_n along the shear span is shown in Fig. 5.10. It

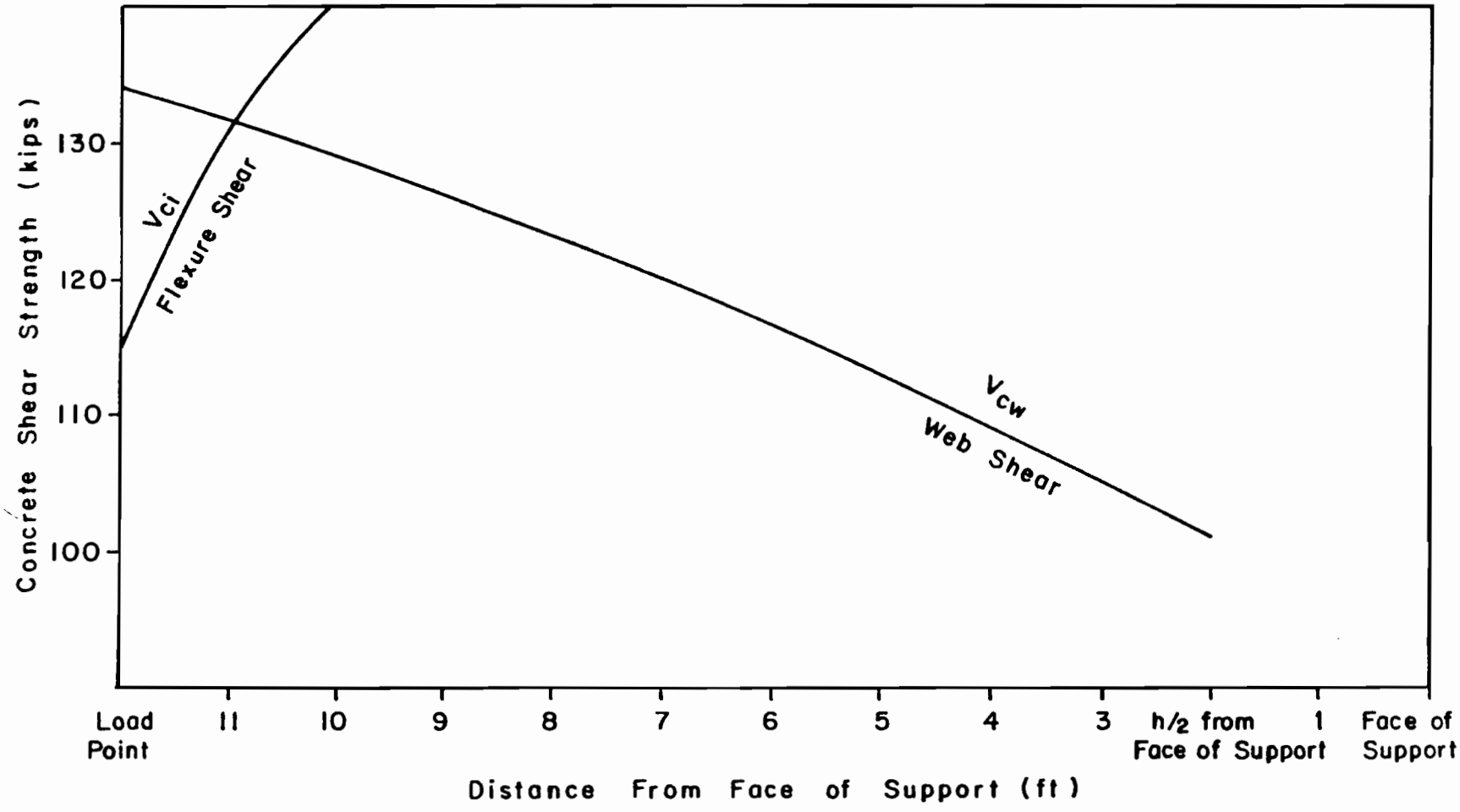

Fig. 5.9 Web shear and flexure shear strength along the shear span for Beam 2

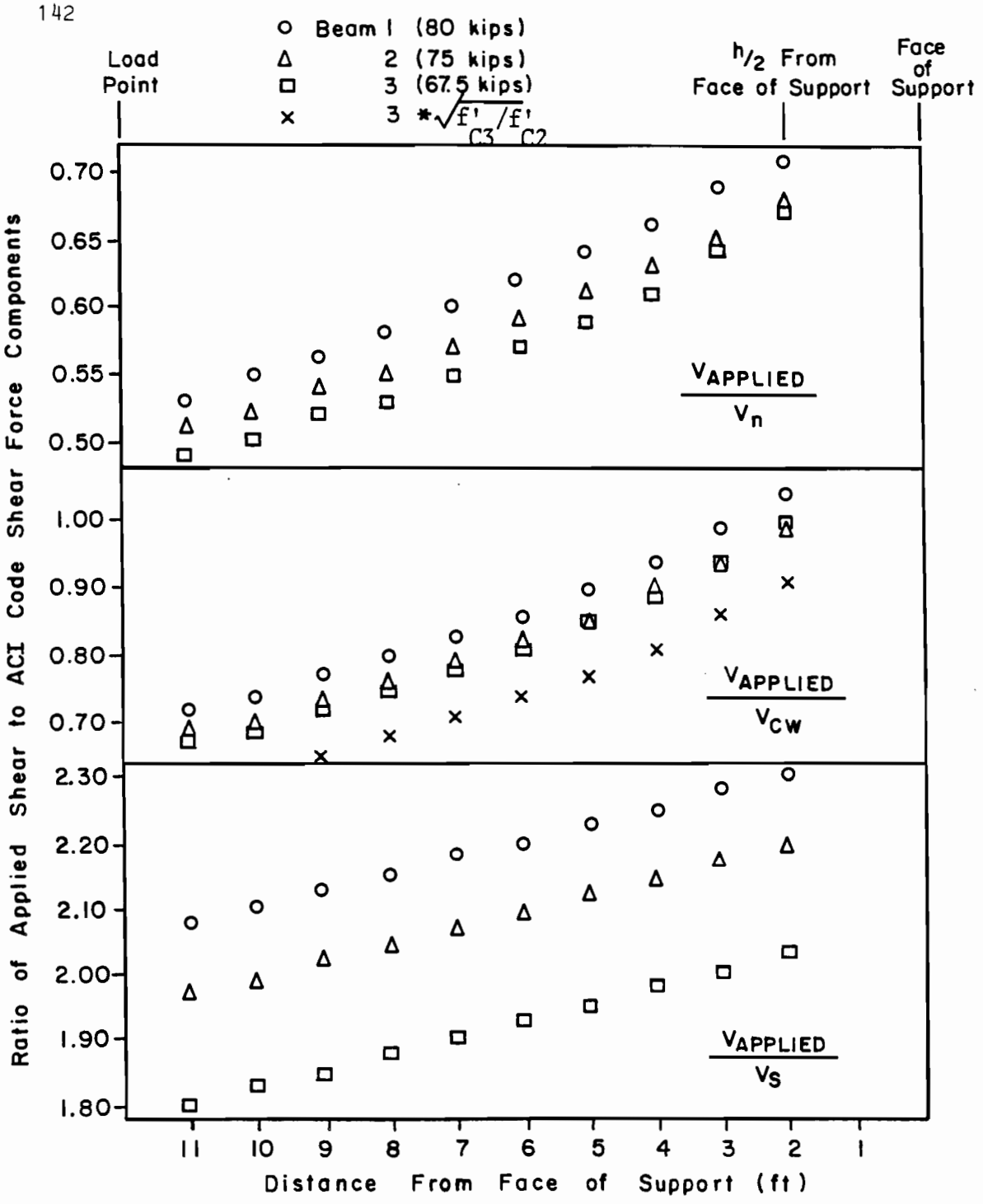

Fig. 5.10 Comparison of applied shear with ACI Code shear-force components

should be noted that only maximum applied load affects the design shear force components. This is why all curves in Fig. 5.10 show increasing values toward the support. If load range were used instead of maximum applied load, the ratio of applied shear to shear force components along the shear span would slope in the opposite direction for $V_{APPLIED}/V_{cw}$ and $V_{APPLIED}/V_n$, and be constant for $V_{APPLIED}/V_s$.

The applied shear was less than the shear strength for all specimens with the highest ratio being 0.71 at h/2 from the face of support for Beam 1. The applied shear slightly exceeded the concrete shear strength, V_c, (based on ACI Eq. 11-13), with the highest ratio being 1.04 for Beam 1, yet all specimens had fatigue fracture of stirrups. Beam 2 and Beam 3 had very similar values for the $V_{APPLIED}$ to V_{cw} ratio. This is because the lower applied load on Beam 3 was approximately cancelled out by the lower strength of concrete and lower effective prestress. Yet Beam 2 and Beam 3 had greatly different behavior in fatigue of the concrete. Beam 2 developed inclined cracking at 200,000 load cycles, while Beam 3 did not develop inclined cracking after 3,133,000 load cycles. Beam 3 had to be cracked during a static test at a maximum applied shear of 115 kips ($V_{APPLIED}/V_{cw}$ = 1.24) at h/2 from the face of the support. From the tests it appeared that maximum load and load range had the greatest effect on concrete fatigue strength in shear. This agrees with results obtained from shear fatigue tests of reinforced concrete beams performed in Japan by Okamura et al. The ratios of $V_{APPLIED}$ to V_{cw} for Beam 2 and Beam 3 are separated significantly when the effect of concrete strength is excluded as shown in the additional curve in Fig. 5.10. This supports the thought that load range and maximum load have a greater effect than compressive strength on fatigue of concrete in shear.

The values of the ratios of $V_{APPLIED}$ to V_s varied from a minimum of 1.80 at h/4 from the load point to maximum of 2.30 at h/2 from the face of the support. This shows that the ACI equation for shear strength due to the web reinforcement, V_s, would have predicted yielding of the stirrups if shear strength of the concrete, V_c, was not considered. The ACI equations would probably produce safe stirrup fatigue designs if the concrete contribution to shear strength was greatly reduced or ignored.

The equation for web shear strength of a concrete section is based on inclined cracking at a principal tensile stress of $4\sqrt{f'_c}$. In fact, the ACI Code allows one to calculate V_{cw} as the shear force required to produce a principal tensile stress of $4\sqrt{f'_c}$ at the centroidal axis of a member, since this is

where elastic theory would predict maximum shear stress. In composite members principal tensile stress is computed at the centroid of the composite section or at the top of the web, whichever is lower in the section. A plot of the maximum principal tensile stress in the web of the section and its inclination from the horizontal is shown in Fig. 5.11 for Beam 2 (Beams 1 and 3 are similar). The following observations can be made:

1. The maximum principal tensile stress occurs at a distance h/2 from the face of the support at the top of the web as the ACI equation predicts.

2. Principal tensile stress decreases from the support to the load point along the top of the web (centroid) and increases from the support to the load point along the bottom of the web.

3. Inclined cracks formed along a diagonal line between the load point and the support point. They did not form along the line of maximum principal tensile stress.

Figure 5.12 is a plot of the concrete stress range along the axis of the principal tensile stress. This plot looks similar to Fig. 5.11. Once again, cracks did not form along the line of maximum stress range.

Because plots of principal tensile stress and stress range along the axis of the principal tensile stress did not appear to compare well with actual behavior in cracking, it was decided to look at principal compressive stresses and associated stress ranges. Figure 5.13 is a plot of principal compressive stress along the shear span. It is seen that the maximum principal compressive stresses occur generally along the line of cracking. Figure 5.14 is a plot of stress range along the axis of principal compressive stress. It is interesting to note that isobars on the section correspond with the inclination of the concrete compression diagonals in the truss model.

In summary, the ACI approach to shear strength using components for concrete and steel strength does not adequately predict the shear fatigue behavior. Elastic theory did not predict the locations of crack initiation, but did predict the orientation of compression struts that developed in shear spans after diagonal web cracks had formed.

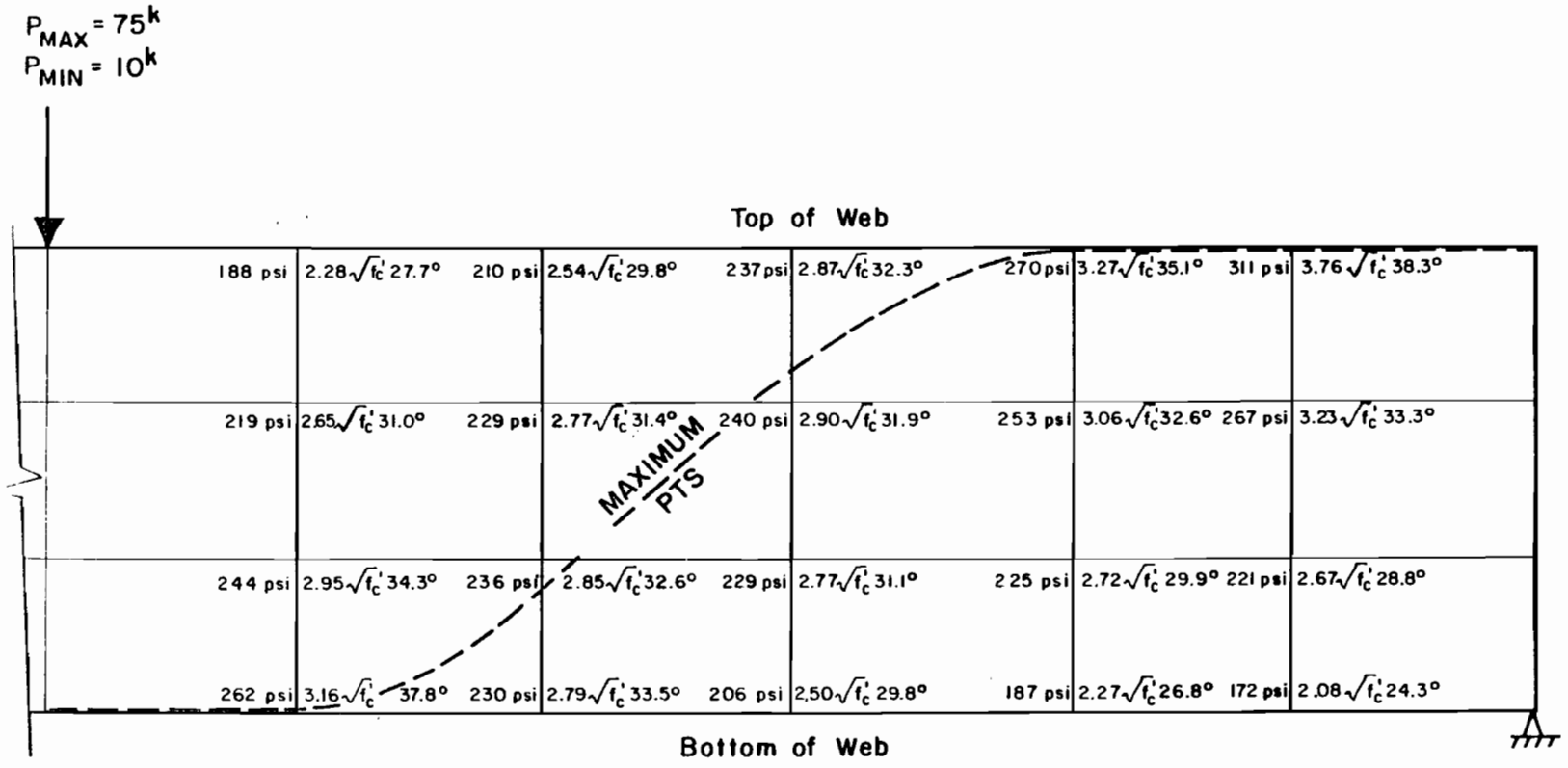

Fig. 5.11 Principal tensile stress and angle from horizontal for Beam 2

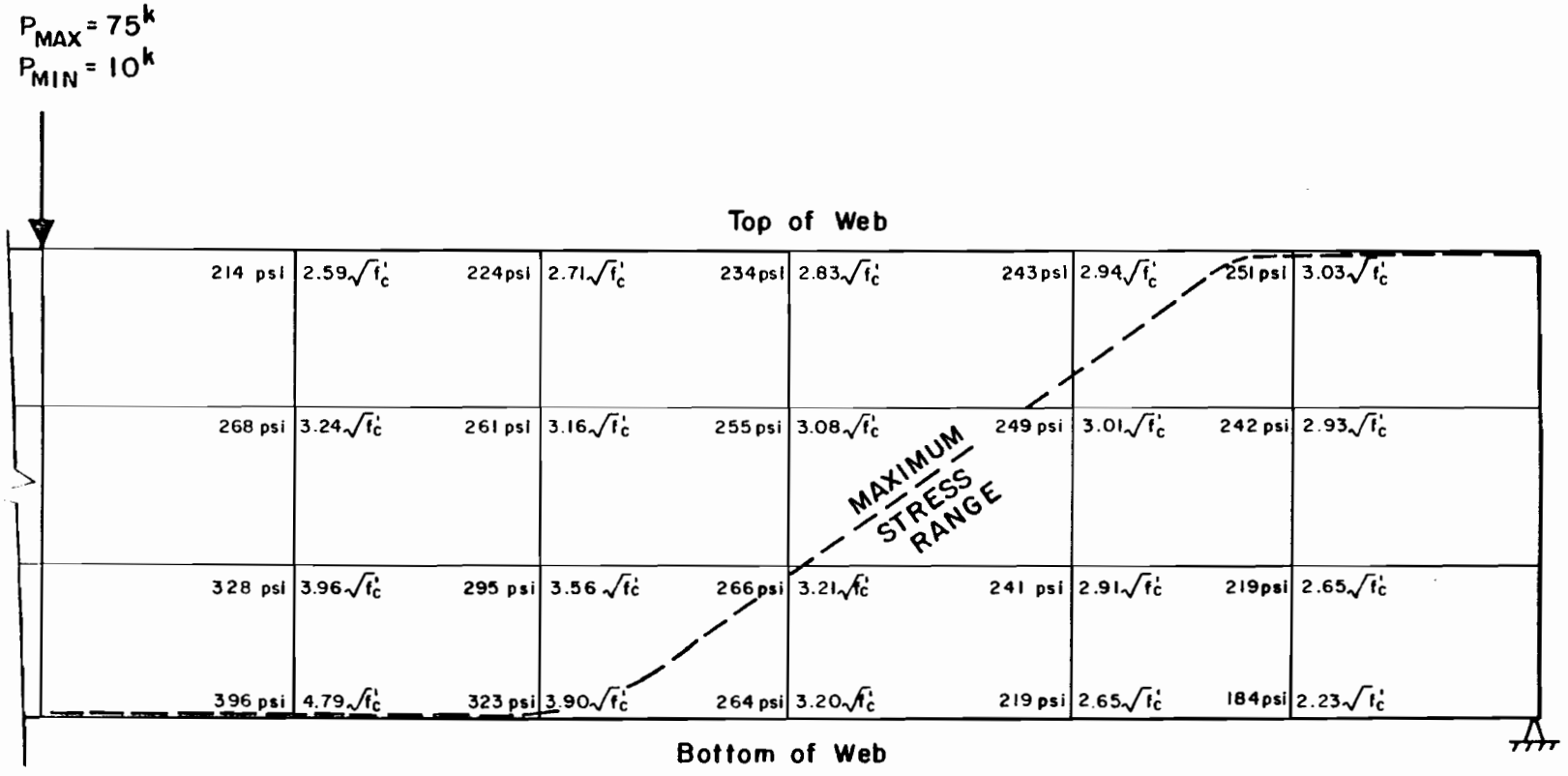

Fig. 5.12 Concrete stress range along axis of principal tensile stress for Beam 2

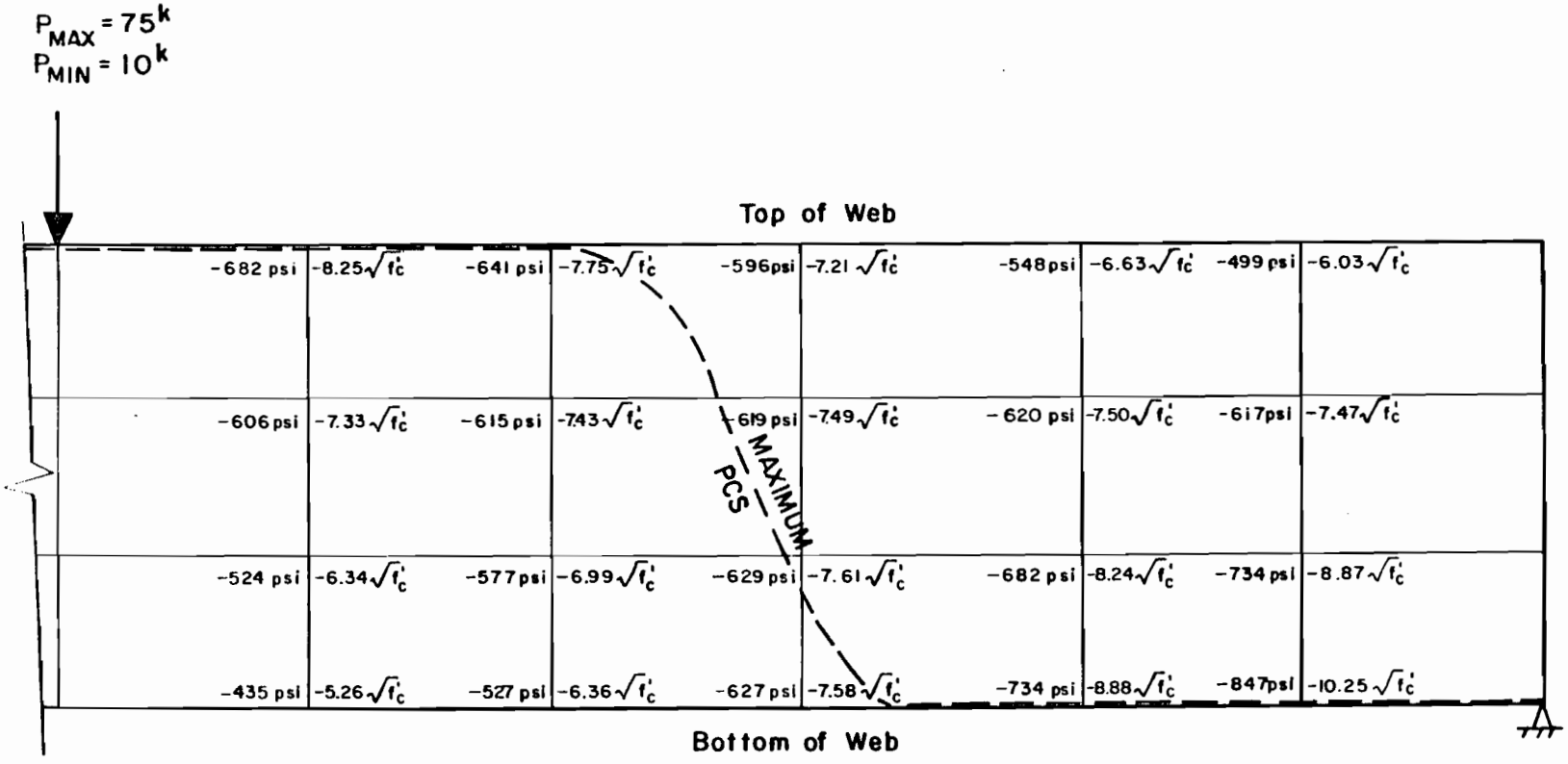

Fig. 5.13 Principal compressive stress for Beam 2

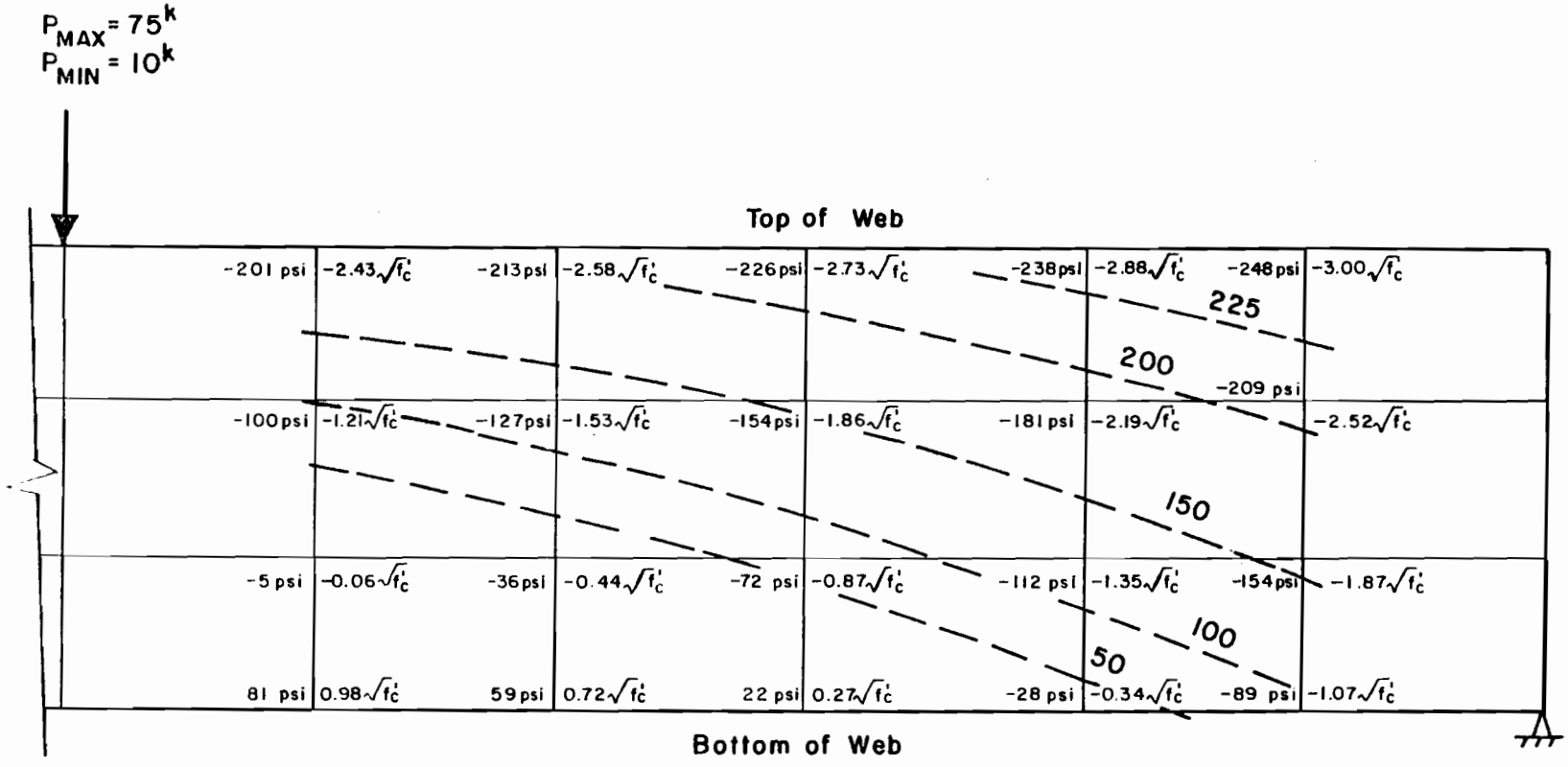

Fig. 5.14 Concrete stress range along axis of principal compressive stress for Beam 2

5.5.2 ACI Committee 215--Considerations for Design of Concrete Structures Subjected to Fatigue Loading. The ACI Committee 215 report consists of an introduction, a chapter on fatigue of component materials, and a chapter on fatigue of beams and pavements. It also has an extremely complete reference list with 108 entries, and an appendix which gives a summary of American, Japanese, and West German specifications relating to fatigue.

The chapter on fatigue properties of component materials contains information in sections on plain concrete (2.1) and reinforcing bar (2.2) that is pertinent to shear fatigue behavior. The fatigue strength of concrete for a life of ten million cycles for compression, tension, and flexure is given as approximately 55% of the static strength. Although shear is not mentioned explicitly, it is known that inclined cracks form due to diagonal tension caused by shear. The influence of load range is discussed with the suggestion of a modified Goodman diagram for fatigue design. Figure 5.15 is the diagram shown in the report for a design life of one million cycles. All tests of specimens described here had a lower shear force of 35 kips (includes self weight of girder) at h/2 from the face of the support. The static, plain concrete strength was not determined experimentally but was at least 115 kips because this was the shear force at which inclined cracking developed in Beam 3 during a static test. Taking the ratio of minimum shear to static shear strength for plain concrete as 30%, the diagram predicts that the upper load required for fatigue failure will be 65% of static strength or a minimum of 75 kips. Beams 1, 2, and 3 were loaded to 105 kips, 100 kips, and 92.5 kips, respectively. Beams 1 and 2 developed inclined cracks in less than one million cycles. Beam 3 was cracked during a static test at 3,133,000 cycles. The method gives a conservative estimate of fatigue life of concrete in shear with the only variable being load range. The effect of load history is discussed with the suggestion that rest periods are beneficial. However, more research is required to substantiate this belief. The effect of rate of loading is stated to have little effect unless the stress level is greater than 75% of the static strength, in which case a higher fatigue strength is encountered with increased loading rates.

The lowest stress range reported in the ACI Committee 215 report known to have caused a fatigue failure of a straight, hot-rolled deformed bar embedded in a concrete beam was 21 ksi after 1,250,000 cycles of loading on a beam containing a No. 11, Grade 60 test bar with a minimum stress level of 17.5 ksi. This agrees with the results of the test program because all bars that

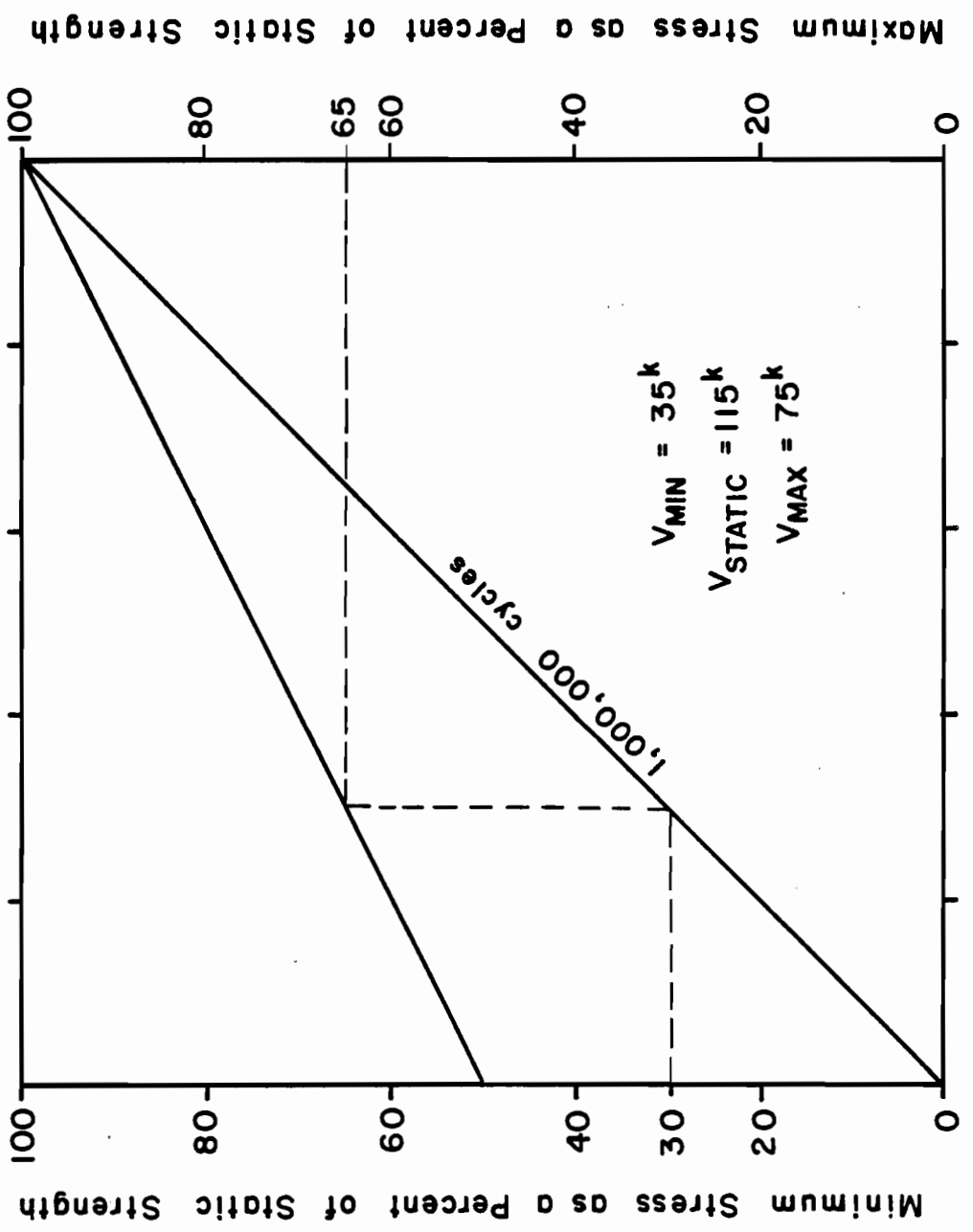

Fig. 5.15 Fatigue strength of plain concrete in tension, compression, or flexure; dashed line indicates value for test specimens (from Ref. 4)

had fatigue fractures experienced larger than 21 ksi stress ranges. The report discusses contradictions in the available research as to whether a bar has the same fatigue strength when tested in air or embedded in a concrete beam. A comparison of UT beam test results with in-air results (Fig. 5.5) indicates that in-air tests exhibit a greater fatigue strength. However, it should be pointed out that the stress range increased with progressive cycles in the beam tests reported here.

A chapter on fatigue of beams and pavements contains some useful guidance for shear fatigue design. Section 3.1 on beams states:

> In order to insure adequate performance at service load levels, beams subjected to repeated loads should be checked for the possibility of fatigue distress. Checking a design for safety in fatigue requires the following three steps:
>
> 1. Projection of a load histogram for the structural member.
>
> 2. Selection of locations where fatigue stresses may be critical.
>
> 3. Determination of critical fatigue stresses and comparison of these stresses with permissible values.

The first requirement means that a design life must be chosen for the member. The second requirement involves determining what type of fatigue to consider. A test by Hanson and Hulsbos is discussed in which a beam had a fatigue failure in shear after only 400,000 cycles of load above design levels (see Sec. 5.2). Warning of fatigue fracture in bends of reinforcement is discussed. The third requirement related to fatigue stresses suggests that minimum stresses are generally due to dead load and maximum stresses are generally due to dead plus live load. No suggestion of how to determine these stresses is provided. The discussion of fatigue of prestressed concrete members refers one to Sec. 2.1 (Plain Concrete) for discussion of fatigue of concrete and to Sec. 3.1.1 (Non Prestressed Members) for discussion of fatigue strength in shear. Mention is made of the fact that tests by Hanson and Hulsbos demonstrate that prestressed beams have a remarkably high shear fatigue strength under very severe loading conditions.

The section on nonprestressed members discusses test results by Hawkins which indicate that special attention should be given to the shear fatigue strength of beams subjected to high nominal shear stresses. The discussion goes on to say:

> Inclined cracking is a prerequisite for a shear fatigue failure. However, it is known that web shear cracks will form under repetitive loads at appreciably lower stresses than those assumed for static loading conditions.
>
> For highly repetitive loading it is recommended that the range in nominal shear stress that is assumed to cause inclined cracking under a zero to maximum loading be taken as one-half the value of nominal shear stress carried by the concrete, v_c, specified in the ACI Code. For other loadings, the range in nominal shear stress shall be linearly reduced from one-half of v_c to zero as the minimum stress is increased to v_c.
>
> Where the nominal shear stress under service loads exceeds the value of v_c specified in the ACI Code, and the shear stress due to the repetitive live load plus impact exceeds 25% of the total nominal shear stress, it is further recommended that the shear carried by the concrete, v_c, be taken as zero for calculations of the required area of shear reinforcement. This recommendation will reduce the risk of a shear fatigue failure at bends in stirrup reinforcement.

All test specimens described here fall into the last category which allows no contribution for concrete strength. The ratio of applied shear to shear carried by stirrups, shown in Fig. 5.10, shows that if this recommendation were followed, all three specimens would be considered underdesigned for shear strength. The amount of web reinforcement would have to be more than doubled at h/2 from the face of the support to meet this requirement if the ACI equation for shear strength provided by web reinforcement were used.

In summary, the ACI Committee 215 report gives some conservative guidelines for determining the strength of prestressed concrete members subjected to shear fatigue. However, little guidance is provided for determining the fatigue stresses resulting from a given loading.

5.5.3 ACI Committee 343--Analysis and Design of Reinforced Concrete Bridge Structures. The ACI Committee 343 report (formerly Committee 443) contains information concerning shear fatigue of prestressed members in Chapter 8, Service Load Analysis and Design, and Chapter 9, Prestressed Concrete. Section 8.3, Fatigue of Materials, presents an equation for maximum allowable stress range for straight, hot-rolled deformed reinforcing bars under live plus impact service loads:

$$f_f = 21 - 0.33 f_{min} + 8 (r/h)$$

where f_f = stress range

f_{min} = minimum stress level

r/h = ratio of base radius to height of rolled-on transverse deformation. Where the actual value is not known, 0.3 is recommended.

This equation can also be found in the AASHTO Code (See Ref. 2). A plot of this equation is shown in Fig. 5.16 for various lug profiles. The r/h radius for the No. 3 bars used as stirrups in this test series was 0.2 [18]. This produces a maximum allowable stress range of 22.6 ksi assuming zero minimum stress in the bars. All reinforcing bars which sustained fatigue fractures exhibited greater stress ranges than 22.6 ksi which is in agreement with the relationship presented above. However, the equation is extremely conservative since the lowest known stress range to have caused a fatigue fracture of a deformed bar embedded in concrete is 21 ksi, as discussed in Sec. 5.5.2. The report suggests that greater stress ranges may be used if demonstrated by fatigue tests on similar reinforcing bars. No guidance is given for determining minimum stress or live-plus-impact stress range. The report also warns that bends and tack welds should not be used in regions of high stress range.

The section pertaining to service load design for shear is nearly identical to Appendix B of the ACI 318-83 Building Code (Alternative Design Method) with the following modifications:

1. Shear stress carried by concrete is limited to $0.95\sqrt{f'_c}$ rather than $1.10\sqrt{f'_c}$.

2. The maximum shear carried by web reinforcement is limited to $4.05\sqrt{f'_c}$ rather than $4.4\sqrt{f'_c}$.

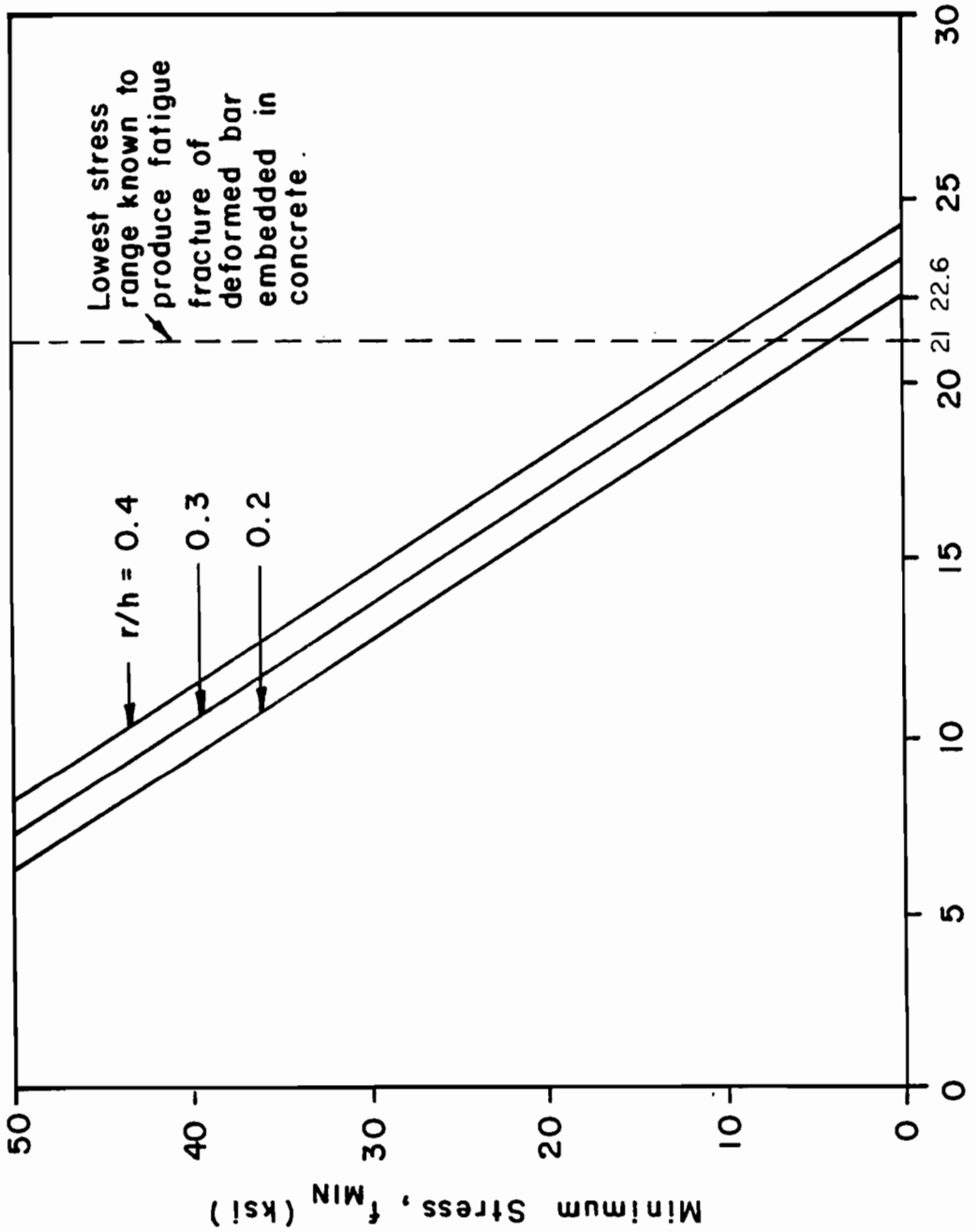

Fig. 5.16 ACI Committee 343 equation for maximum allowable stress range for straight, hot-rolled, deformed reinforcing bars subjected to live-plus-impact service loads

Table 5.3 shows calculated stress range values for the specimens in this test series using the service load design recommendations presented above and the following assumptions:

1. The critical section is located at h/2 from the face of the support.

2. Stress is shared equally by all stirrups crossing a diagonal crack.

3. Minimum stress is produced by dead load plus 10 kips live load (P_{min}).

From the results it is obvious that use of service load design for calculating stress range would produce very conservative designs. Minimum shear is greater than V_c in all cases. The minimum stress range calculated by this method would be 76 ksi for Beam 3 which is greater than nominal yield stress for the stirrups. For shear fatigue considerations, the value allowed for V_c under working stress design is much more reasonable than the value for V_c allowed for ultimate strength design, because fatigue problems are primarily confined to service load levels. The value for V_s is probably too conservative for prestressed concrete because it assumes a 45 degree angle for the inclination of the compression diagonals.

In Chapter 9, Prestressed Concrete, it is stated that prestressed concrete bridges may be designed by the strength or service load design method; however, they must satisfy both criteria. Section 9.2.3 states that:

> Complete freedom from cracking may or may not be necessary at any particular loading stage. When cracking is permitted under service loadings, the possibility of fatigue failure and tendon corrosion should be investigated in accordance with the criteria recommended in Sections 9.12 and 9.17.

Section 9.12.3 has the following to offer regarding shear fatigue:

> The possibility of inclined diagonal tension cracks forming under repetitive loading at appreciably smaller stresses than under static loading should be considered in the design.

TABLE 5.3 Calculated Stress Ranges for Test Specimens Using Service Load Values Recommended by ACI Committee 343

Beam No.	f'_c (psi)	V_c = $0.95\sqrt{f'_c}\, b_w d$ (k)	V_{min} = V_{DL} + 10 (k)	V_{max} = V_{DL} + V_{LL} (k)	V_s = V_{max} - V_{min} (k)	SR = $(V_s S / A_v d)$* (ksi)
1	6870	24.1	35.0	105.0	70.0	92
2	6838	24.0	35.0	100.0	65.0	85
3	5682	21.9	35.0	92.5	57.5	76

*SR = stirrup stress range

Section 9.17 has no reference to shear fatigue since it concerns only unbonded tendons.

5.6 Summary of Evaluation of Test Results

Fatigue loads applied to test specimens were in the range of AASHTO service level loads and resulted in formation of diagonal cracks and fatigue failure of stirrups. Specimens which suffered severe degradation of shear strength resisted shear forces through arch action near the end of the specimen life. It is likely that beams with different prestressing, such as draped or blanketed strands, will not develop the same action observed in the pretensioned beams with straight strands, and fail in a catastrophic manner.

Existing U.S. code provisions provide inadequate guidance for design against shear fatigue. Some proposed Japanese design methods for shear fatigue of reinforced concrete may hold promise for adaptation to design of prestressed concrete members.

CHAPTER 6

SUMMARY AND CONCLUSIONS

6.1 Introduction

Current research on fatigue strength of prestressed concrete girders has been undertaken at the University of Texas to gain a better understanding of fatigue behavior of full-scale beams and component materials. The investigation has examined:

1. Tensile fatigue tests of prestressing strand in air.

2. Flexural fatigue tests of prestressed concrete beams.

3. Shear fatigue tests of prestressed concrete beams.

This report contains information obtained in the third phase of the study.

Limited test results by others [10,12,26] have indicated that shear fatigue may be a problem in thin-web, prestressed concrete beams. The objectives of this exploratory study were to see if shear fatigue may be a problem in prestressed concrete highway girders designed according to current specifications.

6.2 Outline of Investigation

Three full-scale, Texas Type C-16 pretensioned girders with a composite deck slab were tested. All utilized 16 seven-wire, 1/2-in. diameter, Grade 270, stress-relieved strands in a straight pattern. End anchorage and shear reinforcement were provided in accordance with Texas Department of Highways and Public Transportation drawing GpA. The specimens were simply supported with a clear span of 48 ft. Loads were applied at the quarter points for static and fatigue testing, producing a shear span-to-depth ratio of 3.0. Instrumentation was provided to monitor applied loads, deflections, stirrup and prestressing strand stress ranges, inclined crack widths, and to detect the presence of stirrup fatigue fractures.

Variables in the three girders tested were maximum fatigue load, and incidental differences in effective prestress and concrete strength. The lower fatigue load level for all specimens was 10 kips. The emphasis of the test series was on

web-shear cracking. Specimens were not precracked initially in shear so that diagonal tension fatigue of concrete could be explored. After inclined fatigue cracks developed, fatigue strength of web reinforcement was studied.

A companion study on fatigue of deformed reinforcing bars in air was performed by Matsumoto [18] so that comparisons could be made between axial tension fatigue tests in air and fatigue of stirrups embedded in prestressed concrete beams. Reinforcing bars for the in-air tests were of the same mill heat as the reinforcing bars used for the stirrups in the three prestressed concrete beams.

6.3 Response of Specimens

Beam 1 was tested with a maximum fatigue load of 80 kips. The maximum computed diagonal tension stress was 328 psi or $3.96\sqrt{f'_c}$ at a section at the top of the web, 24 in. (h/2) from the face of the support. The corresponding maximum bottom fiber tensile stress at midspan was 500 psi or $6.03\sqrt{f'_c}$. This specimen was intended for the combined investigation of flexural and shear fatigue behavior. The flexural portion of the behavior was reported by Overman [23]. In that series of tests, the specimen was designated Beam C16-NP-6.0-NO-1.91.

The specimen was precracked in flexure at a load of 70 kips with loads applied at the third points. The load frame was then adjusted to provide quarter-point loading for all subsequent testing. Inclined cracking was detected in the north and south shear spans at 300,000 load cycles. Flexural fatigue damage was evident at 1,470,000 cycles. Extensive spalling had occurred and two strands were exposed with visible breaks. At 1,911,000 cycles the load pulsator turned off automatically due to a large increase in deflection. A static strength test was performed at this time. The specimen reached a load of 115 kips (71% of calculated flexural capacity) before it failed in flexure. A post-mortem investigation revealed that six stirrups in the south shear span, all located between the concentrated load and the pickup loop, had experienced fatigue fractures.

The shear fatigue strength of Beam 1 was greatly increased by the presence of the pickup loops near the middle of the shear spans (5 ft from each end of the span). The placement of the pickup loops allowed the girder to carry shear through a secondary truss mechanism after all stirrups between the pickup loops and load points had fractured (Fig. 4.6). It was observed

that the width of the major diagonal crack between the bottom of the pickup loops and the concentrated load point reached a steady state opening prior to flexural failure. The pickup loop had effectively anchored the crack so that it could open no wider nor propagate any further. For subsequent beam tests, pickup loops were placed 1 ft from the ends of each span so that they would not contribute to shear strength.

Beam 2 was tested with a maximum fatigue load of 75 kips. The maximum computed diagonal tension stress was 311 psi or $3.76\sqrt{f'_c}$ at a section at the top of the web, 24 in. (h/2) from the face of the support. The corresponding maximum bottom fiber tensile stress at midspan was 443 psi or $5.36\sqrt{f'_c}$. This specimen was the most informative of the shear fatigue series of specimens reported here. Inclined cracks and stirrup fatigue fractures were developed in both shear spans as the result of fatigue loading. The fatigue behavior was dominated by shear with no indication of flexural distress during the entire test. A conclusive method for detecting fatigue fractures while testing was in progress was used in this test and the following test.

Two cycles of monotonic loading were applied prior to fatigue loading to obtain initial information for the virgin test specimen, and to check the data acquisition systems. Inclined cracking was detected in the south shear span at 210,000 cycles. The first stirrup fracture was detected at 485,000 cycles in the south shear span. Concrete cover was removed to examine the stirrup. Corrosion was detected in the area of the fracture indicating fretting may have taken place. At 500,000 cycles, inclined cracking was detected in the north shear span. By this time, six stirrups had fractured in the south shear span. The first stirrup fracture in the north shear span occurred at 693,000 cycles. At 750,000 cycles, nine stirrups in the south shear span and three stirrups in the north shear span had fractured. Diagonal crack-width range in the south shear span was approximately 0.04 in. and shear failure appeared imminent. The specimen continued to carry load until 891,000 cycles when the load pulsator turned off automatically as the result of a large increase in deflection. A diagonal crack in the south shear span had propagated through the bottom flange. At this time, eleven stirrups in the south shear span and six stirrups in the north shear span had fractured. A strength test was performed and the specimen resisted an applied shear of 80 kips. During the test the inclined cracks opened to greater than 1 in., allowing the research team to see completely through the web of the girder.

During the fatigue history of Beam 2, shear was resisted by three mechanisms:

1. Concrete in diagonal tension with stirrups providing almost no resistance to applied shear as confirmed by strains measured with electrical strain gages.

2. Truss action after diagonal cracking with stirrups acting as vertical tension members and concrete as inclined compression struts.

3. Tied arch, after several stirrups fractured, with concrete forming an arch and prestressing strand acting as a tension tie.

A proportional relationship between stirrup stress range and inclined crack-width range was observed for many of the stirrups, indicating that no significant debonding occurred. It was also observed that stirrup stress and inclined crack width did not increase immediately upon application of load, but after a certain threshold load had been applied. This threshold load decreased with progressive load cycles indicating a decrease in the concrete contribution to shear resistance. Correspondingly, the maximum stirrup stress and stress range increased with progressive load cycles.

Beam 3 was tested with a maximum fatigue load of 67.5 kips for the first million load cycles. The maximum computed diagonal tension stress was 299 psi or $3.97\sqrt{f'_c}$ at a section at the top of the web, 24 in. (h/2) from the face of the support. The corresponding maximum bottom fiber tensile stress at midspan was 414 psi, or $5.49\sqrt{f'_c}$.

Static loads were applied prior to fatigue loading as for previous specimens. Flexural cracks were detected at 1,000,000 cycles but no inclined cracks had developed; the maximum fatigue load was increased to 71.3 kips. Fatigue loading was continued with periodic static tests until 3,133,000 load cycles when flexural fatigue damage was detected through a sudden increase in deflection. Light concrete spalling occurred across the bottom of the section; however, no strands were exposed. A static load test to 90 kips produced inclined cracks in the south shear span. Fatigue loading was resumed at a maximum applied shear of 67.5 kips, the original maximum applied shear. At 3,272,000 cycles, the load pulsator turned off automatically due to a sudden increase in deflection. Severe flexural fatigue damage was evident with two broken strands visible. This was

considered a complete flexural fatigue failure. Fatigue loading was continued with only the south ram applying loads to obtain some shear fatigue data from a specimen that had inadvertently failed in flexure. Maximum and minimum load level fatigue loads were adjusted to produce the same shear and bending moment distribution in the south shear span that had been applied immediately prior to flexural fatigue failure. A stirrup fracture was detected in the south shear span at 3,960,000 cycles. A second stirrup fracture was detected at 4,773,000 cycles at which time flexural failure appeared imminent. Fatigue loading was continued until 5,121,000 cycles when the load pulsator turned off automatically due to a large increase in deflection. No additional stirrups had fractured. A strength test was performed with both rams applying load. The specimen reached a load of 55 kips (35% of calculated flexural capacity) before failing in flexure.

The test results of Beam 3 suggest that an endurance limit exists for diagonal tension fatigue of concrete because no inclined cracks developed through 3,133,000 cycles of fatigue loading. This suggestion is supported by the previous series of tests reported by Overman [23]. In that series of tests only one beam developed inclined cracks during fatigue loading (excluding the flexure-shear specimen) at a maximum applied shear of 75 kips (Beam C-16-UP-8.0-NO-1.73), the highest applied shear in that series. The second highest applied shear in the test series was 71.5 kips (Beam C-16-NP-10.5-NO-0.58), and no inclined cracks developed during fatigue loading through 580,000 load cycles when flexural failure occurred. The third highest applied shear in the test series was 70 kips (Beam C-16-CP-7.2-NO-2.54), and no inclined cracks developed during fatigue loading through 2,540,000 load cycles.

After inclined cracking was produced in the south shear span of Beam 3, an increase in stirrup stress range and inclined crack-width range was observed with additional load cycles as had been observed for Beam 2. However, the increase was much more gradual.

6.4 Summary of Test Results

In any test program involving a limited number of test specimens and variables, it is difficult to draw sweeping conclusions. This is especially true for fatigue testing due to the inherent scatter in test results. This exploratory test series included three specimens and only one controlled variable

(maximum applied shear). Therefore, few absolute conclusions were reached and it may be appropriate to apply those conclusions only to beams similar to Texas Type C girders. In addition, several pertinent observations noted during testing will be reported as secondary conclusions.

6.4.1 Primary Conclusions. The following conclusions are drawn from results of an exploratory study of three Texas Type C prestressed concrete girders:

1. Under fatigue loading, a beam that would have failed in flexure during monotonic loading failed in shear.

2. A shear fatigue failure can occur when diagonal cracks are not present at the start of fatigue loading.

3. Flexural cracking can occur at a maximum applied bottom fiber tensile stress of slightly less than $6\sqrt{f'_c}$ under fatigue loading conditions.

4. Web-shear cracks can occur at a computed maximum diagonal tension stress of slightly less than $4\sqrt{f'_c}$ under fatigue loading conditions. Once formed, web-shear cracks do not close completely upon unloading.

5. Upon formation of inclined cracks, the concrete contribution to the resistance of applied shear is less than the diagonal cracking load. Under fatigue loading conditions the concrete contribution decreases with increasing number of load cycles.

6. After formation of inclined cracks, truss action was indicated through stirrup strain readings.

7. Fatigue fracture of stirrups can occur at a computed maximum diagonal tension stress of less than $4\sqrt{f'_c}$ at h/2 from the face of support when diagonal cracks are present. No fatigue endurance limit was observed for fracture of stirrups once diagonal cracks formed even though applied loads were in the approximate range of AASHTO service level design loads.

8. Loads were resisted by a tied-arch mechanism after most of the stirrups in a shear span had failed. Transition from truss action to tied-arch action occurred gradually as additional stirrups fractured. Straight strands and a low shear span-to-depth ratio permitted tied-arch

action to develop in the girders tested in this study. It is likely that draped or blanketed strands, or a high shear span-to-depth ratio, would prevent tied-arch action and probably result in rapid degradation of truss action followed by a catastrophic shear failure.

9. There was no significant debonding of stirrups after formation of diagonal cracks.

10. Stirrups are subjected to modest bending stresses as well as axial tension stresses at the location of an inclined crack.

11. Stirrup stress ranges and diagonal crack-width ranges increase approximately proportionately with additional fatigue load cycles. Stirrups exhibit a large increase in stress range immediately before fracture occurs.

12. The fatigue life of deformed reinforcing bars tested in air is greater than the fatigue life of similar reinforcing bars tested in concrete. This is probably due to bending stresses induced in the stirrups embedded in concrete, fretting at the crack interface, and a rapid increase in the maximum stirrup stress level during load cycles immediately preceding fracture.

13. Shear and flexural fatigue failures may occur even when the load-deflection response of the beam is essentially linear.

14. ACI Code and AASHTO Specification prestressed concrete shear provisions are inadequate for predicting shear fatigue strength of pretensioned concrete beams. Shear fatigue can be minimized by neglecting the concrete contribution to shear strength while designing web reinforcement.

6.4.2 Secondary Conclusions. Some important observations made during the fatigue tests could not be included in the general set of conclusions; the limited number of test specimens in this exploratory series did not provide for replication of all the observed phenomena. These secondary conclusions are listed below:

1. Propagation of diagonal web cracks into the bottom flange led to strand slip at beam ends which resulted in accelerated flexural fatigue.

2. A fatigue endurance limit for diagonal tension cracking of concrete was observed. The primary variables affecting diagonal tension fatigue appeared to be maximum applied shear and shear range with concrete strength being of less importance.

3. Fretting corrosion of a stirrup can occur near the location of a diagonal crack.

4. There can be some reserve capacity in pretensioned beams with straight strands after the shear fatigue failure occurs. In this series of tests, extension of a diagonal crack through the tension flange (Beam 2) was considered a shear fatigue failure.

5. Placement of pickup loops can dominate shear fatigue behavior by providing increased shear strength and controlling width and propagation of diagonal cracks.

6.5 Recommendations

The following recommendations are made based on the results of this exploratory investigation:

1. A better understanding of how laboratory testing conditions compare with actual field service loads is needed. The effect of moving loads, with varying load magnitude and cycle time, and their effect on cumulative damage, needs to be explored. The entire subject of load distribution on an overall bridge, and a better assessment of actual service loads experienced by a single bridge girder needs to be determined.

2. Limit states for shear fatigue design need to be established. The following questions need to be answered: can inclined cracking be allowed to develop; if inclined cracks develop, what concrete contribution to shear resistance should be allowed?

3. Bridge inspection programs should include examination for inclined cracks. It has been documented that inclined cracks are visible when no live load is present. In addition, tests have demonstrated that stirrup fatigue fracture is not possible unless inclined cracks are present.

4. An appropriate analytical model needs to be developed for shear behavior under fatigue loading conditions. This model should include: the effects of fatigue loading on diagonal cracking strength with an accurate assessment of controlling variables, the effect of inclined cracking on the concrete contribution to shear resistance and the possibility of decreasing concrete contribution with progressive load repetitions, and an accurate method of determining stirrup stresses and stress ranges with progressive load cycles. The Japanese have proposed such a model for reinforced concrete.

5. Shear and flexural fatigue interaction need to be more closely examined. The effects of inclined cracking on flexural behavior, and the effect of shear span-to-depth ratio need to be examined. A method of determining which type of failure will occur for different span lengths and loading conditions needs to be determined.

6. The effect of stirrup spacing on crack width control and subsequent fatigue behavior should be examined.

7. A better understanding of the relationships between fatigue strength of reinforcing bars tested in air and fatigue strength of reinforcing bars embedded in beams needs to be developed.

8. Shear fatigue tests should include instrumentation to positively determine the presence of fatigue fractures while testing is in progress, such as the system employed in this test series. Accurate instrumentation should be provided to determine stirrup stress ranges, inclined crack widths, and resistance to applied shear provided by web reinforcement throughout the fatigue history.

NOTATION

a = length of shear span

b_w = web width

c_D = cumulative damage index

d = effective depth

f'_c = concrete compressive strength

f_f = stress range

f_{min} = minimum stress

f_{pu} = tensile strength of prestressing tendons

f_{se} = effective prestress

f_{si} = initial prestress

f_y = yield strength of nonprestressed reinforcement

f_v = stirrup stress

f_{wmax} = maximum stirrup stress

f_{wmin} = minimum stirrup stress

f_{wr} = stirrup stress range

h = overall height of prestressed section

h = deformed bar lug height

j = ratio of internal lever arm to effective depth in a concrete section

k_1 = constant for residual stress

k_2 = constant of proportion for shear force carried by stirrups

r = deformed bar lug radius

r = ratio of minimum to maximum applied shear

s = stirrup spacing

s_{max} = maximum stress

s_{min} = minimum stress

s_R = stress range

v_c = service load shear strength provided by concrete

x = distance from face of support

y_B = distance from bottom of composite section to center of gravity of composite section

z = distance between centroid of tension and compression force in a concrete section

A = area of precast section

A_s = area of steel

A_v = area of web reinforcement in a distance "s"

A_w = area of web reinforcement in a distance "s"

C_b = distance from bottom of precast section to center of gravity of precast section

C_t = distance from top of precast section to center of gravity of precast section

CG_c = center of gravity of precast concrete section

CG_{ps} = center of gravity of prestressing steel

E = modulus of elasticity

I = moment of inertia of precast section

I_{TOTAL} = moment of inertia of composite section

N = number of fatigue load cycles

N_f = number of cycles to inclined cracking (Japanese equations)

N_f = number of cycles to complete beam collapse (Price and Edwards)

N_1 = number of cycles to first stirrup fracture

P = applied load

R = correlation coefficient

S_b = section modulus to bottom of precast section

S_e = standard error of estimate

S_t = section modulus to top of precast section

S_y = yield stress

SR = stress range

$V_{APPLIED}$ = maximum shear force

V_c = nominal shear strength provided by concrete

V_{ci} = nominal shear strength provided by concrete when diagonal cracking results from combined shear and moment

V_{co} = concrete shear strength at start of fatigue history

V_{cw} = nominal shear strength provided by concretre when diagonal cracking results from excessive principal tensile stresses in web

V_{DL} = shear force due to weight of composite section

V_{LL} = shear force due to applied loads

V_{max} = maximum applied shear force

V_{min} = minimum applied shear force

V_n = nominal shear strength

V_s = nominal shear strength provided by shear reinforcement

V_{STATIC} = monotonic load required to produce cracks in concrete

V_u = ultimate shear force

β_x = reduction factor for shear force carried by web reinforcement

δ = deflection

ε = strain

σ_y = vertical compressive stresses in a horizontal beam

ρ_w = ratio of area of web reinforcement (A_s) to effective area of web ($b_w d$)

REFERENCES

1. AASHO, Standard Specifications for Highway Bridges, 8th Ed., American Association of State Highway Officials, Washington, 1961.

2. AASHTO, Standard Specifications for Highway Bridges, 13th Ed., American Association of State Highway and Transportation Officials, Washington, 1986.

3. ACI 318-83, Building Code Requirements for Reinforced Concrete, American Concrete Institute, Detroit.

4. ACI Committee 215, "Considerations for Design of Concrete Structures Subjected to Fatigue Loading," ACI Manual of Concrete Practice, Part 1, 1984, pp. 215R-1 - 215R-25.

5. ACI Committee 343, "Analysis and Design of Reinforced Concrete Bridge Structures," ACI Manual of Concrete Practice, Part 4, 1984, pp. 343R-1 - 343R-118.

6. ASCE-ACI Task Committee 426 on Shear and Diagonal Tension, "The Shear Strength of Reinforced Concrete Members," Proceedings of the American Society of Civil Engineers, Journal of the Structural Division, Vol. 99, ST6, June 1973, pp. 1091-1187.

7. Chang, T.S., and Kesler, C.E., "Static and Fatigue Strength in Shear of Beams with Tensile Reinforcement," Journal of the American Concrete Institute, June 1958, pp. 1033-1057.

8. Chang, T.S., and Kesler, C.E., "Fatigue Behavior of Reinforced Concrete Beams," Journal of the American Concrete Institute, August 1958, pp. 245-254.

9. Frey, R., and Thurlimann, B., "Ermudungsversuche an Stahlbeton-balken mit und ohne Schubbewehrung (Fatigue Study of Reinforced Concrete Beams With and Without Web Reinforcement)," Institut fur Baustatik and Konstruktion, ETH Zurich, Report No. 7801-1, September 1983. (in German with English summary)

10. Hanson, J.M., and Hulsbos, C.L., "Fatigue Tests of Two Prestressed Concrete I-Beams with Inclined Cracks," Highway Research Record 103, Highway Research Board, January 1965, pp. 14-30.

11. Hanson, J.M., Burton, K.T., and Hognestad, E., "Fatigue Tests of Reinforcing Bars--Effect of Deformation Pattern," Journal of the PCA Research and Development Laboratories, Vol. 7, No. 3, September 1968, pp. 2-13.

12. Hanson, J.M., Hulsbos, C.L., and Van Horn, D.A., "Fatigue Tests of Prestressed Concrete I-Beams," Proceedings of the American Society of Civil Engineers, Journal of the Structural Division, Vol. 96, ST11, November 1970, pp. 2443-2464.

13. Helgason, T., Hanson, J.M., Somes, N.F., Corley, W.B., and Hognestad, E., "Fatigue Strength of High Yield Reinforcing Bars," National Cooperative Highway Research Program, Report 164, 1976.

14. Higai, T., "Fundamental Study on Shear Failure of Reinforced Concrete Beams," Concrete Library of Japanese Society of Civil Engineers, Vol. 1, July 1983, pp. 25-39 (translation from Proceedings of Japanese Society of Civil Engineers, No. 279, 1978).

15. Lin, T.Y., and Burns, N.H., Design of Prestressed Concrete Structures, 3rd Ed., John Wiley and Sons, New York, 1981.

16. MacGregor, J.G., and Jhamb, I.C., "Effect of Surface Characteristics on Fatigue Strength of Reinforcing Steel," Abeles Symposium on Fatigue of Concrete, SP-41, American Concrete Institute, Detroit, 1974, pp. 39-67.

17. MacGregor, J.G., Jhamb, I.C., and Nutall, N., "Fatigue Strength of Hot-Rolled Reinforcing Bars," Journal of the American Concrete Institute, Vol. 68, No. 3, March 1971, pp. 169-179.

18. Matsumoto, N., "A Fatigue Study of Deformed Reinforcing Bars," unpublished M.S. Thesis, The University of Texas at Austin, May 1985.

19. Okamura, H., and Farghaly, S., "Shear Design of Reinforced Concrete Beams for Static and Moving Loads," Concrete Library of Japanese Society of Civil Engineers, Vol. 1, July 1983, pp. 72-81 (translation from Proceedings of Japanese Society of Civil Engineers, No. 287, July 1979).

20. Okamura, H., and Higai, T., "Proposed Design Equation for Shear Strength of Reinforced Concrete Beams without Web Reinforcement," Concrete Library of Japanese Society of Civil Engineers, Vol. 1, July 1983, pp. 96-106 (translation from Proceedings of Japanese Society of Civil Engineers, No. 300, August 1980).

21. Okamura, H., Farghaly, S., and Ueda, T., "Behavior of Reinforced Concrete Beams with Stirrups Failing in Shear under Fatigue Loading," Concrete Library of Japanese Society of Civil Engineers, Vol. 1, July 1983, pp. 82-95 (translation from Proceedings of Japanese Society of Civil Engineers, No. 308, April 1981).

22. Okamura, H., and Ueda, T., "Behavior in Shear of Reinforced Concrete Beams under Fatigue Loading," Concrete Library of Japanese Society of Civil Engineers, Vol. 2, December 1983, pp. 37-69 (translation from Journal of the Faculty of Engineering, The University of Tokyo (B), Vol. 37, No. 1, 1983).

23. Overman, T.R., Breen, J.E., and Frank, K.H., "Flexural Fatigue Behavior of Pretensioned Concrete Girders," Research Report 300-2F, Center for Transportation Research, The University of Texas at Austin, November 1984.

24. Paulson, C., Frank, K.H., and Breen, J.E., "A Fatigue Study of Prestressing Strand," Center for Transportation Research Report 300-1, The University of Texas at Austin, April 1983.

25. Pfister, J.F., and Hognestad, E., "High Strength Bars as Concrete Reinforcement, Part 6, Fatigue Tests," Journal of the PCA Research and Development Laboratories, Vol. 6, No. 1, January 1964, pp. 65-84.

26. Price, K.M., and Edwards, A.D., "Fatigue Strength in Shear of Prestressed Concrete I-Beams," American Concrete Institute Journal, April 1971, pp. 282-292.

27. Rabbat, B.G., Karr, P.H., Russell, H.G., and Bruce, N.G., "Fatigue Tests of Full Size Prestressed Girders," Research Report 113, Portland Cement Association, June 1978.

28. Reese, G.A., "Fatigue Strength of Prestressed Concrete Girders," unpublished M.S. Thesis, The University of Texas at Austin, August 1983.

29. Rehm, G., "Contributions to the Problem of Fatigue Strength of Steel Bars for Concrete Reinforcement," Preliminary Publication--6th Congress of the IABSE (Stockholm, 1960), International Association for Bridge and Structural Engineering, Zurich, 1960, pp. 35-46.

30. Ruhnau, J., "Influence of Repeated Loading on the Stirrup Stress of Reinforced Concrete Beams," Shear in Reinforced Concrete, SP-42, Vol. 1, American Concrete Institute, Detroit, 1974, pp. 169-181.

31. Suttikan, C., "A Generalized Solution for Time Dependent Response and Strength of Non-Composite and Composite Prestressed Concrete Beams," Ph.D. Dissertation, The University of Texas at Austin, August 1978.

32. Yates, D., "Flexural Fatigue Behavior of Post-Tensioned Partial-Beam Concrete Specimens," unpublished M.S. Thesis, The University of Texas at Austin, December 1987.

33. Diab, J., "An Exploratory Investigation of Flexural Fatigue Behavior of Post-Tensioned Concrete Girders," unpublished M.S. Thesis, The University of Texas at Austin, December 1987.

34. Collins, M.P., and Mitchell, D., "Shear and Torsion Design of Prestressed and Non-Prestressed Concrete Beams," PCI Journal, Vol. 25, No. 5, September-October 1980, pp. 32-100.

35. Marti, P., "Basic Tools of Reinforced Concrete Beam Design," Journal of the American Concrete Institute, Vol. 82, No. 1, January-February 1985, pp. 46-56.

36. Marti, P., "The Use of Truss Models in Detailing," Concrete International, Vol. 7, No. 12, December 1985, pp. 66-73.

37. Ramirez, J.A., and Breen J.E., "Proposed Design Procedures for Shear and Torsion in Reinforced and Prestressed Concrete," Research Report 248-4F, Center for Transportation Research, The University of Texas at Austin, December 1983.

38. Thurliman et al., Anwendungen der Plastizitatstheorie auf Stahlbeton Vorlesung zum Forthbildungskurs fur Bauingenieure. Institut fur Baustatik und Konstruktion ETH Zurick 1983.

39. Schlaich, J., Zum einheitlichen Bemessen von Stahlbetontragwerken, Beton-und Stahlbetonbau, Heft 4, 1984, S. 89-96.

40. Schlaich, J., Schafer, K., and Jennewein, M., "Towards a Consistent Design of Structural Concrete," PCI Journal, Vol. 32, No. 3, May-June, 1987.

41. Bachman, P.M., "An Exploratory Investigation of Shear Fatigue Behavior of Pretensioned Concrete Girders," unpublished M.S. Thesis, The University of Texas at Austin, August 1985.